Katabatic wind and Boundary Layer Front Experiment around Greenland ("KABEG '97")

Field Phase Report
compiled by Günther Heinemann

Ber. Polarforsch. 269 (1998)
ISSN 0176 - 5027

Corresponding author address: Dr. Günther Heinemann, Meteorologisches Institut der Universität Bonn, Auf dem Hügel 20, D 53121 Bonn, Germany. (email: gheinemann@uni-bonn.de)

METEOROLOGISCHES INSTITUT
DER UNIVERSITÄT BONN
1998

Contents

Abstract

The aircraft-based experiment KABEG'97 (**Ka**tabatic wind and **b**oundary layer front **e**xperiment around **G**reenland) was performed in April/May 1997. The experimental investigations comprised the katabatic wind system over Greenland and measurements of boundary layer fronts (BLFs) over the Davis Strait. Both phenomena are important for the understanding of the climate of the Arctic and the Antarctic.

The research aircraft POLAR2 owned by the Alfred-Wegener-Institut (AWI) was based at Kangerlussuaq. During the experiment, surface stations were installed at five positions on the ice sheet and in the tundra. The GPS navigated aircraft was instrumented with the turbulence measuring device "METEOPOD", allowing high-resolution measurements and the determination of turbulent momentum, sensible and latent heat fluxes. In addition, downward and upward solar and terrestrial radiation and surface temperature were measured; a high-resolution laser altimeter registered surface roughness structures. The GPS dropsonde facility of the aircraft was used for the BLF program over ocean.

A total of 13 flights have been performed, three of them were BLF flights. The BLF flights took place during cold air outbreaks over the Davies Strait under conditions of low-level flow parallel to the sea ice edge wind speeds of about 20 m/s. The katabatic wind flights were performed during quite different synoptic situations and surface conditions, and low-level jets with wind speeds up to 25 m/s were measured under strong synoptic forcing of the katabatic wind system.

1. Introduction

1.1 Goals

The aircraft-based experiment KABEG'97 (Katabatic wind and boundary layer front experiment around Greenland) was performed in April/May 1997 in the area of southern Greenland. The experimental investigations comprised the katabatic wind system over Greenland and measurements of boundary layer fronts (BLFs) over the Davis Strait. Both phenomena are important for the understanding of the climate of the Arctic and the Antarctic. The main goals of KABEG are as follows:

(A) "The katabatic wind system near Greenland"
- development of the katabatic flow under high pressure conditions;
- channeling of the katabatic flow and synoptic forcing;
- modification of the katabatic flow in the transition zones ice/ocean and ice/tundra.

(B) "Boundary layer studies near the sea ice edge"
- development and structures of BLFs at the sea ice edge under conditions of a flow parallel to the sea ice front.

1.2 Participating institutions and participants, acknowledgments

KABEG was an experiment of the Meteorologisches Institut der Universität Bonn (MIUB) in cooperation with the Alfred-Wegener-Institut (AWI). My thanks go to C. Kottmeier, J. Hartmann and W. Cohrs (AWI) for their help during the pre-experiment phase. The aircraft POLAR2 was operated by the Deutsches Zentrum für Luft- und Raumfahrt (DLR), the logistics of the aircraft mission was organized by H. Finkenzeller (DLR). My thanks go also to Aerodata, which was responsible for the operation of the POLAR2 measurement system.

The KABEG team at Greenland consisted of R. Henrici, H. Hettinger and H. Christen (all three from DLR), P. Wachs, E. Schmidt (both from Aerodata) and C. Drüe and G. Heinemann (both from MIUB). Without the experience and skill of all in the team the quality of the KABEG data set would have been significantly reduced. The author is also grateful to the DMI (Copenhagen and Kangerlussuaq) and the Institute of Marine and Atmospheric Research University Utrecht (IMAU) for support. The assistance from Greenlandair and Air Traffic Control at Kangerlussuaq is acknowledged. Thanks go also to all people at MIUB, who helped in the preparation and organization of KABEG.

The KABEG data set is completed by various data sources. Additional AWS data useful for KABEG has been provided by the University of Colorado and IMAU. Infrared and visible satellite imagery was acquired from the Satellite Active Archive of NOAA/NESDIS, and high-resolution HRPT data from the Canadian Weather Service. SSM/I data were provided by the Global Hydrology Resource Center (GHRC) at the Global Hydrology and Climate Center (Huntsville, Alabama, USA), ERS data were made available by IFREMER

(Brest, France). KABEG is supported by the German Federal Ministery of Education, Science, Research andTechnology under grant BMBF-03PL020F, the aircraft program was funded by AWI.

1.3 Time schedule of KABEG

Pre-experiment phase:
8-10 October 1996: planning meeting and testflights with the POLAR2 at Braunschweig
28 December 1996: application for the experiment at the Danish Polar Centre
24 February 1997: planning meeting at Braunschweig
10 March 1997: test of the laseraltimeter data logging
25 March 1997: planning meeting and final testflights with the POLAR2 at Braunschweig
until 2 April 1997: preparation and packing of material and instruments
2 April 1997: transportation of all material and instruments to Greenland

Experiment (9 April to 20 May 1997)
9 to 10 April: installation of an energy balance station with profile measurements and a sonic anemometer near Kangerlussuaq (station S)
12 April: installation of the stations A1, A2 and A3[1] on the inland ice, transport by a Hughes 500 helicopter
15 April: flight BLF1[2]
16 April: installation of the station A4 on the inland ice, transport by a AS350 helicopter
18 April: flight KA1
19 April: flight BLF2
21 April: flight KA2
22 April: flight KA3
24 April: flight BLF3
29 April: flight KA4
30 April: inspection and data backup at the stations A1-A4, transport by a Hughes 500 helicopter
2 May: flight KA5
11 May: flights KA6 and KA7
13 May: flight KA8
14 May: flight KA9
15 May: dismount of the station S
17 May: dismount of the stations A1-A4, transport by a Bell UH1D helicopter
18 to 19 May: packing of material and instruments, transport to Germany

post-experimental phase:
12 June: de-briefing of KABEG at Bonn

---

[1] see Section 3

[2] BLF = boundary layer front flight mission
KA = katabatic wind flight mission

2. Scientific background

2.1 Katabatic wind

The katabatic wind system represents a key factor for the near-surface wind field over the large ice sheets of the Antarctic and Greenland. It is particularly essential for the exchange of energy and momentum between atmosphere and the underlying surface. Considering the large area of the Antarctic continent (about 14×10^6 km^2, including ice shelf surfaces), this topographically induced wind system plays an important role in the global energy and momentum budget. But also over Greenland, which is much smaller than the Antarctic continent, the katabatic-driven near-surface wind regime plays an important role in questions of the mass balance of the ice sheet. The coastal zones of the Antarctic and Greenland generally reveal a strong topographic gradient (Fig.2.1), and are associated with a wind regime dominated by katabatic forcing with wind speeds up to gale force (Putnins, 1970; Ball, 1960; Wendler, 1990). The so-called "piteraq", which is a strong synoptically enforced katabatic wind at the Greenlandic coast, represents a well-known phenomenon to the Inuits at Greenland (Rasmussen, 1989).

Despite the fact that the physical processes of the dynamics of the katabatic wind system are thought to be well understood, detailed observational studies are quite rare for both polar regions. Most of our understanding of the 3D structure of the katabatic wind relies on numerical simulations, and there is a lack of an adequate validation data set. At this point two main characteristics of the term "katabatic wind" used in this study should be stressed:

1) it is a gravity-driven airflow, i.e. a stably stratified boundary layer is a necessary condition;
2) the Coriolis force is important, i.e. a relatively large horizontal scale of the wind system.

Most of the past observational studies of the katabatic wind use data from surface measurements (e.g. Oerlemans und Vugts, 1993; Wendler, 1990; Bromwich, 1989). Measurements of the vertical structure are very rare and result from data of sounding systems at few points. For the Antarctic, measurements of the wind speed profile of katabatic wind events show a typical vertical extent of 100-200 m (see Schwerdtferger, 1984; Sorbjan et al., 1986). Strong winds with high temporal constancy are generally observed to be associated with confluence zones due to topographic structures (Schwerdtfeger, 1984). Sorbjan et al. (1986) use a tethersonde system for the investigation of the katabatic wind structure over East Antarctica during spring (Fig.2.2). The mean profiles show a pronounced daily cycle with the largest near-surface wind speed (about 10 m/s) during the early morning hours. A detailed investigation of the (less accurate) profiles from Antarctic synoptic stations using wind data from radiosoundings and pilot balloons is presented by Phillpot (1997). To the author's knowledge, only two studies of the katabatic wind using an instrumented aircraft exist for the Antarctic. Parish und Bromwich (1989) investigate the channeling of the katabatic flow in the area of the Ross Ice Shelf by flying at a constant level of about 200 m relative to the topography. No

information about the vertical structures can be obtained from this study. The flights of Gosink (1982) in the same area also represent single level data and gave an indication of the presence of a hydraulic jump in the coastal area.

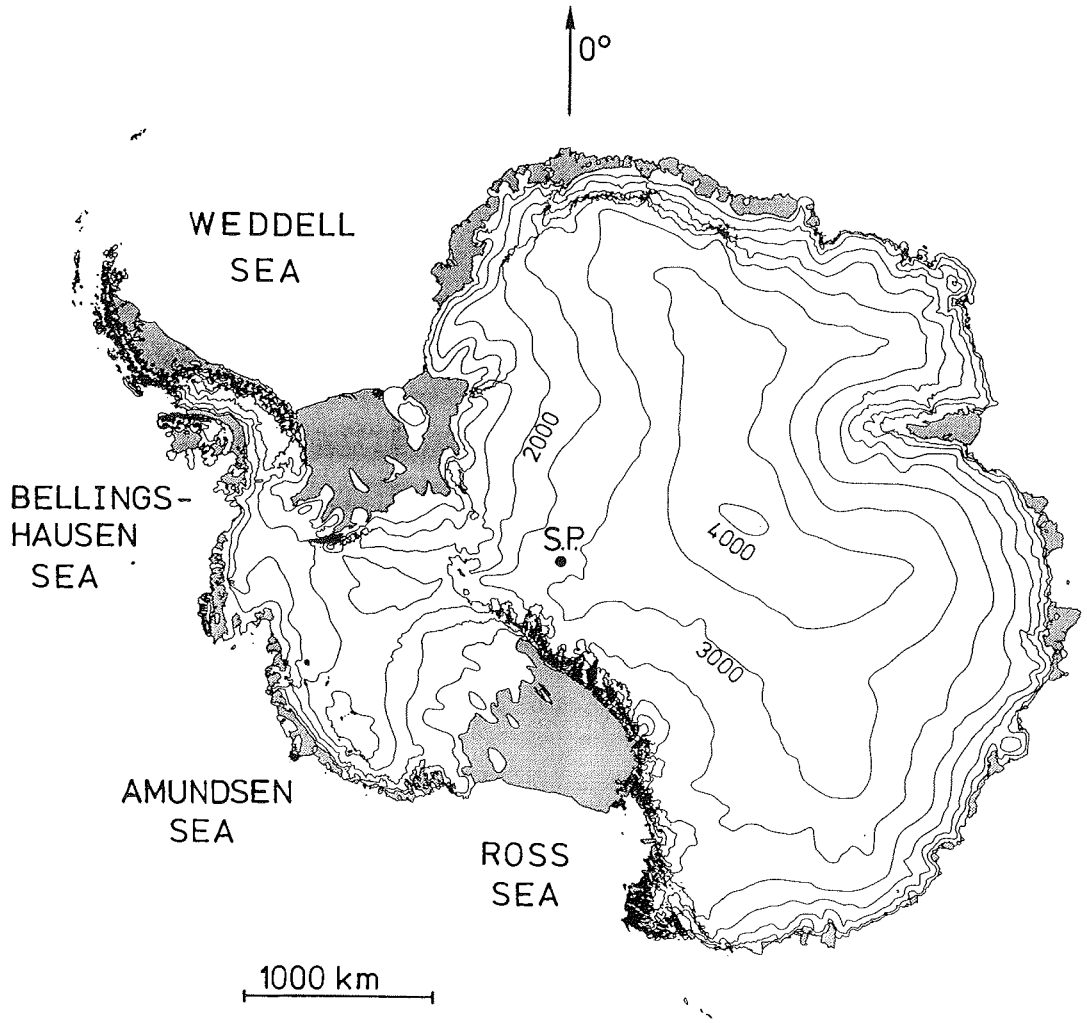

Fig.2.1a: Map of Antarctica with topography (isolines every 500 m), ice shelf surfaces are shaded (data taken from Antarctic Digital Database, BAS et al., 1993).

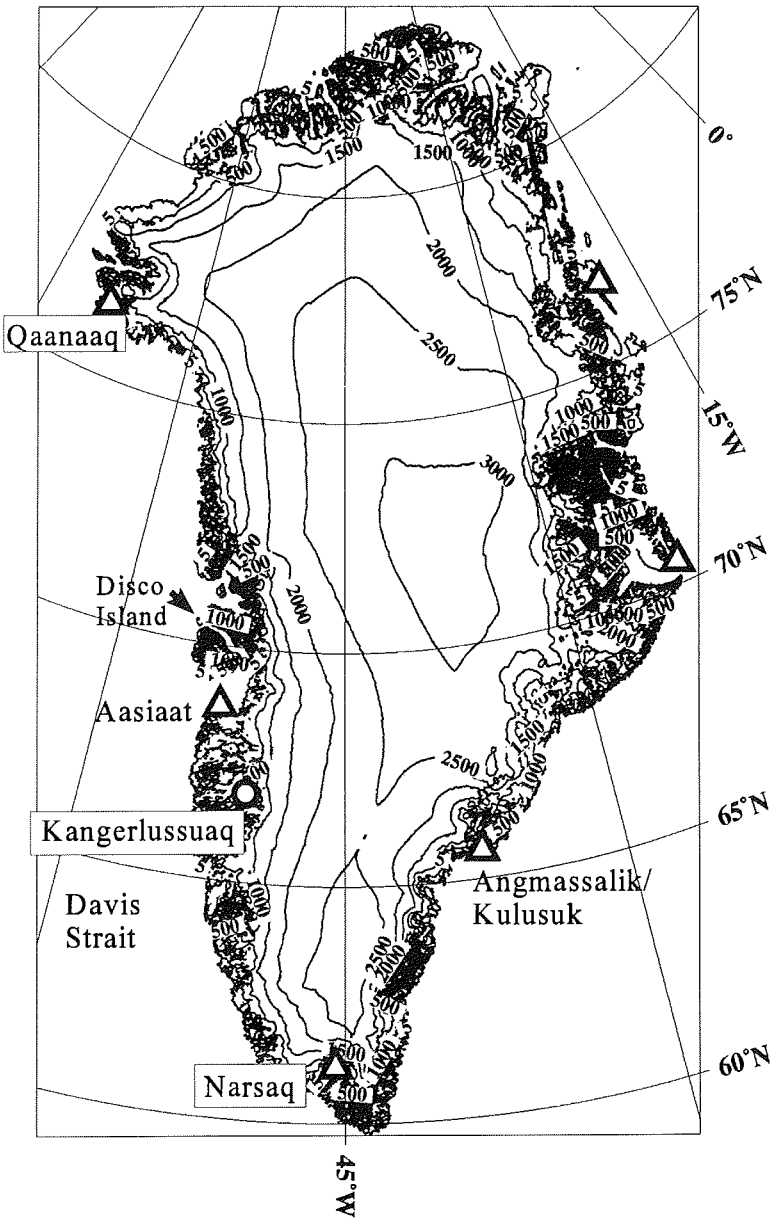

Fig.2.1b: Map of Greenland with topography (isolines every 500 m) from high resolution (2 km) topography data (Ekholm, 1996). Triangles mark the radiosonde stations.

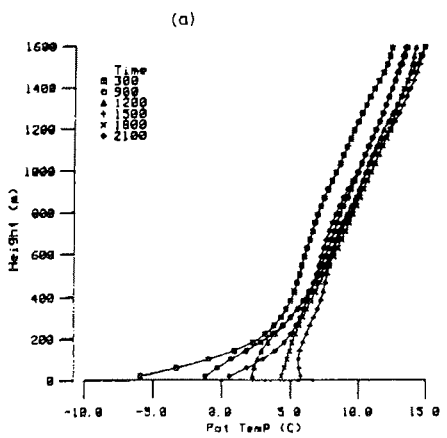

Fig.2.2a: Profile of mean potential temperature for November/December 1985 at station D47 (1560 m) near the Adélie Coast (from Sorbjan et al., 1986).

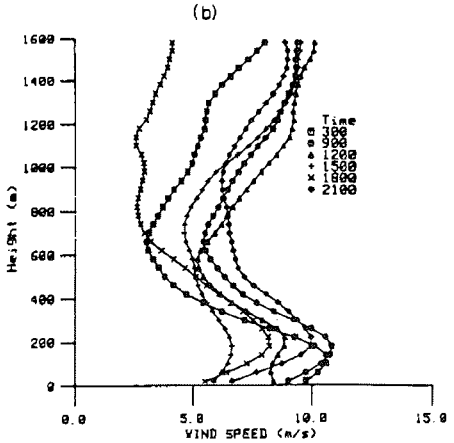

Fig.2.2b: As Fig.2.2a, but for the wind speed (a total of 52 profiles).

Besides the channeling effects, the modification of katabatically generated air flows near the margin of the ice sheets is a special point of interest. This interaction with an ice or open water surface with considerably different surface energy and momentum fluxes compared to the continental ice regions is poorly understood.

The situation for experimental data over Greenland is problably worse than for the Antarctic. A major effort for the investigation of the katabatic wind system over Greenland was made during the GIMEX experiment (Oerlemans und Vugts, 1993). In addition to data from surface stations, the katabatic wind at the ice margin was studied using a tethered sonde for summertime conditions (Van den Broeke et al., 1994). For this summertime situation, the measurements and also numerical simulations of Meesters (1994) show the development of a shallow, weak katabatic flow (Fig.2.3). In contrast to the summertime situation for the Antarctic (and wintertime situations for Greenland), melting occurs at the ice surface of the Greenland ice sheet during summer. As a result, the katabatic wind system of the GIMEX study is not driven by the nighttime cooling of the snow surface, but instead by the daytime warming of the tundra boundary layer. Because of the dominating thermal forcing by the daily cycle of the tundra boundary layer, the maximum wind speeds

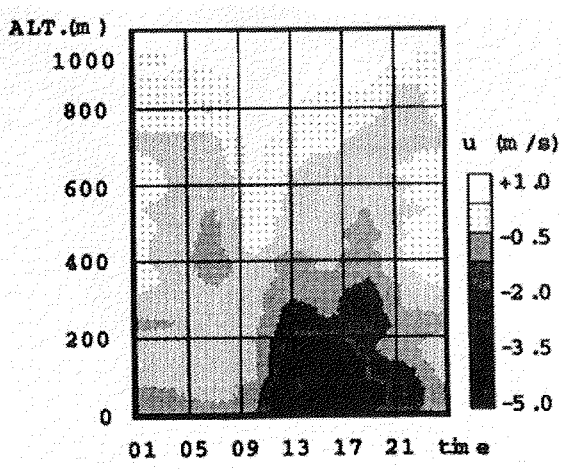

Fig.2.3: Mean daily cycle of the downslope wind component from GIMEX during 5-24 July 1991 (from van den Broeke et al., 1994)

are found to be present during the afternoon. The mean downslope wind maximum for July 1991 has values of less than 5 m/s and lies about 100 m above the surface.

In recent years, a couple of numerical investigations of the katabatic wind system in the Antarctic and Arctic (Greenland) have been performed using idealized simulations with 3D meso-scale models. Heinemann (1997) and Bromwich et al. (1994) show the development of katabatic winds in the Antarctic under highly simplified boundary values and initial atmospheric conditions. The synoptic forcing, the daily course of the net radiation during summer and the surface conditions in the transition zone ice/ocean are found to be important for the katabatic wind structure. A more realistic approach is presented by Hines et al. (1995), who run a meso-scale model in a nested mode with global analyses for the period of one month (June 1988) for the whole Antarctic. Interestingly, Hines et al. show that the structures found by these realistic simulations for the near-surface wind field as a one month mean are quite similar to the wind field structures found by idealized simulations over 1-2 days. The conclusion of this comparison is that the forcing of the topography over the Antarctic continent represents the dominant forcing term for the near-surface wind field, and that the influence of synoptic-scale cyclones is small in the average. However, the synoptic forcing term can be of great importance regarding shorter periods of a few days (Bromwich et al., 1994; Heinemann, 1995; Engels and Heinemann, 1996).

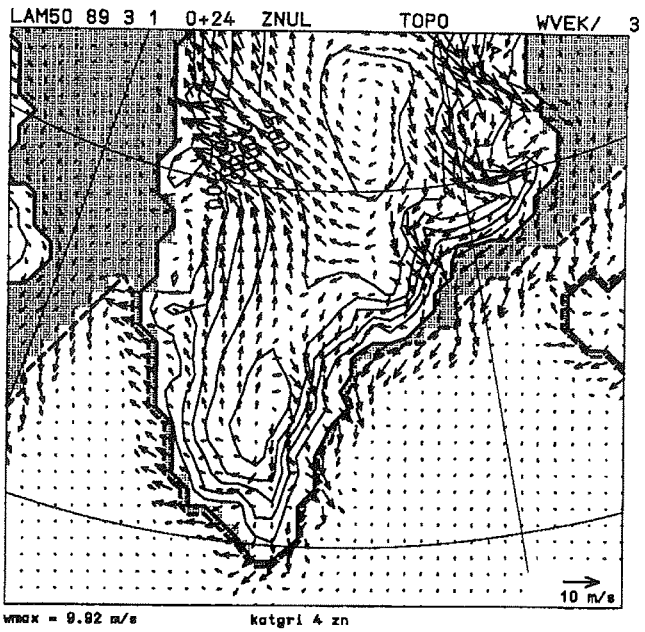

Fig.2.4: Topography (full lines, isolines every 500 m) and wind vectors at the lowest sigma level for South Greenland after 24 h simulation starting from a state of rest (from Heinemann, 1996a)

During the planning of the katabatic wind flights of KABEG, model simulations were also taken into account. Idealized simulations for Greenland are shown by Bromwich et al. (1996) and Heinemann (1996a). These simulations reflect the dominant influence of the topography structure on the near-surface wind field (Fig.2.4). While a relative homogeneous structure is found over the inner part of the Greenlandic ice sheet and over West Greenland, channeling effects are present in areas of coastal fjords. Very pronounced channeling effects occur near Angmagssalik and Kangerdlugssuaq at the coast of East Greenland. These confluence zones can be enforced for the case of a synoptic-scale cyclone near Iceland (Bromwich et al., 1996).

The katabatic wind measurements during KABEG were performed in order to address the following questions:

(a) What are the 3D structures of the katabatic wind field over topographically structured terrain and over relatively homogeneous terrain? In several studies for West Greenland, 2D numerical modelling was thought to be sufficient for the description of the katabatic wind field (e.g. for the GIMEX study, Gallée and Duynkerke, 1997).

(b) How can the katabatic wind development quantitatively be described in terms of the budgets of momentum and energy? Aircraft-based turbulence measurements (thus representing not only point measurements or only low levels) have not yet been performed in a katabatic wind system.

(c) How is the katabatic wind triggered by the synoptic-scale forcing?

(d) How is the performance of mesoscale numerical models in simulating the boundary layer structure of the katabatic flow? In this respect, the KABEG data set will be the first data set with a detailed 3D resolution covering grid points of operational mesoscale models.

2.2 Boundary layer fronts

The sea ice edge represents an area with strong gradients of surface temperature, roughness and albedo (the latter being of minor importance during wintertime conditions). Due to the different energy budget of the boundary layer above the sea ice and open water, strong horizontal temperature gradients in the atmospheric boundary layer can establish. This "boundary layer front" (BLF) associated with the sea ice front represents a low-level baroclinic environment where polar mesocyclones can develop (Fett, 1989). These mesocyclones typically occur as shallow vortices with fronts (Heinemann, 1996b; Douglas et al., 1995). A pronounced BLF forms when the flow direction in the boundary layer is almost parallel to the sea ice front. In this case, differential heating can generate strong low-level baroclinicity with a low-level jet (Shapiro and Fedor, 1989; Shaw et al., 1991). Frontogenetic processes lead to the formation of a pronounced cloud band parallel to the sea ice front in many cases, which represents the signature of the BLF on satellite images. With the onset of substantial off-ice wind components connected with cold air outbreaks or cyclogenesis, the BLF can be advected over the open ocean.

Aircraft-based observational studies of the Arctic boundary layer in the vicinity of the sea ice front have been carried out during the experiments MIZEX (Johannessen, 1987; Kellner et al., 1987; Fairall and Markson, 1987), CEAREX (Shaw et al., 1991), ACE (Shapiro and Fedor, 1989), ARKTIS'88 (Brümmer et al., 1992) and REFLEX (Hartmann et al., 1992; Kottmeier, 1994). While Brümmer et al. (1992) and Kellner et al. (1987) document the air mass transformation during off-ice flow, the structures of BLFs during flow conditions parallel to the sea ice front are investigated by Shaw et al. (1991) and

Shapiro and Fedor (1989). The latter find a low-level jet (LLJ) of up to 30 m/s in a BLF west of Spitzbergen. A case study of the energy budget of the boundary layer associated with a BLF is shown by Shaw et al. (1991), who use eddy correlation flux measurements. Their vertical profiles of temperature and humidity over ice and open water (Fig.2.5) reflect the strong heating over the open water in the lowest 600 m resulting in gradients of about 10 K and 1 g/kg over a distance of 200 km perpendicular to the sea ice edge. Shaw et al. show for the sensible heat budget that the contributions of the horizontal advection and the vertical divergence of the turbulent heat flux are the dominating terms. The dynamics associated with BLFs can be also relevant for the whole atmosphere/ocean system, since increased wind speeds in the vicinity of a BLF influence the mixing processes in the oceanic boundary layer as well as the drift of sea ice (Phee et al., 1987).

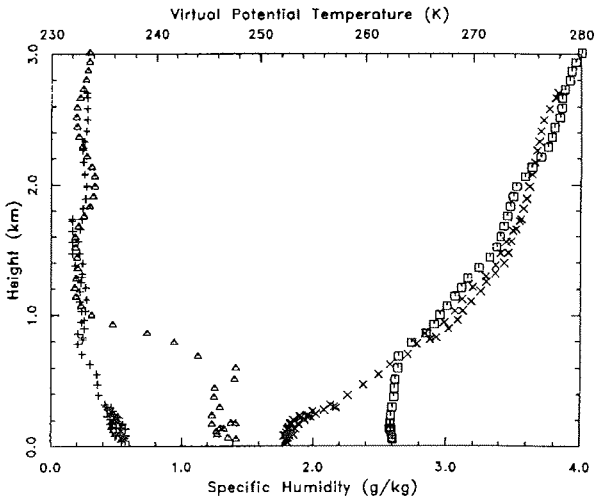

Fig. 2.5: Composite profiles of vitual potential temperature and specific humidity over the ice (crosses and pluses) and over water (squares and triangles) for the CEAREX BLF study (from Shaw et al., 1991).

The KABEG measurements for BLFs were performed in order to address the following questions:

(a) What is the 3D structure of BLFs and how can their developments quantitatively be described in terms of the budgets of momentum and energy and in terms of the analysis of the frontogenesis? To the author's knowledge, the study of Shaw et al. (1991) is the only case of a BLF budget study; thus it cannot be judged about its representativeness.

(b) Are the parameterizations of mesoscale numerical models realistic enough and do they correctly simulate the boundary layer structure of the BLFs? In this respect, the KABEG data set can be used for the validation on different scales, since the flight legs were sufficiently long to extent over several grid points of operational mesoscale models.

3. Experiment setup

3.1 Experimental area

The research aircraft POLAR2 owned by the Alfred-Wegener-Institut (AWI) was based at Kangerlussuaq (former Søndre Strømfjord, West Greenland, see Tab.3.1 for coordinates) at a distance of about 20 km from the glaciers of the inland ice sheet. Kangerlussuaq was selected for two reasons. Firstly, BLFs which were expected to develop over the Davis Strait, were in the range of the aircraft taking into account the position of the sea ice front for April/May. Secondly, this area was selected to investigate the development of the katabatic flow over relatively homogeneous topography under different synoptic conditions and the modification of the katabatic flow in the transition zone ice/tundra. The regions for the investigation of channeling effects of the katabatic wind were near Ilulissat (West Greenland) and southwest of Angmagssalik (East Greenland), where pronounced valley structures with steep topographic gradients are present (see Fig.3.1).

3.2 Surface stations

During the experiment, surface stations were installed at five positions (Tab.3.1). Near Kangerlussuaq a station with direct turbulent heat flux and momentum measurements, and a station measuring the surface layer profile, the soil temperature profile and net radiation was built up in order to determine surface energy balance components. These stations were built up in order to represent the tundra area. Along a line orientated parallel to the fall line at about 50 km north of Kangerlussuaq four stations were installed: A1 over the tundra close to the edge of the inland ice; A2 over the inland ice close to the ice edge (both being wind recorders); and two surface energy balance stations over the ice at distances of about 30 km (A3) and 70 km (A4) from the ice edge (see Tab.3.1). In the area of Kangerlussuaq the University of Utrecht (IMAU) is also operating two automatic weather stations on the ice sheet, but only one of them had recorded data during April and May 1997 (at 67.0764°N/49.3714°W, 1015 m). Additional data for the KABEG period is also available from AWS of the University of Colorado at the positions "Dye2" (66.490°N/46.300°W, 2100 m) and at "Swiss Camp" (69.572°N/49.305°W, 1200 m) at the Ilulissat glacier. Fig.3.1 shows a high-resolution digital topography with the positions of the above mentioned AWS.

3.3 Aircraft data

The GPS navigated aircraft was instrumented with the turbulence measuring device "METEOPOD", allowing high-resolution measurements and the determination of turbulent momentum, sensible and latent heat fluxes. In addition, downward and upward solar and terrestrial radiation and surface temperature were measured; a high-resolution laser altimeter registered surface roughness structures (see Tab.3.2 and Tab.3.3). The GPS dropsonde facility of the aircraft was used for the BLF program over ocean.

Table 3.1: Surface stations operated by MIUB during KABEG

Site	asl in m	measured quantity	height in m	Instrument
A1 67°24'50"N 49°59'24"W	600	wind vector	2	Mechanical windrecorder (Thies)
A2 67°27'09"N 49°36'04"W	760	wind vector	2	Mechanical windrecorder (Thies)
A3 67°29'02"N 48°59'58"W	1200	Air temperature+ humidity Wind speed Wind direction Pressure Snow temperature Net radiation	1.0, 2.2 1.0, 2.1 2.4 0 -0.4, -0.7 1.0	Electrically ventilated thermistor (Grant) + Humicap (Vaisala) Cup anemometer (Vector Instr.) Wind vane (Vector Instr.) Piezoresistive pressure sensor (Honeywell) Thermistor (Grant) Net pyrradiometer (Middleton)
A4 67°29'51"N 47°59'48"W	1600	Air temperature Wind speed Wind direction Pressure Snow temperature Net radiation	0.3, 0.8, 1.9 0.3, 0.8, 1.9 2.4 0 -0.2, -0.25, -0.3, -0.4, -0.7 1.4	Electrically ventilated PT100 Cup anemometer (Vector Instr.) Wind vane (Vector Instr.) Piezoresistive pressure sensor (Honeywell) PT100 Net pyrradiometer (Thies)
S 67°01'32"N 50°36'11"W (Kanger-lussuaq)	40	Air temperature+ 3D wind vector Air temperature+ humidity Wind speed Wind direction Pressure Soil temperature Net radiation	3.3 0.5, 0.8, 1.1, 1.7, 2.7 0.5, 0.8, 1.1, 1.7, 2.6 3.2 0 -0.02, -0.05, -0.1, -0.2, -0.5 1.4	3D sonic anemometer + thermometer (Metek) Electrically ventilated psychrometer (PT100) Cup anemometer (Vector Instr.) Wind vane (Thies) Piezoresistive pressure sensor (Honeywell) PT100 Net pyrradiometer (Thies)

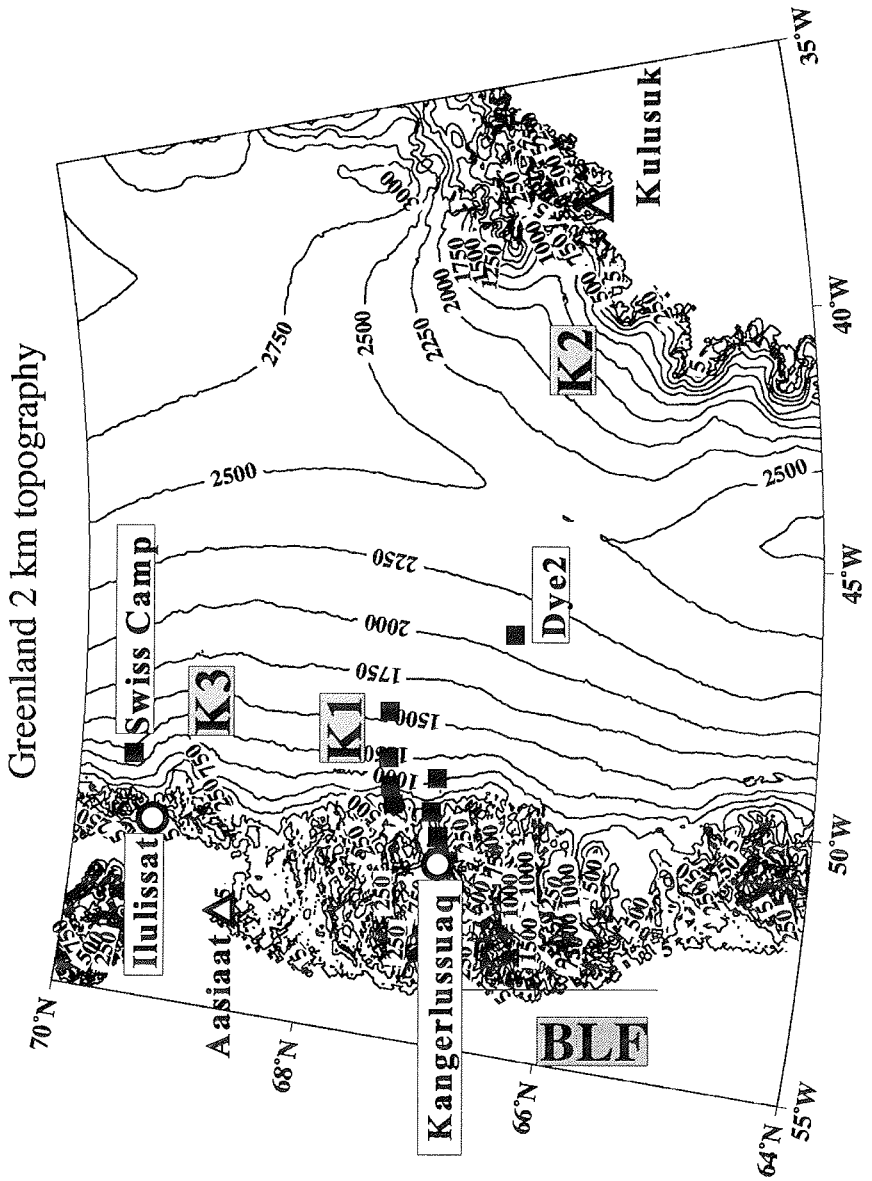

Fig.3.1: High-resolution (2 km) topography (data from Ekholm, 1996) for the KABEG area. Triangles mark the radiosonde stations Aasiaat (Egedisminde, West Greenland) and Angmassalik (East Greenland); the full squares mark the AWS from MIUB, IMAU and University of Colorado. The areas for the BLF and katabatic wind programs are indicated (see text).

Table 3.2: METEOPOD instrumentation and laser altimeter

Measured quantity	Sam-pling in Hz	Instrument
Air temperature	120	PT100 open wire (Rosemount)
Air temperature	120	PT100 open wire (AWI)
Air humidity	120	Lyman-α (AIR)
Air humidity	12	Humicap, PT100 in Rosemount housing (Aerodata)
Air humidity	12	Dew point mirror (Gen. Eastern)
Air pressure	12	Pressure sensor (Rosemount)
3D wind vector	120	5-hole-probe (Rosemount)
METEOPOD acceleration	60	Attitude and Heading Reference System LTR81 (Litton)
Height	120	Radar altimeter (TRT)
Height	500	Laser altimeter (Ibeo)

Table 3.3: Equipment of the research aircraft "Polar2" (basic instruments and dropsonde system).

Measured Quantity	Sam-pling in Hz	Instrument
Air temperature	12	PT100 (Rosemount)
Air humidity	12	Humicap, PT100 in Rosemount housing (Aerodata)
Air pressure	12	Pitot-static tube and absolute pressure sensor (Rosemount)
Wind vector	12	Calculated from navigation system and air pressure measurements
Aircraft accereration	60	LaserNav Inertial Platform Navigation (Honeywell)
Position	12	GPS (SEL)
Height	12	Radar altimeter
Surface temperature	12	KT4 (Heimann), 8-14 µm, 0.6° opening angle
Downward and upward radiation fluxes	12 12	Short-wave: pyranometer (Eppley PSP) Long-wave: pyrgeometer (Eppley PIR)
Profiles of temperature, humidity, wind speed and direction	2	MARWIN dropsonde system (Vaisala RS80), naturally ventilated thermistor, Humicap, wind from GPS

3.4 Satellite data

Visible and infrared imagery

The DMI was operating a High-Resolution Picture Transmission (HRPT) data receiving station at Kangerlussuaq, but for the KABEG period most of the data was lost because of a malfunction of the magneto-optical disk device. Fortunately, Global Area Coverage (GAC) data with a reduced resolution of 4 km (nadir) was acquired from the Satellite Active Archive (SAA) of NOAA/NESDIS and high-resolution HRPT data with a nadir resolution of 1.1 km were provided by the Canadian Weather Service for most of the flight missions. The availability of the latter data is summarized in Tab.3.4. Except for the flight mission on 18 April, HRPT data was archived by the Canadian Weather Service for each KABEG flight.

Tab.3.4: HRPT data available for the KABEG flights.

Satellite	Date	Time	Lines
noaa-14	97/04/15	15:55:52	4072
noaa-14	97/04/15	17:33:33	5415
noaa-14	97/04/15	19:16:05	4258
noaa-12	97/04/15	20:20:05	3930
noaa-12	97/04/15	21:57:06	5305
noaa-14	97/04/19	16:50:46	5075
noaa-14	97/04/19	18:30:41	5158
noaa-12	97/04/19	20:31:56	4221
noaa-12	97/04/19	22:09:32	5306
noaa-14	97/04/21	05:00:38	3453
noaa-14	97/04/21	06:39:44	5568
noaa-14	97/04/21	08:20:58	4624
noaa-12	97/04/21	10:02:39	4781
noaa-12	97/04/21	11:42:26	5241
noaa-12	97/04/21	13:23:53	2776
noaa-14	97/04/22	04:58:52	3040
noaa-14	97/04/22	06:28:47	5534
noaa-14	97/04/22	08:10:00	4842
noaa-12	97/04/22	09:41:21	4168
noaa-12	97/04/22	11:20:26	5340
noaa-12	97/04/22	13:01:12	3818
noaa-12	97/04/24	10:36:37	5314
noaa-12	97/04/24	12:16:53	4893
noaa-14	97/04/24	15:57:54	4103
noaa-14	97/04/24	17:37:05	4694
noaa-12	97/04/29	10:27:09	5253
noaa-12	97/04/29	12:07:23	5040
noaa-14	97/04/29	16:42:17	4917
noaa-14	97/05/02	06:19:57	5487
noaa-14	97/05/02	08:01:02	5078
noaa-12	97/05/02	09:22:53	3484
noaa-12	97/05/02	11:01:24	5398
noaa-12	97/05/02	12:41:54	4354
noaa-14	97/05/11	06:21:59	5503
noaa-14	97/05/11	08:03:07	5046
noaa-12	97/05/11	09:25:35	3631
noaa-12	97/05/11	11:04:16	5427
noaa-12	97/05/11	12:44:48	4282
noaa-14	97/05/11	16:12:17	4489
noaa-14	97/05/11	17:50:35	5474
noaa-14	97/05/11	19:34:05	3731
noaa-14	97/05/13	06:02:26	5286
noaa-14	97/05/13	07:40:59	5334
noaa-14	97/05/13	09:23:59	2323
noaa-12	97/05/13	10:20:32	5228
noaa-12	97/05/13	12:00:41	5111
noaa-14	97/05/14	05:49:26	5113
noaa-14	97/05/14	07:29:58	5411
noaa-14	97/05/14	09:12:21	2957
noaa-12	97/05/14	09:58:58	4768
noaa-12	97/05/14	11:38:39	5298
noaa-12	97/05/14	13:20:11	2921

Microwave data

Two kinds of microwave data can be used for the KABEG period. Firstly, scatterometer (ERS-SCAT) data of the Active Microwave Instrument on board the polar orbiting ERS-2

satellite is available. This type of data allows the determinination of near-surface wind vectors over ice-free ocean from the backscattered microwave radiation. The ERS-SCAT data is available as ERS off-line scatterometer wind products, which were generated at the Institut Français de Recherche pour l'Exploitation de la Mer (IFREMER) using the Centre ERS d'Archivage et de Traitement (CERSAT) algorithms. The spatial resolution is about 50 km with a pixel spacing of 25 km and a 500 km swath width. Due to the large gaps between the swaths of two subsequent orbits, the area of the Davis Strait is only covered once or twice per day.

Secondly, multi-frequency, dual polarisation data of the SSM/I sensor is available. This type of data allows the retrieval of several atmospheric parameters over the ice-free ocean with a resolution of 30-70 km, particularly the sea ice extent, near-surface wind speed, cloud liquid water and integrated water vapour. This data was obtained from the Global Hydrology Resource Center (GHRC) at the Global Hydrology and Climate Center (Huntsville, Alabama, USA). Using two satellites, a coverage of four times daily is typical polewards of 60° latitude. For KABEG SSM/I data of the following three satellites are available: DMSP F10 (1 April-31 May), DMSP F13 (31 March-31 May) and DMSP F14 (8 May-31 May). Thus, even three satellites can be used during May.

4. First results of the surface stations

In order to give an overview over the whole measurement period, Fig.4.1 shows selected data from station "S" near Kangerlussuaq (see Tab.3.1) being representative for the tundra area. Using the mean daily temperature (upper panel) and the surface pressure (lowest panel), the KABEG period can be devided into four main phases. The first days of the period (phase 1, until Julian day 107) were characterized by low temperatures (around -10°C) and high pressure. This phase was followed by almost one week of mean temperatures around 0°C, in which the first three katabatic wind flights were made (phase 2, Julian day 107-113). After 8 days with relatively cold mean temperatures and relatively low pressure (phase 3), a considerable warming occurred and the mean temperatures were around +5°C. While at the beginning of KABEG the tundra was snow covered and the soil was frozen, the snow melted during phase 2 and a transition to almost summertime conditions took place in phase 4, when maximum temperatures at 2 m were around +15°C. The net radiation reveals a pronounced daily cycle with typical maximum values of about 450 W/m^2. Only low wind speeds (less than 5 m/s) were recorded throughout the period, on a few days signals of a valley wind in the Kangerlussuaq fjord were observed.

Over the inland ice, quite different conditions were observed. Fig.4.2 shows the same data as Fig.4.1, but for the station A4 at the line about 50 km north of Kangerlussuaq at a distance of about 70 km from the ice edge. At this station (height about 1600 m) phase 3 is associated with mean temperatures of less than -25°C, while temperatures are about 10°C higher during phase 4. The net radiation also reveals a clear daily cycle, but is negative in the daily mean and maximum values are around +40 W/m^2 only. In contrast to the tundra station, a clear forcing of the net radiation on the daily course of the wind speed can be seen: for most of the days the maximum wind speed is present during the early morning hours. It should be noted that the UTC times are about 3 hours later than the local solar time at Kangerlussuaq. Thus the nighttime katabatic wind regime is well established nearly for all days. The wind increase caused by the katabatic wind is about 5 m/s and is associated with a marked change in wind direction towards a more downslope direction.

The daily cycle of the katabatic wind system near the surface can also be found in the data of other surface stations. As an example, the measurements at the AWS "Dye2" (Fig.4.3) show a similar amplitude in wind speed and also the daily course of the wind direction. "Dye2" lies in an area with a topography gradient comparable to that at A4, but farer inland (see Fig.3.1). The above mentioned coupling between nighttime cooling and katabatic wind can be seen quite well in a close-up for a few days with weak synoptic forcing (Fig.4.4). The data of the shortwave radiation (Kdown) show undisturbed (cloud-free) conditions between Julian day 116 and 122 (the daily course of the net radiation seems to be not reliable; probably this sensor is disturbed by the mast of the AWS or ice on the sensor). The minimum of the wind speed is measured shortly after local noon, during the cooling phase the wind turns from 180-210 deg to 150 deg and highest wind speeds are observed during the early morning hours. This daily cycle of the katabatic wind system is also present in the data of other AWS on the ice (not shown).

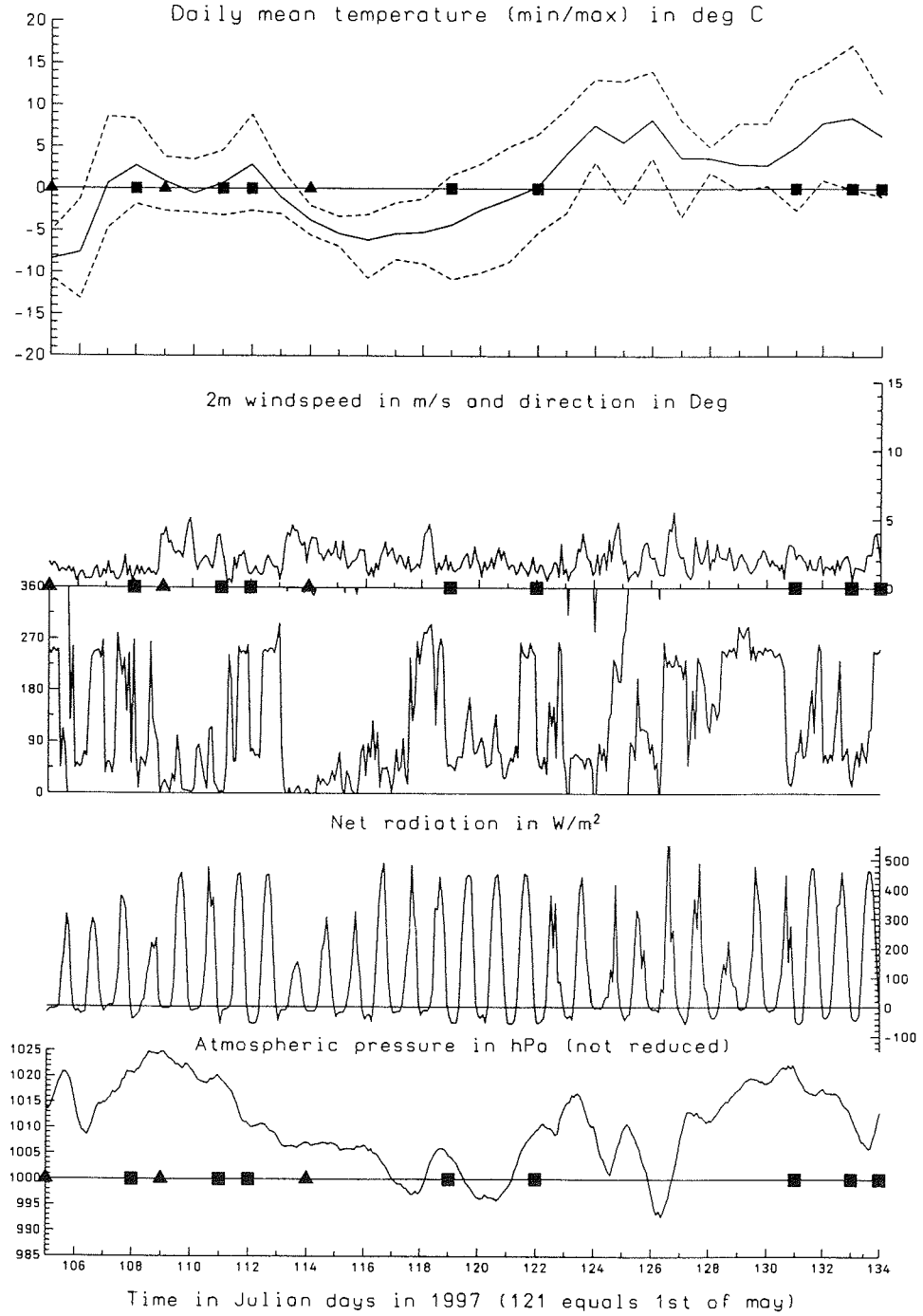

Fig.4.1: Overview over the KABEG period at AWS S in the fjord near Kangerlussuaq: mean daily temperature and daily minimum and maximum; wind speed at 2.6 m; wind direction at 3.3 m; net radiation and pressure. The triangles and squares indicate days with BLF and katabatic wind flights flights, respectively.

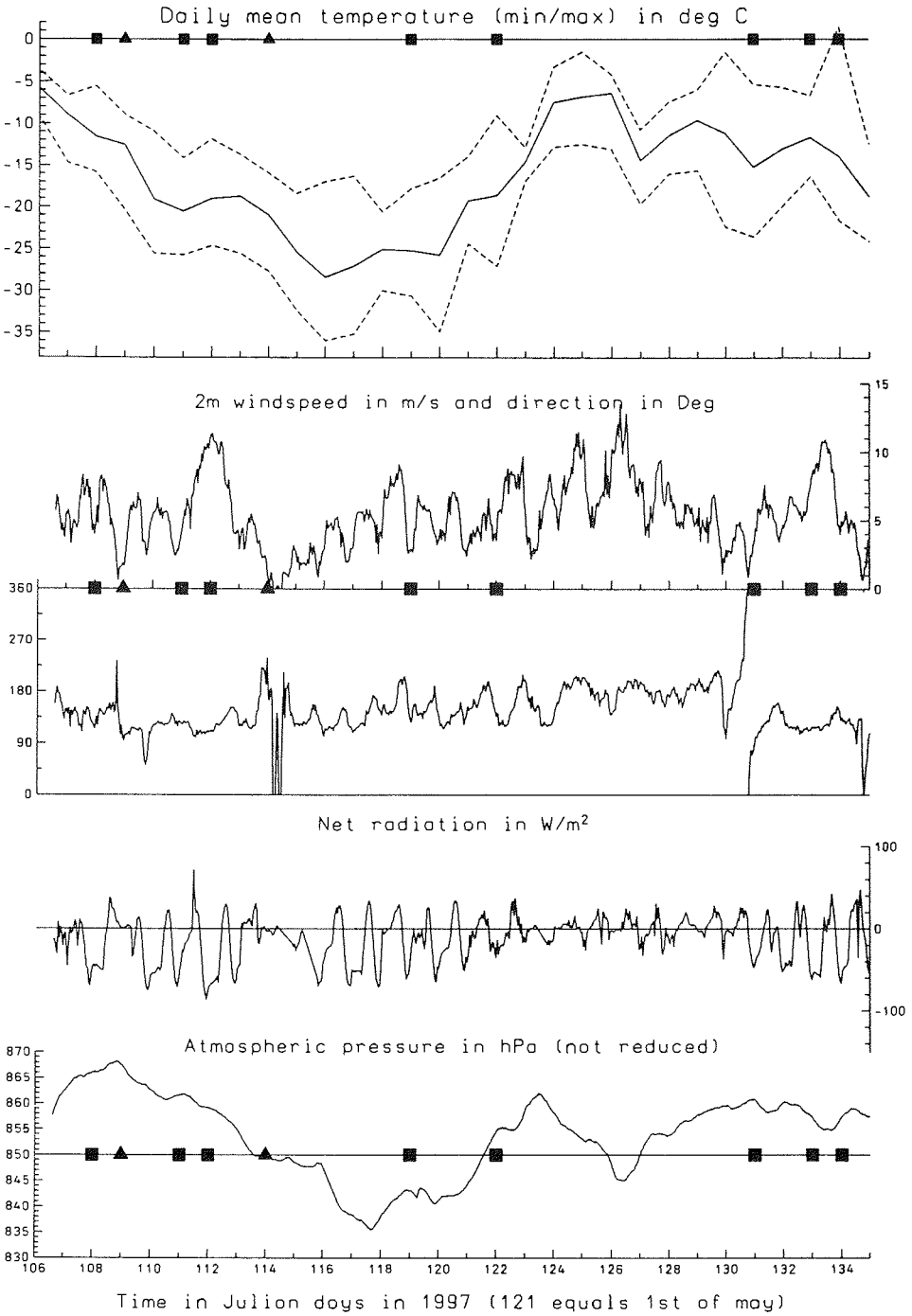

Fig.4.2: As Fig.4.1, but for the AWS A4 on the inland ice at a height of 1600 m (note the change in scale for the net radiation.

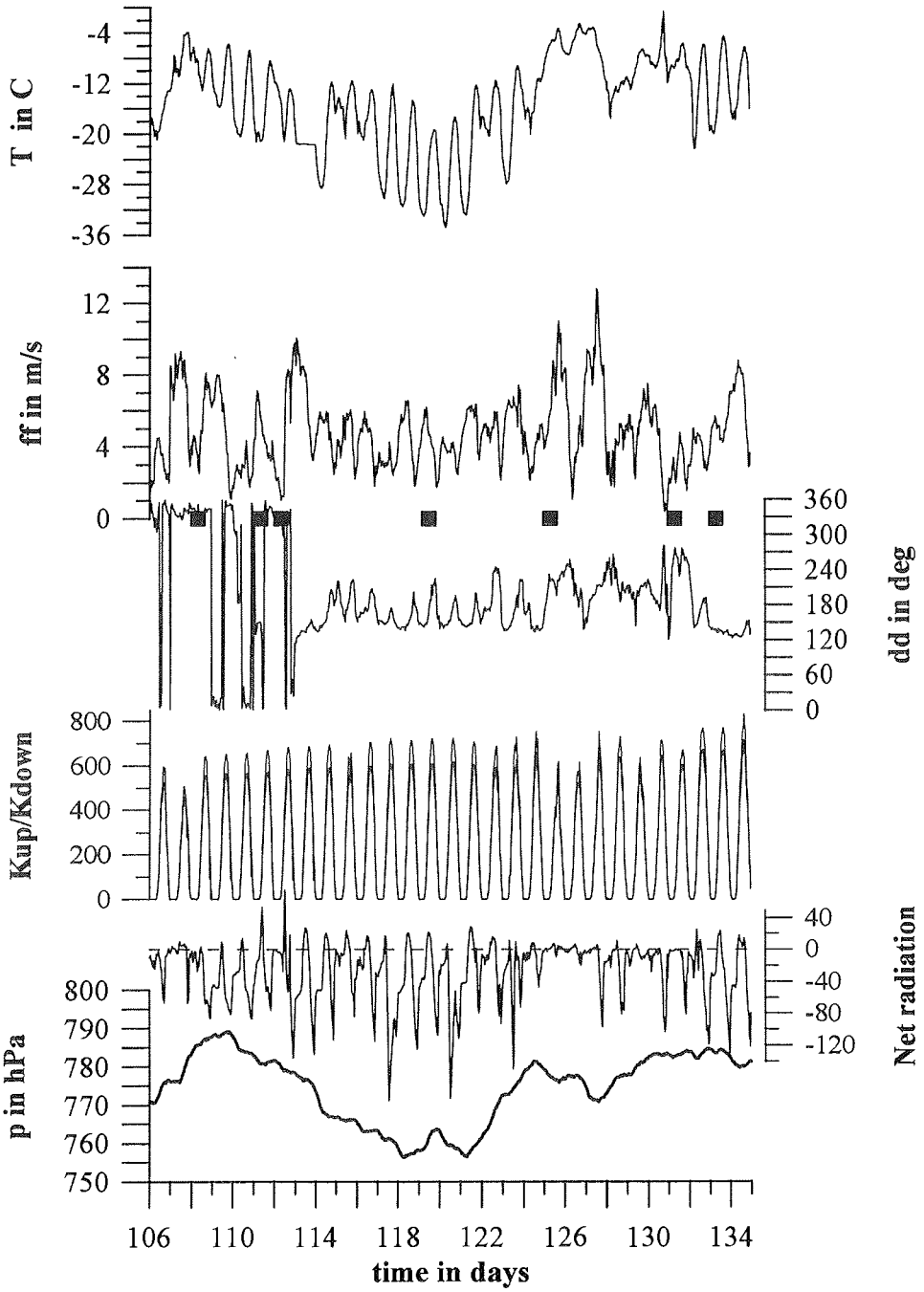

Fig.4.3: Overview over the KABEG period at AWS "Dye2" on the inland ice: temperature at about 3 m; wind speed at about 3 m; wind direction at about 3 m; shortwave downward and upward radiation; net radiation and pressure. The squares indicate days with katabatic wind flights.

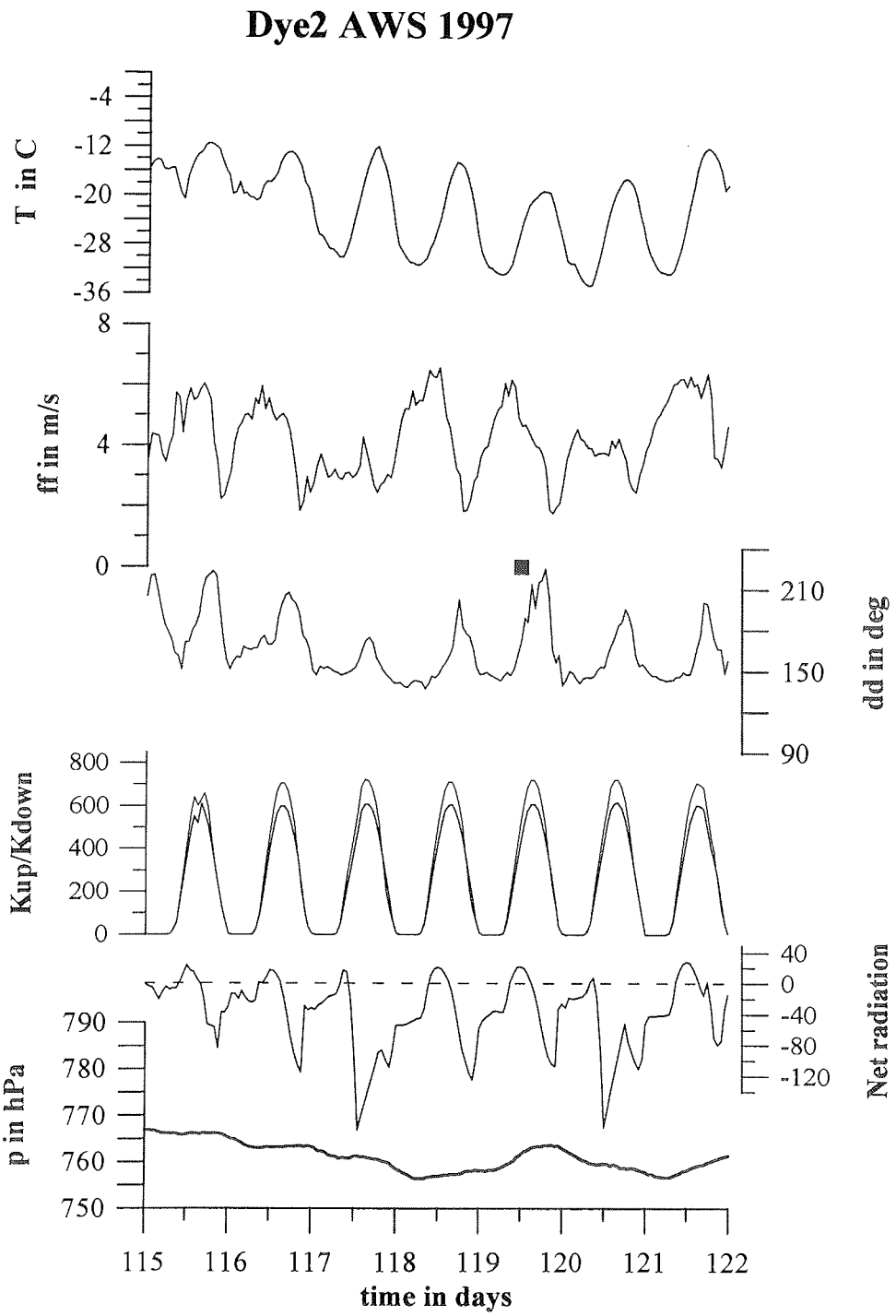

Fig.4.4: As Fig.4.3, but for the period between Julian day 115-122 (25 April-2 May 1997).

5. Overview over the flight missions

5.1 Flight strategy

Katabatic wind flights over homogeneous terrain

This part of the katabatic wind program (K1) was flown in the area of Kangerlussuaq, taking the KABEG surface station line north of Kangerlussuaq as a ground reference (marked P in Fig.5.1). A1-A4 and S are the AWS described in Tab.3.1, U1 and U2 are the two stations operated by IMAU. The flight strategy for a cross-section along line P was to fly aircraft temps and constant level legs at different heights above the surface. The data of this pattern should allow to produce a 2D cross-section of mean quantities along to the slope and in the transition zone to the tundra, to resolve small-scale horizontal structures and to obtain turbulent fluxes at different heights. In the presence of a low-level jet, the plan was to have one flight level beneath the wind maximum, one in the maximum itself and one above. Information about the 3D structure and advection terms should be derived from the cross legs Q1 and Q2 in form of aircraft temps and a low-level flight leg. As an alternative flight pattern, a box was flown including the legs Q1 and Q2. During the first flights it turned out that the low-level leg at Q2 was too difficult to fly; therefore, only aircraft temps were flown during the later flight missions. In order to obtain the development in time, cross-section P was flown two times.

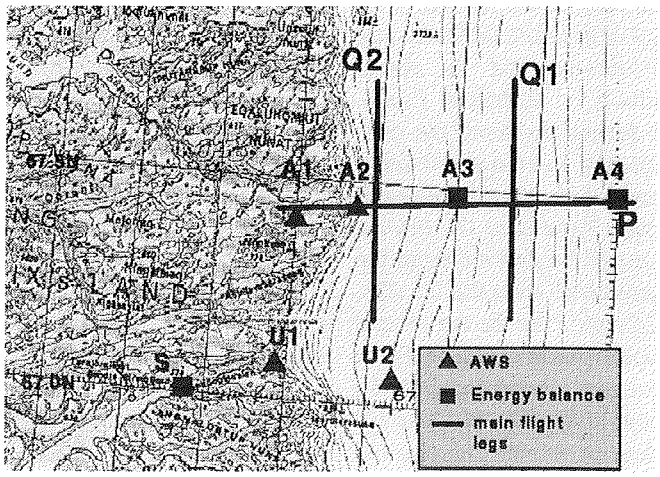

Fig.5.1: Basic flight pattern for the katabatic wind flights near Kangerlussuaq (see text).

Katabatic wind flights in confluence zones

This part of the katabatic wind program was flown in two different areas. One area for the investigation of channeling effects of the katabatic wind was in a valley west of Angmagssalik (East Greenland, K2, see Fig.5.2). Kulusuk (marked KUL in Fig.5.2) is the nearest airport and it was initially planned to use it as an temporarily base for a few days for this part of the program. But, during the KABEG period, this airport turned out to have such bad conditions for most of the time (fog or bad weather) that it would not be suitable as a base for the aircraft missions. As a consequence, the program K2 was only flown once starting at Kangerlussuaq. Several pronounced valley structures with steep topographic gradients are present west and southwest of KUL. Taking into account the limited range of POLAR2, the valley closest to KUL was selected for K2.

The flight strategy for K2 was to fly aircraft temps and a constant level leg along the line Pa-Pe (Fig.5.2). The data of this pattern should allow to produce a 2D cross-section of mean quantities along to the slope and in the transition zone to the sea ice, to resolve small-scale horizontal structures and to obtain low-level turbulent fluxes. Information about the confluence and the possible extent of the channeled katabatic flow over the sea ice should be derived from the cross legs over the ice (Q1, Q2) and over the sea ice and open water (Q3, Q4) in form of aircraft temps and a low-level leg. No surface data as ground reference is available for this area.

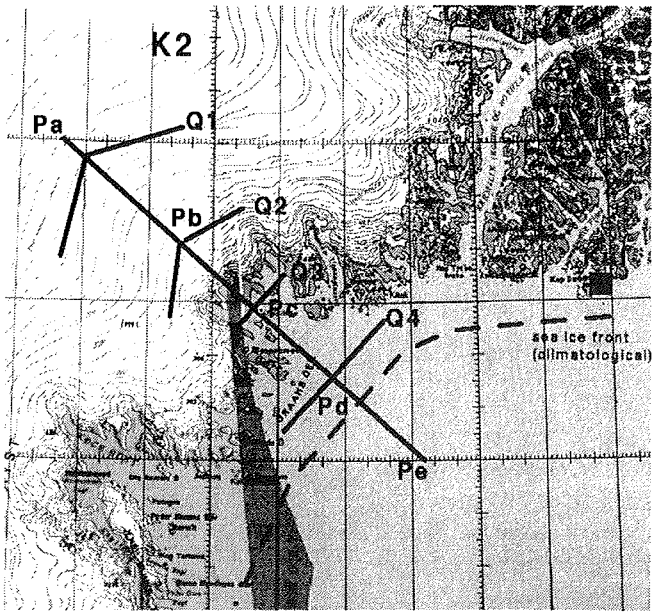

Fig.5.2: Flight pattern for the katabatic wind flight in the confluence zone near Angmassalik (see Text).

The program K3 was flown near Ilulissat (West Greenland) over the area of the Ilulissat glacier, which is the fastest flowing glacier of the world and is also associated with a pronounced valley structure and steep topographic gradients. In this area, the AWS "Swiss Camp" could be used as a ground reference for the aircraft data. The flight strategy for K3 was similar to K2, but only cross profiles over the ice were planned.

BLF flights

The strategy for the BLF flights was to fly an U-form pattern at during cold air outbreaks over the Davis Strait under conditions of low-level flow parallel to the sea ice edge (Fig.5.3). With the information from AVHRR satellite images and sea ice maps produced by DMI, the first flight leg was used to find the actual position of the sea ice edge and to define the position of the flight pattern. The U-form pattern consisted of a 80 km long profile perpendicular to

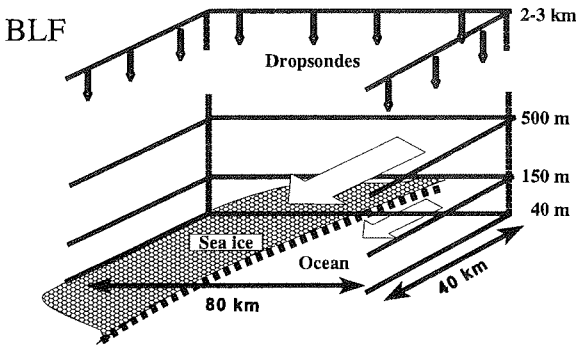

Fig. 5.3: Schematic flight pattern for the BLF missions over the Davis Strait.

the sea ice edge and two 40 km legs over the sea ice and the open water, repectively. While the GPS dropsondes should yield a 2D cross-section of mean quantities, constant level legs at different heights above the surface should allow to resolve small-scale horizontal structures and to measure turbulent fluxes at different heights. In order to get the development in time, one level in the middle of the boundary layer was flown two times (or alternatively a second cross-section by aircraft temps). Taking the advection terms from the data of the 40 km legs this data should allow a complete budget study of the BLF.

5.2 Summary of the flight missions

A total of 13 flights (duration of each flight 5 to 6 h) have been performed, three of them were BLF flights. The BLF flights took place during cold air outbreaks over the Davies Strait under conditions of low-level flow parallel to the sea ice edge wind speeds of up to 20 m/s. A summary of the BLF flights is given in Tab.5.1. The synoptic environment was different for each BLF flight, and only during April temperatures were low enough for the formation of a BLF due to differential heating of the sea ice and ocean.

The katabatic wind flights for K1 were flown under different synoptic situations and surface conditions (Tab.5.2). As discussed in Section 4, the surface conditions over the tundra area were typical of wintertime conditions during the first part of the KABEG period and changed to conditions typical to summertime conditions in May. With the exception of the flights in the dissipating katabatic wind system, a well-developed low-level jet was found in all flight missions at different heights and intensities. The strength of the surface inversion over the ice showed also a large range for the different flights.

Tab.5.1: Aircraft flights for the BLF program ($\partial T/\partial x$ is the horizontal temperature gradient)

Date	**flight program**	**characteristics**			
time in UTC (duration in h)		**general**	**inversion**		**upper air flow in m/s (direction)**
			height in m	**strength in K**	
15.4.97 16.00-21.40 (5h40)	BLF, at 66°N, dropsondes and aircraft temps	flow parallel to the sea ice edge, 20 m/s (N), $\partial T/\partial x$=2.5K/20km	500	5	6 (NO)
19.4.97 15.35-21.00 (5h25)	BLF, at 67°N, aircraft temps	flow parallel to the sea ice edge, 20 m/s (N), $\partial T/\partial x$=1K/20km	400	9	16 (NNO)
24.4.97 11.30-16.30 (5h00)	BLF, at 66°N, aircraft temps	flow parallel to the sea ice edge, 16 m/s (N), $\partial T/\partial x$=1K/20km, cloud streets	700	5	20 (N)

Tab. 5.2: Aircraft flights for the katabatic wind programs K1-K3 (ΔTs are the temperature differences between the temperature at the top of the surface inversion and at the lowest flight height (MFH) and the radiometrically measured surface temperature, respectively).

Date time in UTC (duration in h)	**flight program**	**characteristics**					
		general	**inversion**		**LLJ**		**upper air flow in m/s (direction)**
			height in m	**strength in K ΔT(MFH) /ΔT(0)**	**height in m**	**max. in m/s**	
18.4.97 7.00-11.45 (4h45)	K1 P, Q1	advection of clouds over the tundra	150	6 / 9	80	16	2-3 (S)
21.4.97 6.30-11.50 (5h20)	K1 P, Q1, Q2	clouds over the tundra, snow drift	70	3 / 8	60	17	6 (ESE)
22.4.97 7.05-12.10 (5h05)	K1 P, aircraft temps in box Q1/Q2	cloud-free, snow drift	150	10 / 12	100	22	13 (S)
29.4.97 10.20-15.40 (5h20)	K1 P, Q1	decaying during the flight	100	5 / 7	80	12	0-5 (S)
2.5.97 6.05-11.50 (5h45)	K1 P, aircraft temps in box Q1/Q2	snow drift	180	10 / 15	60	18	5 (SE)
11.5.97 6.35-11.30 (4h55)	K2 ("Kulusuk") KP, KQ	flow channeling, dissipation over the ice slope	100	10 / 14	60	22	12 (N)
11.5.97 13.00-17.40 (4h40)	K2 ("Kulusuk") KP, KQ	decaying	200	6 / 6	100	15	6 (N)
13.5.97 6.00-12.05 (6h05)	K1 P, aircraft temps in box Q1/Q2	snow drift, severe turbulence at the ice edge	200	16 / 20	90	24	10 (SE)
14.5.97 6.00-11.35 (5h35)	K3 ("Ilulissat") IP, IQ1, IQ2	flow channeling, snow drift, dissipation over the ice slope	200	9 / 13	70	15	3 (E)

5.3 A brief description of the katabatic wind flight missions

In the following, the synoptic situation is described using forecasts of the DMI operational model HIRLAM and satellite imagery. AVHRR channel 4 (infrared) data are shown as an overview over a larger area (GAC data) as well as for the subarea of the aircraft flights (HRPT data, except for 18 April). For each flight, a table with the flight legs, a schematic plot of the flight pattern, a table with the geographic coordinates of the way points and 2D and 3D plots of the flight path superimposed on a high-resolution topography is shown.

The synoptic situation is described by HIRLAM forecasts of mean sea level pressure (MSLP, isolines every 5 hPa) and 10 m wind vectors (full barb: 5 m/s; half barb: 2.5 m/s), which were operationally received at the DMI office at Kangerlussuaq. The initial times of the forecasts are 00 and 12 UTC. The maps are taken for the time being closest to the mean time of the flights. The flight pattern was flown in different ways. "Profile" means a flight leg at a constant height, either in terms of barometric height (BH) or in terms of radar height relative to the surface (SH)."Temp" means aircraft temps (ascents or descents). The flight path is shown superimposed on a high-resolution topography (Ekholm, 1996) as a 2D plot (upper panel, isolines every 100 m, areas lower than 800 m shaded) as well as a 3D plot. The advantage of the latter plot is that it demonstrates the spatial data distribution of the aircraft temps and legs flown at different heights. For the K1 plots the triangles mark the positions of the surface stations A1-A4 and S.

5.3.1 KA1 18 April 1997

The synoptic situation was characterized by high pressure systems over southeastern Greenland and over Baffin Island. The satellite image shows these areas as being almost cloud-free. Most of the ice sheet of southwest Greenland was cloud-free, but north of Kangerlussuaq and over southeast Greenland significant cloudiness can be found. Over the area of K1 only weak pressure gradients were present. Forecasted 10 m winds were around 3 m/s in the K1 area. The katabatic wind system was disturbed by stratus clouds (St), which were advected from the tundra over the ice. The St can be seen in the satellite image as a warm signature, because cloud top temperatures are higher compared to the surface as a result of the inversion. No snow drift was observed during the flight.

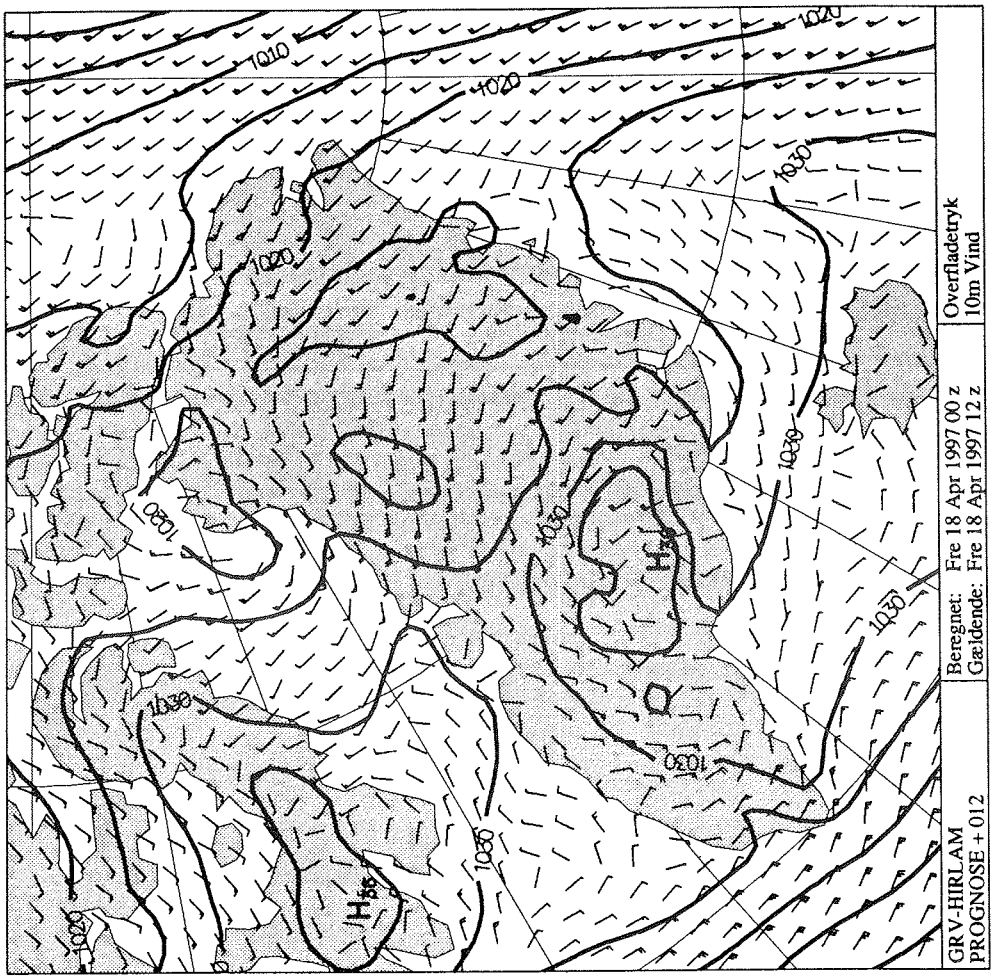

Fig.5.4a: HIRLAM forecasts of mean sea level pressure (MSLP, isolines every 5 hPa) and 10 m wind vectors (full barb: 5 m/s; half barb: 2.5 m/s), valid for 12 UTC 18 April 1997.

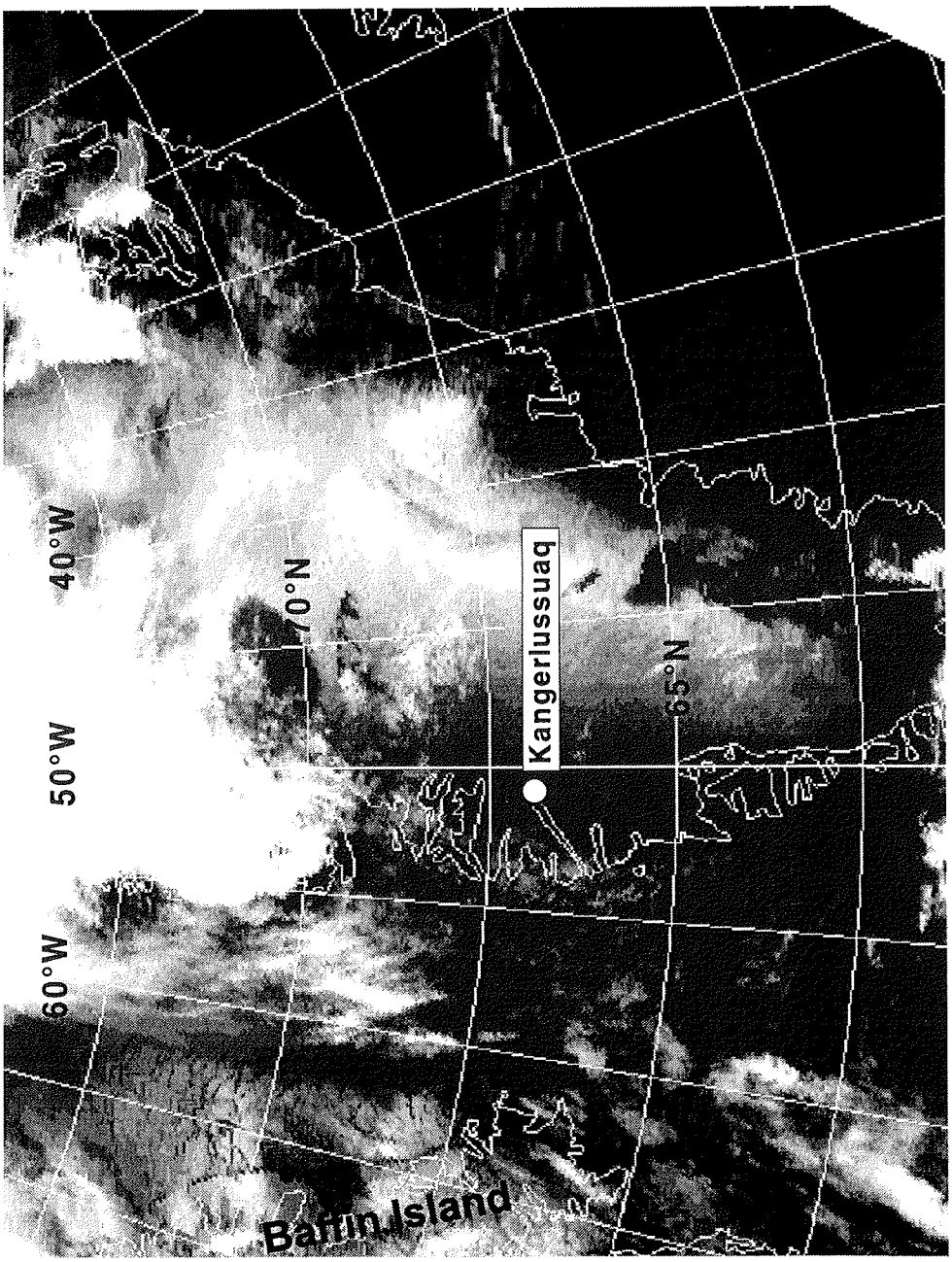

Fig.5.4b: GAC infrared image for 07 UTC 18 April 1997 (reduced resolution).

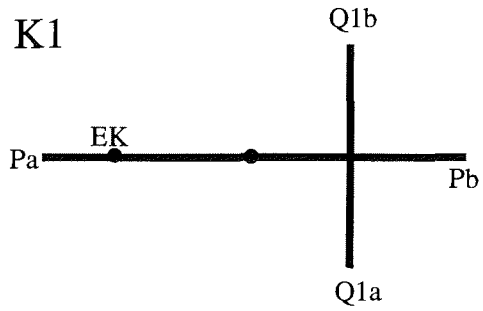

Way point coordinates		
Long.	Lat.	
-50.708	67.013	Kan
-50.090	67.420	Pa
-47.800	67.485	Pb
-48.500	67.200	Q1a
-48.500	67.730	Q1b
-49.500	67.170	Q2a
-49.500	67.710	Q2b
-49.700	67.435	EK

Fig.5.5a: Schematic plot of the flight pattern and a table with the geographic coordinates of the way points for KA1 on 18 April 1997.

The measurement flight startet with a P cross-section with temps, then four profiles along P were flown (one well above the LLJ, three in the vicinity of the LLJ). One Q1 cross-section (temps and low-level profile) was flown, and again a second P cross-section with two profiles Pa-Pb and temps between Pb and EK. At that time stratus clouds (St) were advected from the tundra over the ice and the flight program was stopped.

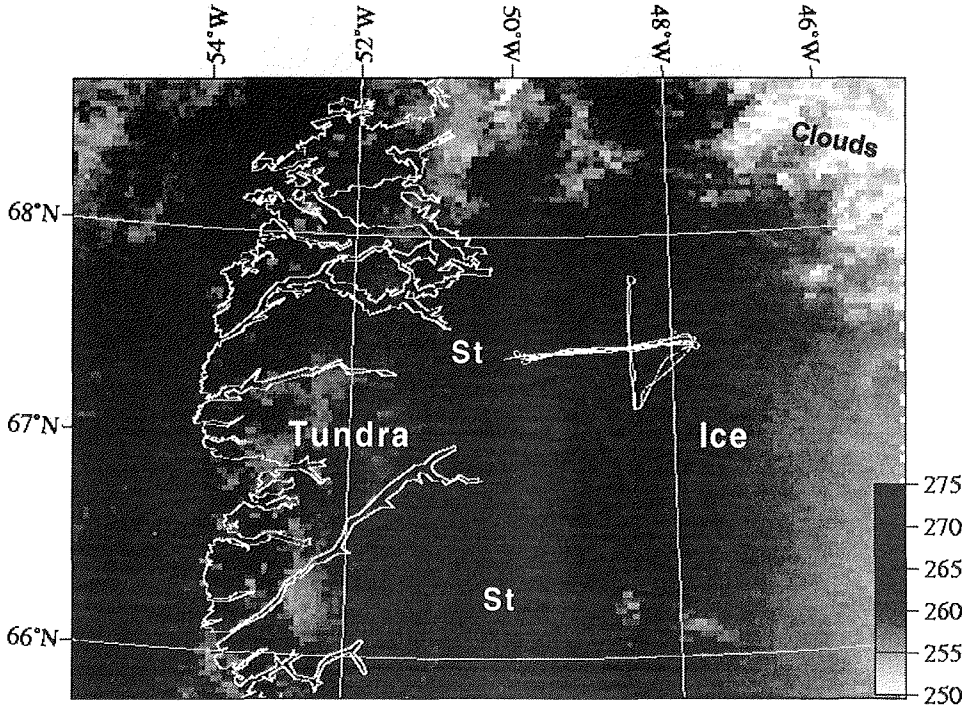

Fig.5.5b: GAC infrared image for 18 April 1997, 07 UTC with the flight path superimposed.

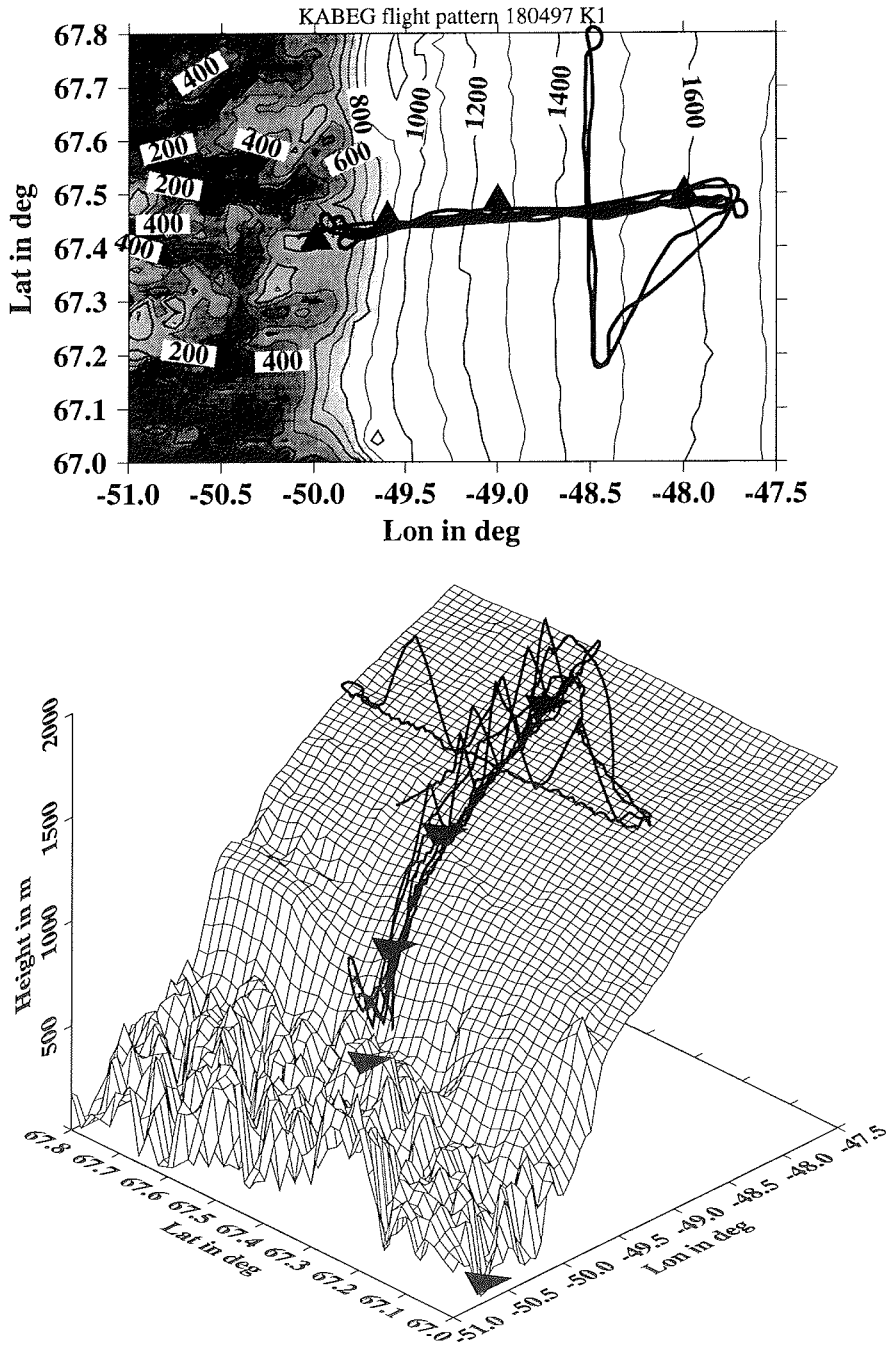

Fig.5.5 (continued): Flight path superimposed on a high-resolution topography as a 2D plot (upper panel, isolines every 100 m, areas lower than 800 m shaded) as well as a 3D plot. The triangles mark the positions of KABEG surface stations.

5.3.2 KA2 21 April 1997

An intense high pressure system lay over central Greenland and strong pressure gradients were present over the area of north of K1. Over the area of K1 forecasted 10 m winds were around 5 m/s. Greenland was almost cloud-free at both coasts. The satellite image near the beginning of the flight (Fig.7.7b) shows an area of low clouds or surface fog southeast of the flight pattern. Intense winds and snow drift were observed during the flight.

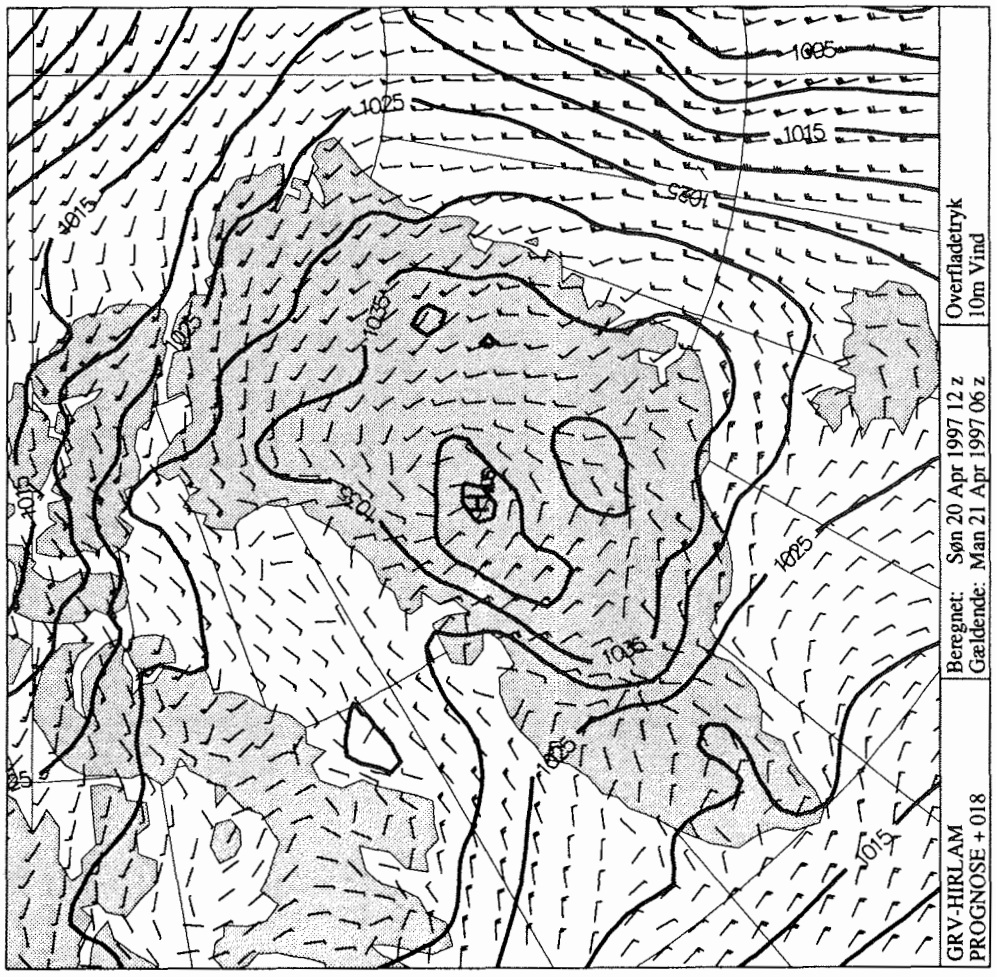

Fig.5.6a: As Fig.5.4a, but valid for 06 UTC 21 April 1997.

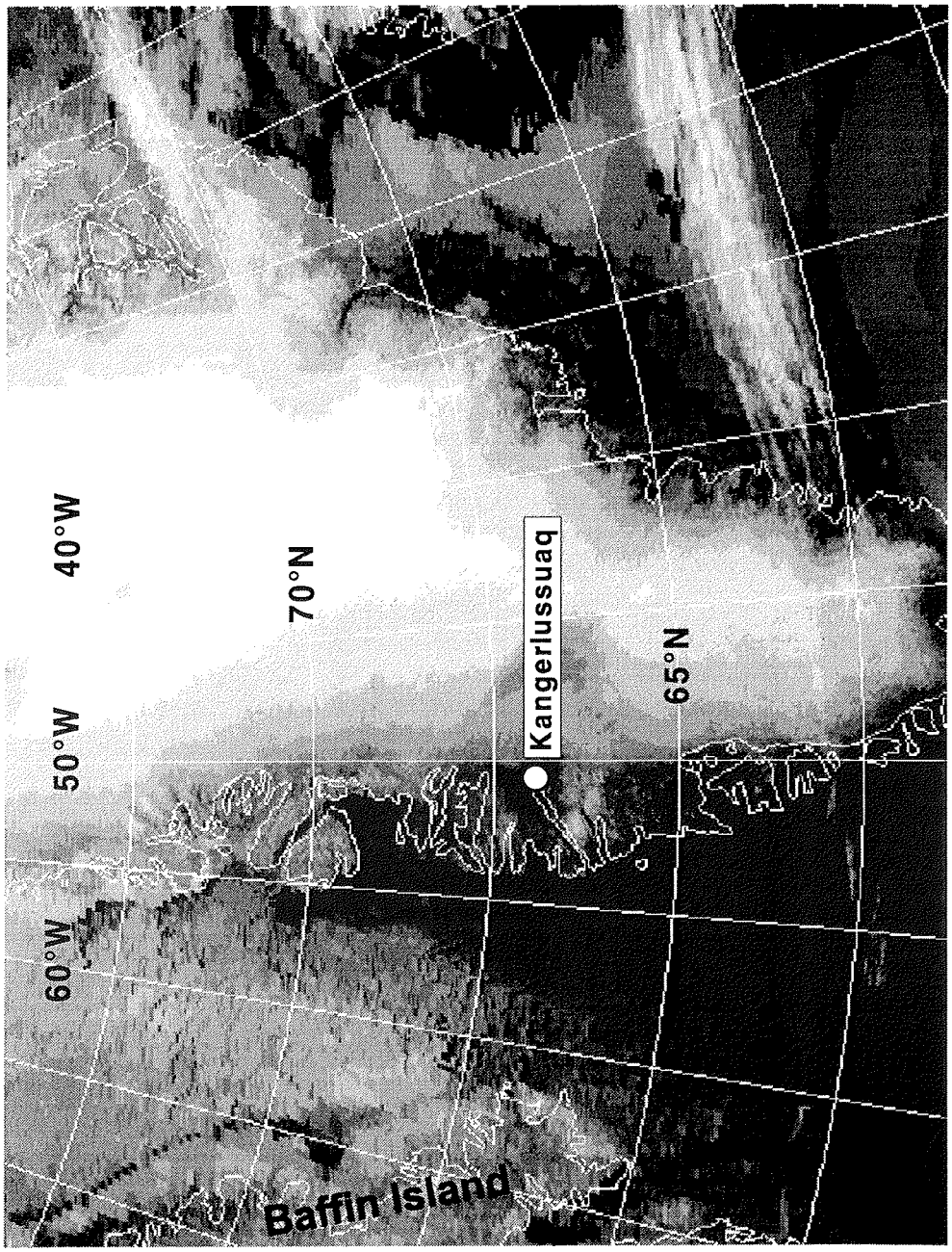

Fig.5.6b: GAC infrared image for 06 UTC 21 April 1997 (reduced resolution).

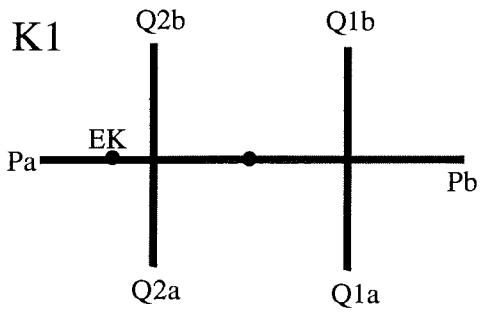

Way point coordinates		
Long.	Lat.	
-50.708	67.013	Kan
-50.090	67.420	Pa
-47.800	67.485	Pb
-48.500	67.200	Q1a
-48.500	67.730	Q1b
-49.500	67.170	Q2a
-49.500	67.710	Q2b
-49.700	67.435	EK

Fig.5.7a: Schematic plot of the flight pattern and a table with the geographic coordinates of the way points for KA2 on 21 April 1997.

During the first part of the flight the tundra was covered by a low St, but no clouds were observed over the ice. First, temps were performed along P, then four profiles were flown between Pb and EK in order to measure the ABL structure in, below and above the LLJ. One Q1 cross-section (temps and low-level profile) was flown, and again a second P cross-section with two profiles and temps between Pb and EK. The flight ended with a Q2 cross-section (temps and low-level profile).

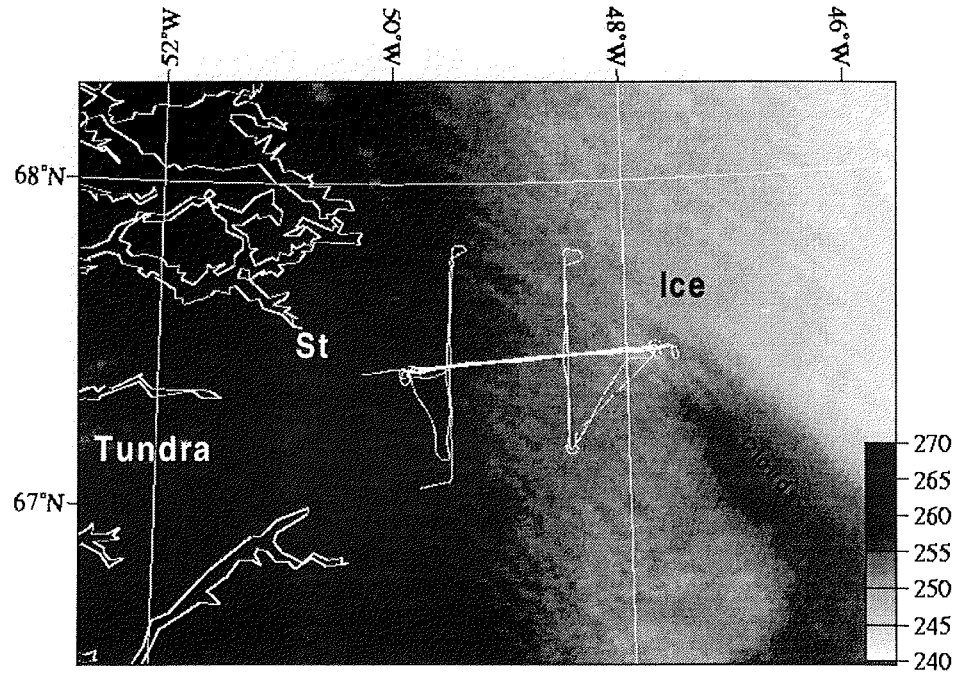

Fig.5.7b: HRPT infrared image for 21 April 1997, 06 UTC with the flight path superimposed.

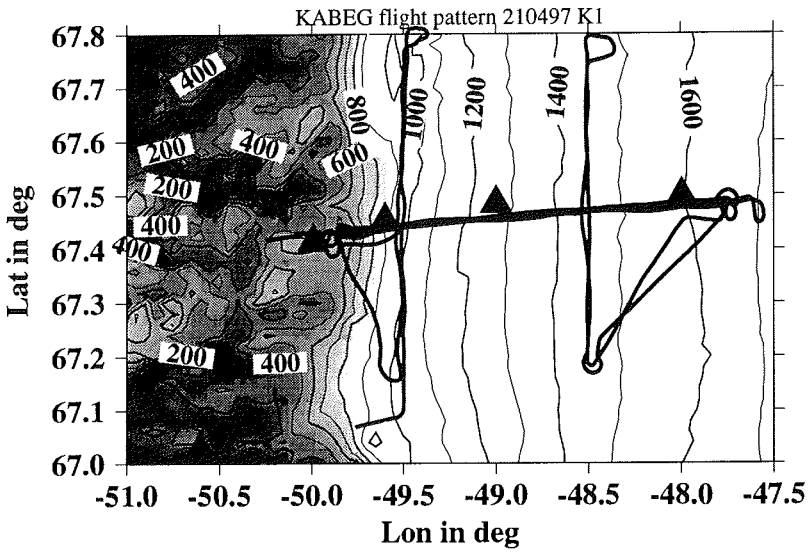

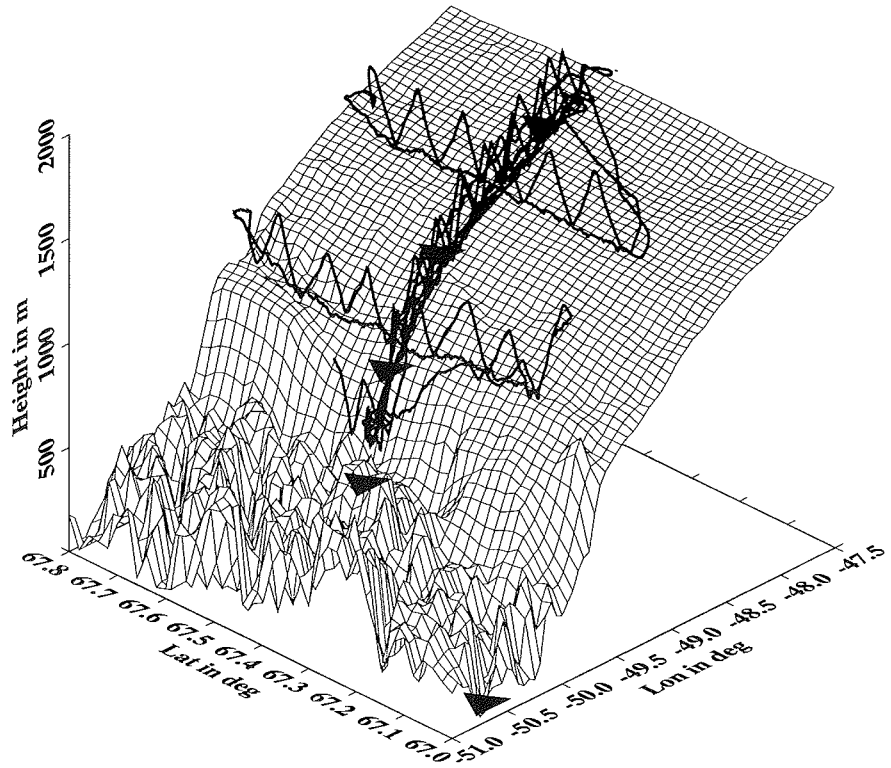

Fig.5.7 (continued): As Fig.5.5, but for the flight path KA2.

5.3.3 KA3 22 April 1997

As the day before, an intense high pressure system lay over central Greenland and strong pressure gradients were now present also over the area of of K1. Forecasted 10 m winds were around 5-10 m/s. No clouds were present, neither over the tundra nor over the ice. Intense winds and snow drift were observed during the flight.

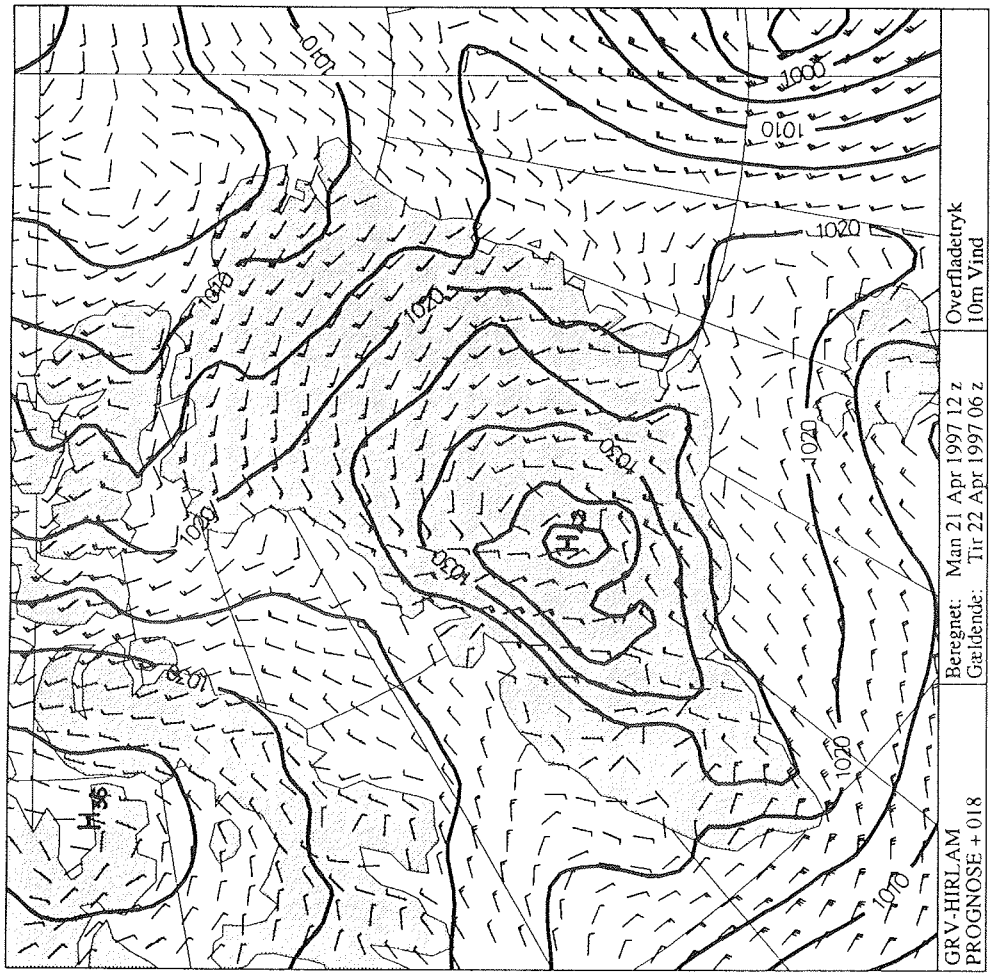

Fig.5.8a: As Fig.5.4a, but valid for 06 UTC 22 April 1997.

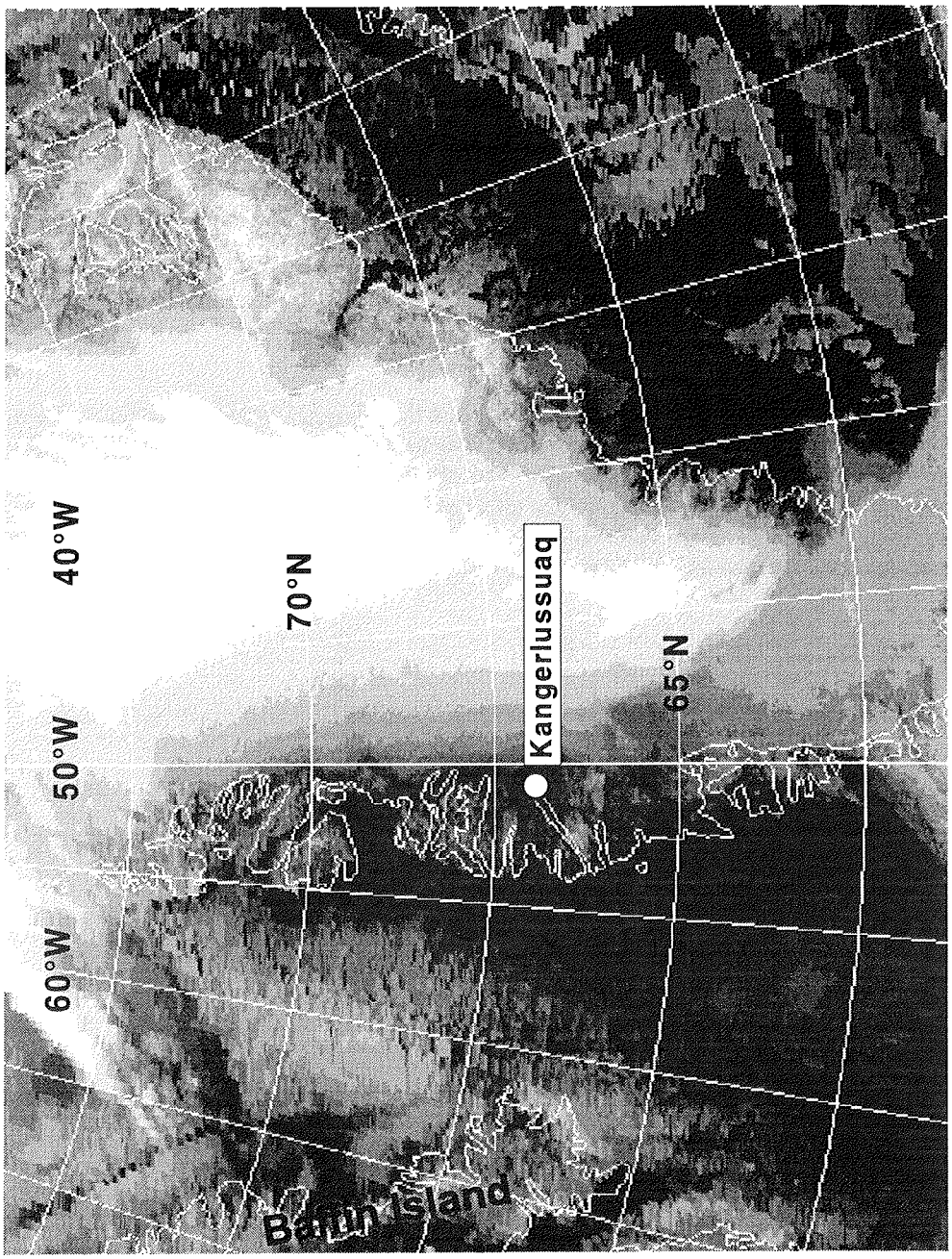

Fig.5.8b: GAC infrared image for 06 UTC 22 April 1997 (reduced resolution).

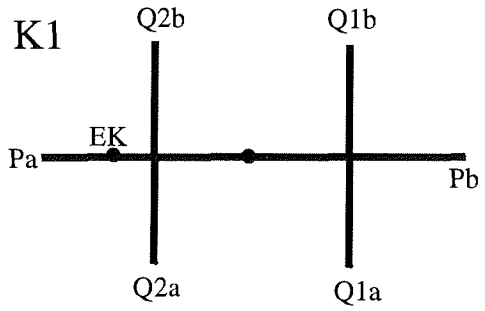

Way point coordinates	
Long.	Lat.
-50.708	67.013 Kan
-50.090	67.420 Pa
-47.800	67.485 Pb
-48.500	67.200 Q1a
-48.500	67.730 Q1b
-49.500	67.170 Q2a
-49.500	67.710 Q2b
-49.700	67.435 EK

Fig.5.9a: Schematic plot of the flight pattern and a table with the geographic coordinates of the way points for KA3 on 22 April 1997.

Two P cross-sections and aircraft temps in a box including Q1 and Q2 were flown. First, temps were performed along P, then four profiles were flown between Pb and EK in order to measure the ABL structure in, below and above the LLJ. Cross-sections with temps were flown along Q1a-Q1b-Q2b-Q2a-Q1a, and a second P cross-section with temps between Pb and Pa. Then two profiles were performed at constant SH over the ice and constant BH over the tundra in order to investigate the transition zone at the ice edge.

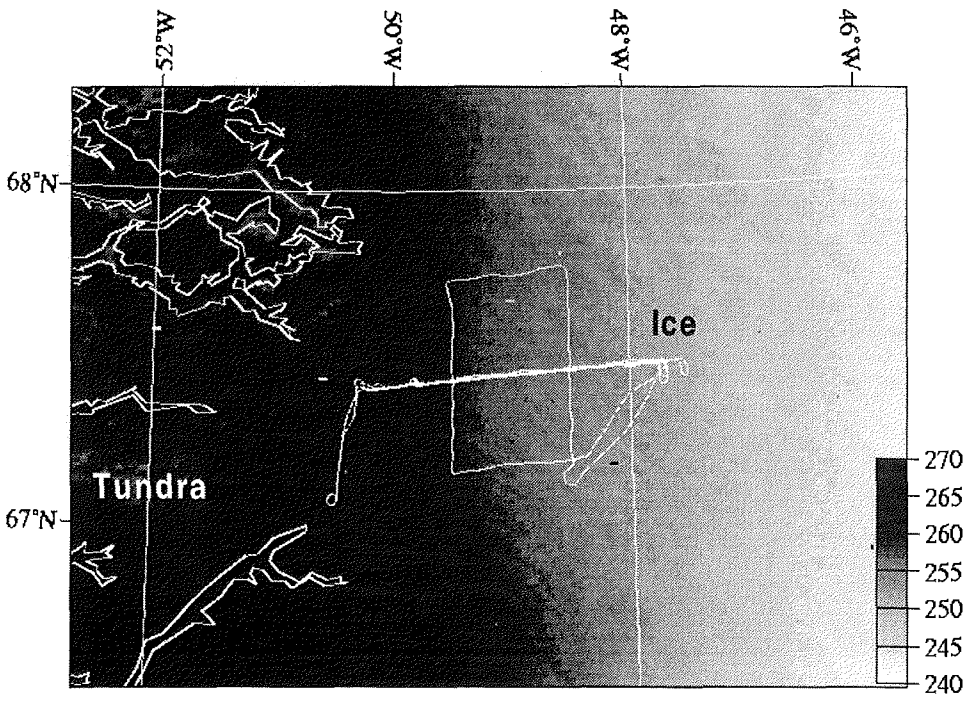

Fig.5.9b: HRPT infrared image for 22 April 1997, 06 UTC with the flight path superimposed.

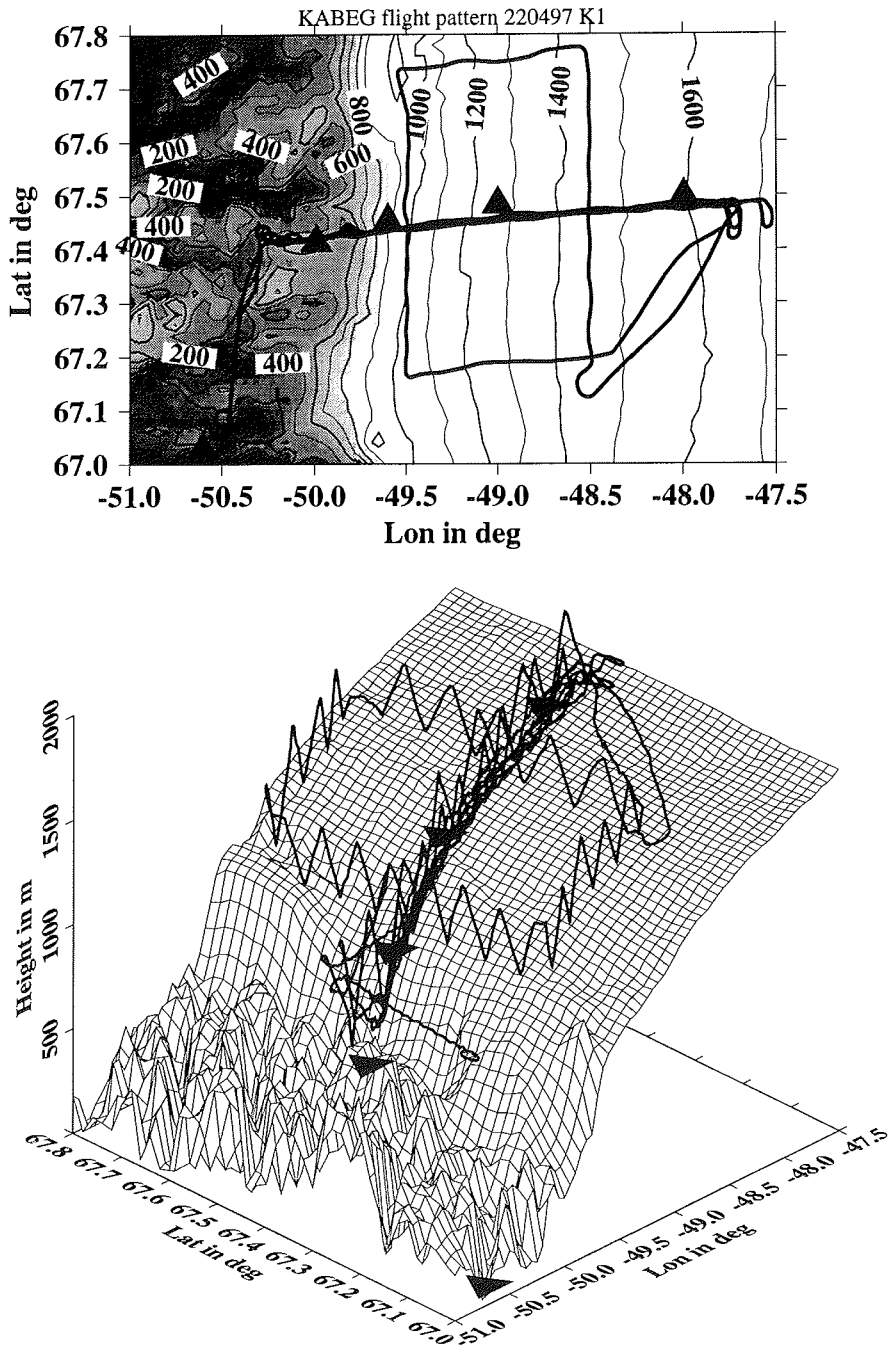

Fig.5.9 (continued): As Fig.5.5, but for the flight path KA3.

5.3.4 KA4 29 April 1997

While a synoptic cyclone lay at the coast of East Greenland, a weak high pressure system lay over West Greenland. Only weak pressure gradients were present over the area of of K1. Forecasted 10 m winds were 0-2.5 m/s. The flight was started at a relatively late time (see Tab.5.2) and captures the decaying katabatic wind system. A few Sc over the tundra and high As over the ice were present.

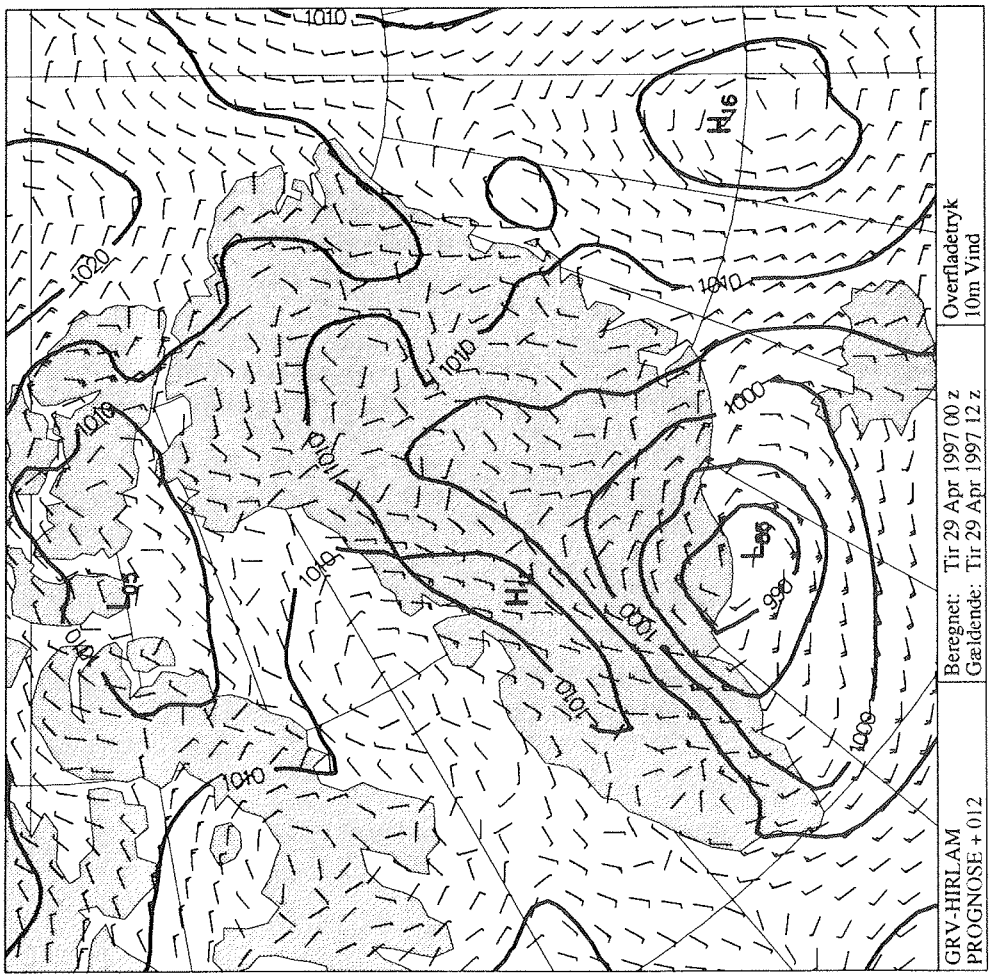

Fig.5.10a: As Fig.5.4a, but valid for 12 UTC 29 April 1997.

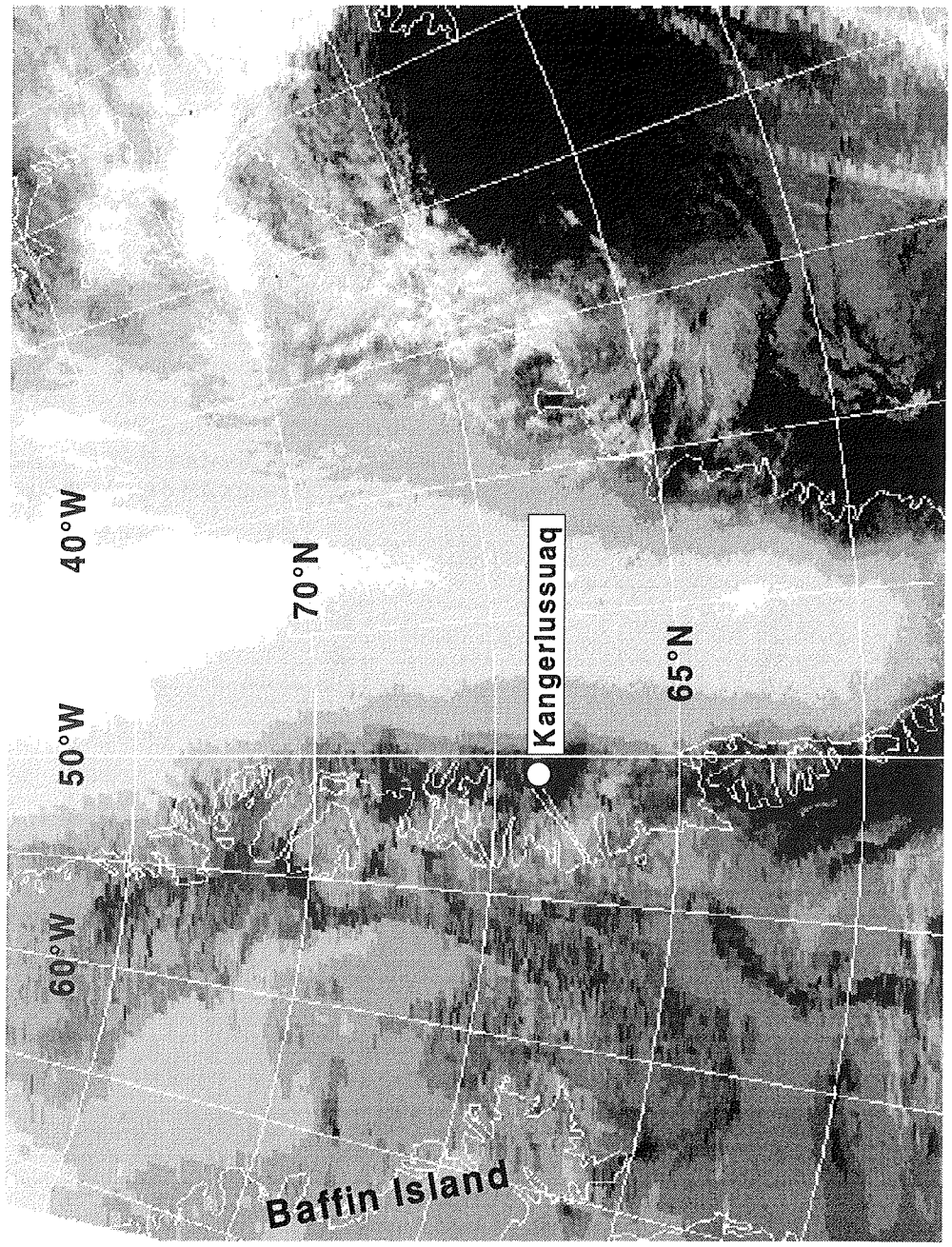

Fig.5.10b: GAC infrared image for 10 UTC 29 April 1997 (reduced resolution).

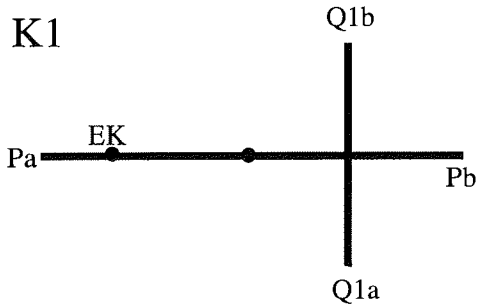

Way point coordinates		
Long.	Lat.	
-50.708	67.013	Kan
-50.090	67.420	Pa
-47.800	67.485	Pb
-48.500	67.200	Q1a
-48.500	67.730	Q1b
-49.700	67.435	EK

Fig.5.11a: Schematic plot of the flight pattern and a table with the geographic coordinates of the way points for KA4 on 29 April 1997.

Three P cross-sections and two Q1 cross-sections were flown. First, temps along P and two profiles were performed between Pb and EK. Cross-section Q1 was flown with temps and a low-level profile, then a second P cross-section with temps and a low-level profile between Pb and EK. Cross-section Q1 was flown a second time (temps and a low-level profile). A third P cross-section with temps, one low-level profile between Pb and EK and one profile between Pb and Pa (constant SH over the ice and constant BH over the tundra) were performed at the end of the flight.

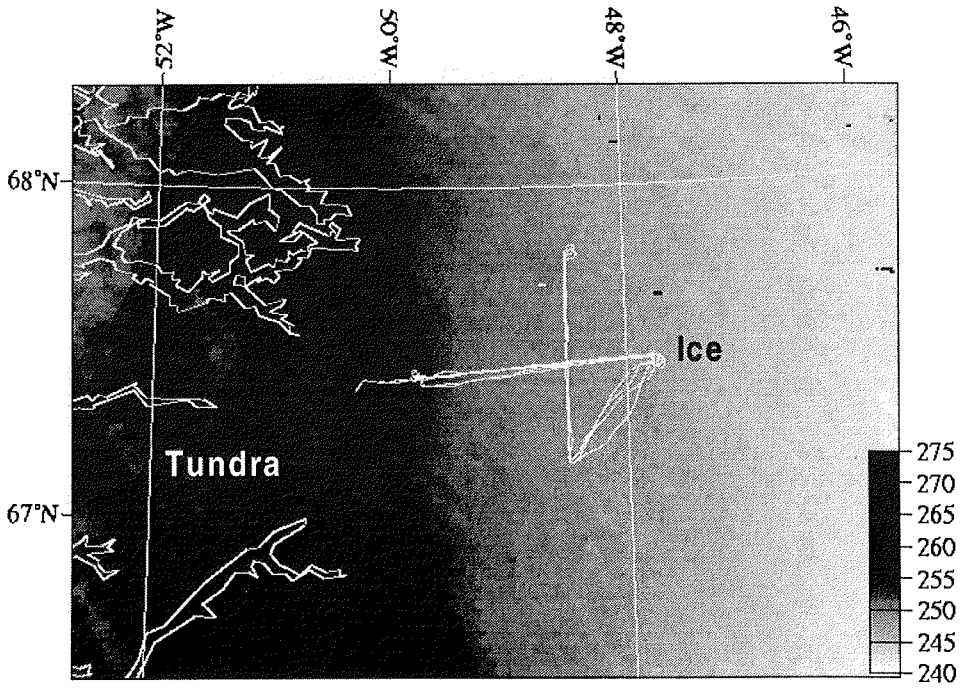

Fig.5.11b: HRPT infrared image for 29 April 1997, 10 UTC with the flight path superimposed.

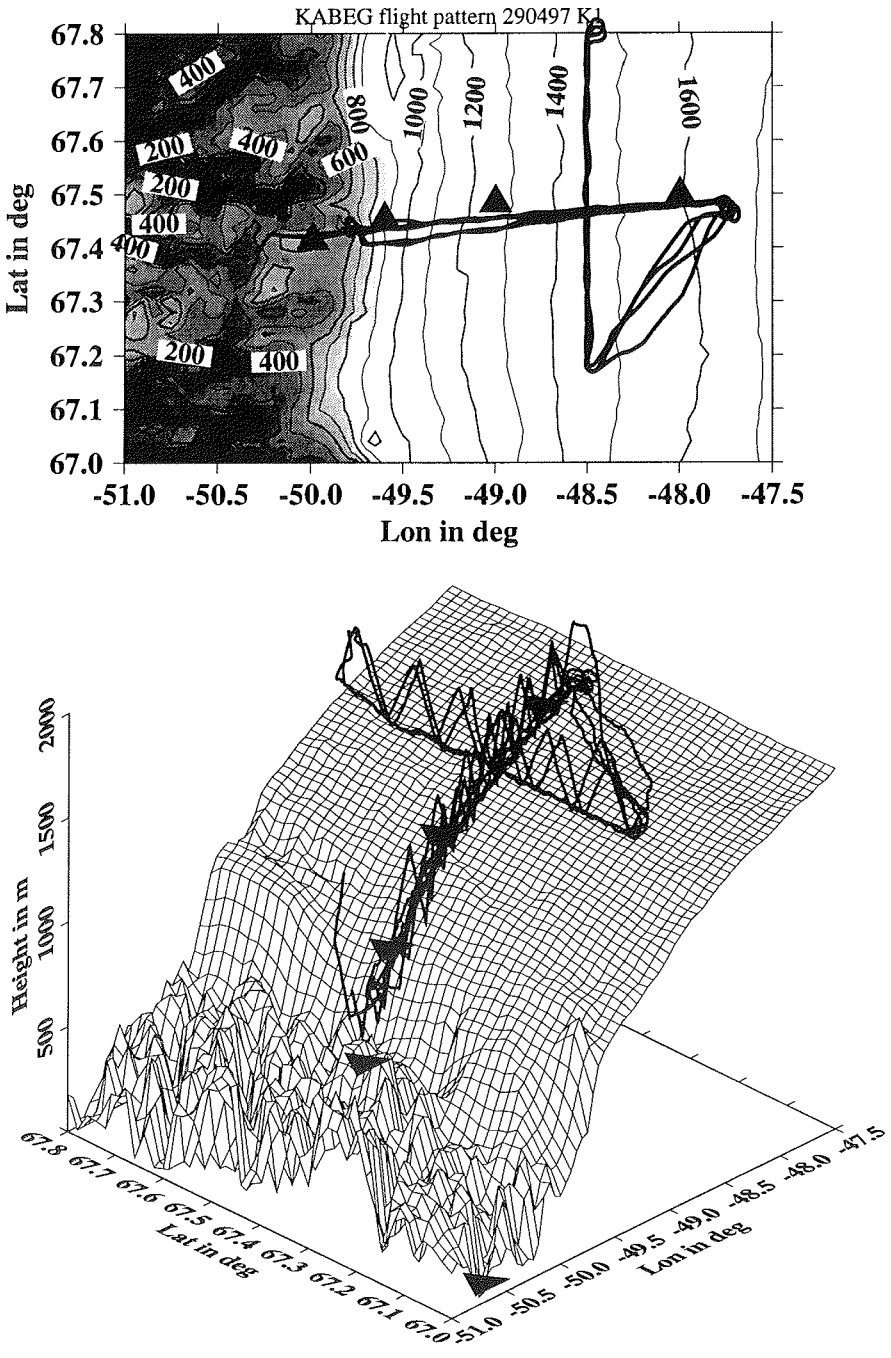

Fig.5.11 (continued): As Fig.5.5, but for the flight path KA4.

5.3.5 KA5 2 May 1997

The synoptic situation was characterized by a moderate high pressure system over southeast Greenland and a low over Baffin Island and the Davis Strait. Over the area of K1 forecasted 10 m winds were around 3-5 m/s. At the beginning of the flight, the conditions were cloud-free, later the tundra and the ice were covered by 4/8 Ci/As. Intense winds and snow drift were observed during the flight.

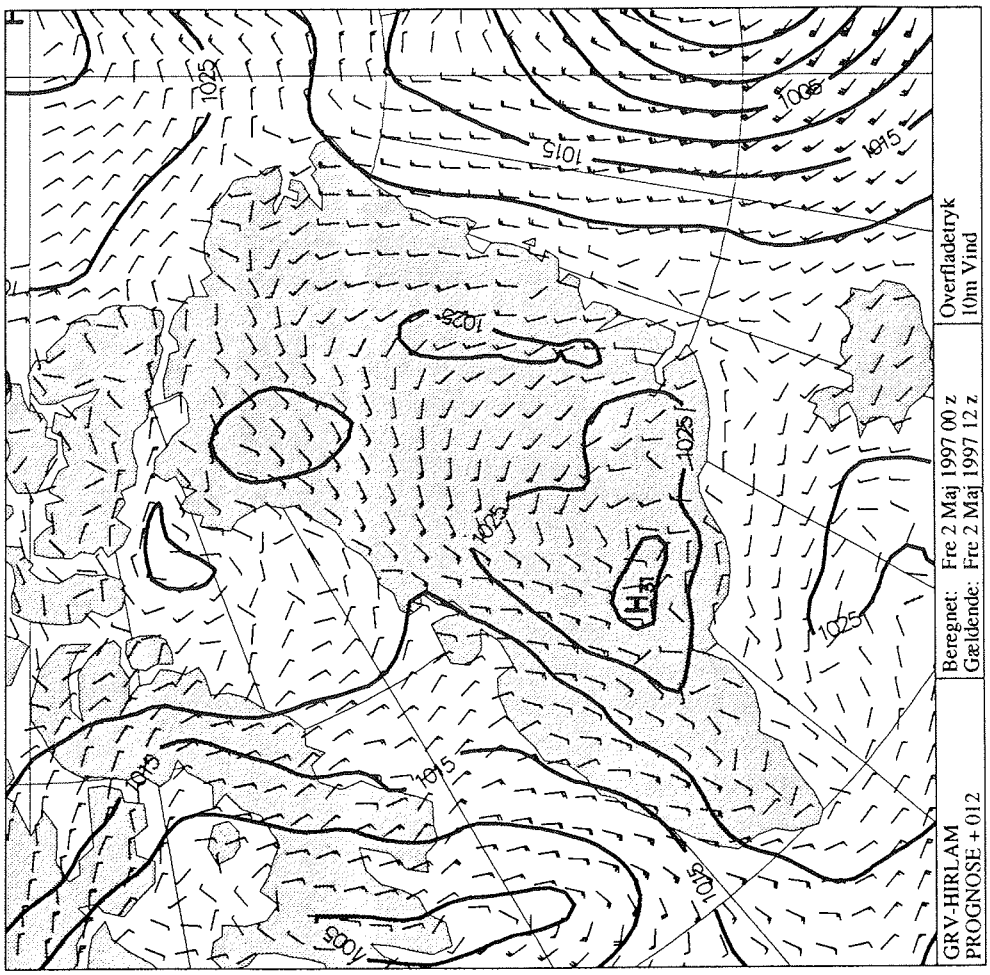

Fig.5.12a: As Fig.5.4a, but valid for 12 UTC 2 May 1997.

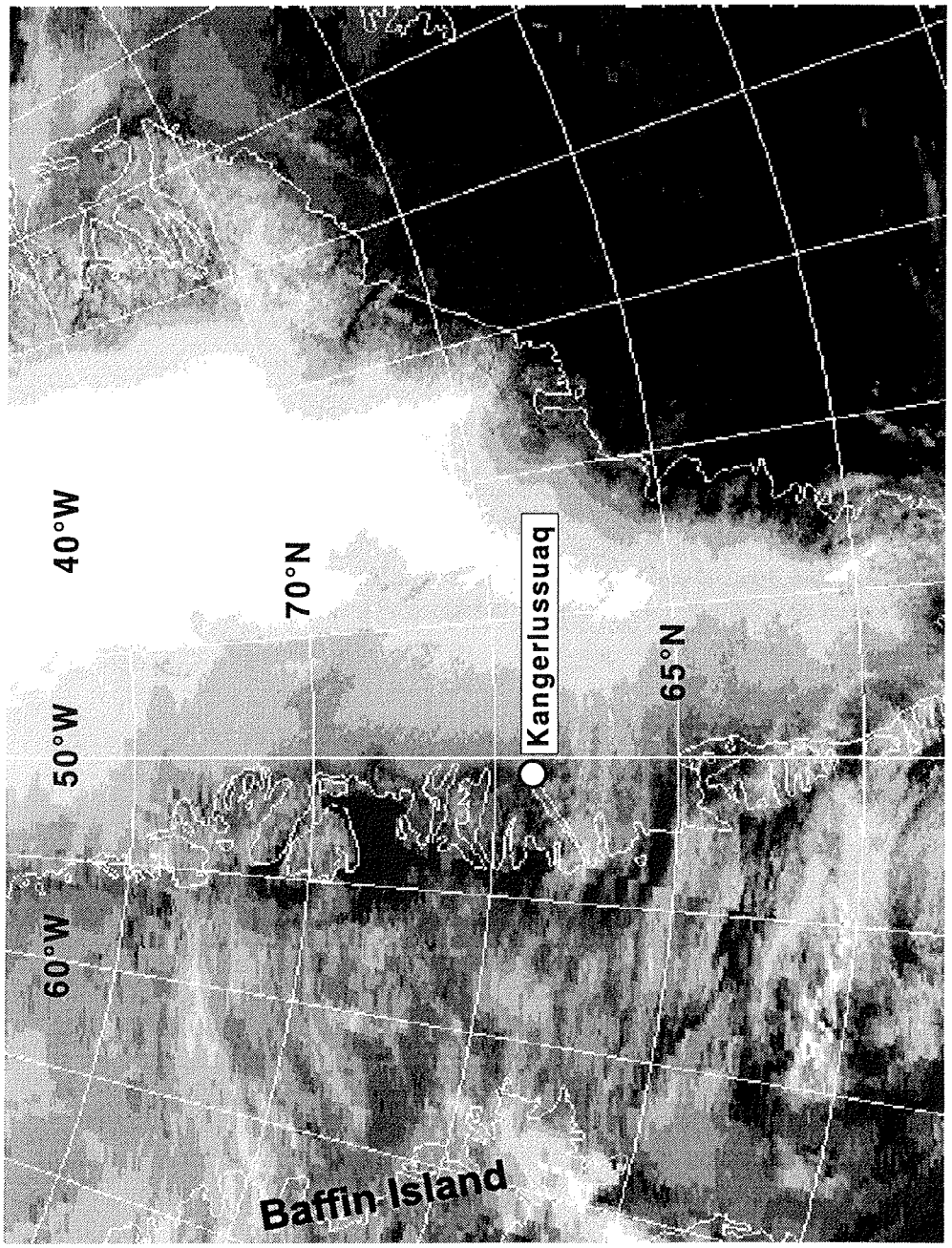

Fig.5.12b: GAC infrared image for 06 UTC 2 May 1997 (reduced resolution).

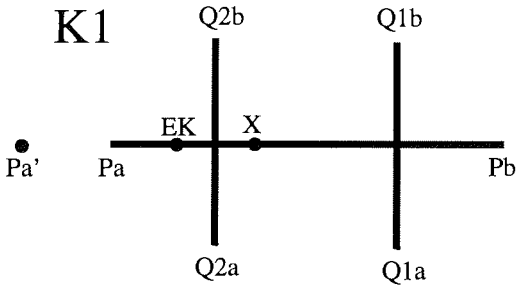

Way point coordinates		
Long.	Lat.	
-50.708	67.013	Kan
-50.860	67.416	Pa'
-50.090	67.420	Pa
-47.800	67.485	Pb
-48.500	67.200	Q1a
-48.500	67.730	Q1b
-49.500	67.170	Q2a
-49.500	67.710	Q2b
-49.700	67.435	EK
-49.077	67.458	X

Fig.5.13a: Schematic plot of the flight pattern and a table with the geographic coordinates of the way points for KA5 on 2 May 1997.

Two P cross-sections and aircraft temps in a box including Q1 and Q2 were flown. In addition, flight legs at constant pressure levels and additional temps were flown near the ice edge in order to investigate the dissipation of the katabatic wind in the transition zone ice/tundra. The cross-section P was extended to Pa' with temps and four profiles. This flight pattern was followed by temps along Q1a-Q1b-Q2b-Q2a-Q1a, and a second P cross-section with temps and two profiles between Pb and Pa. At the end of the flight, the area near the ice edge between EK and X was investigated by two profiles and temps.

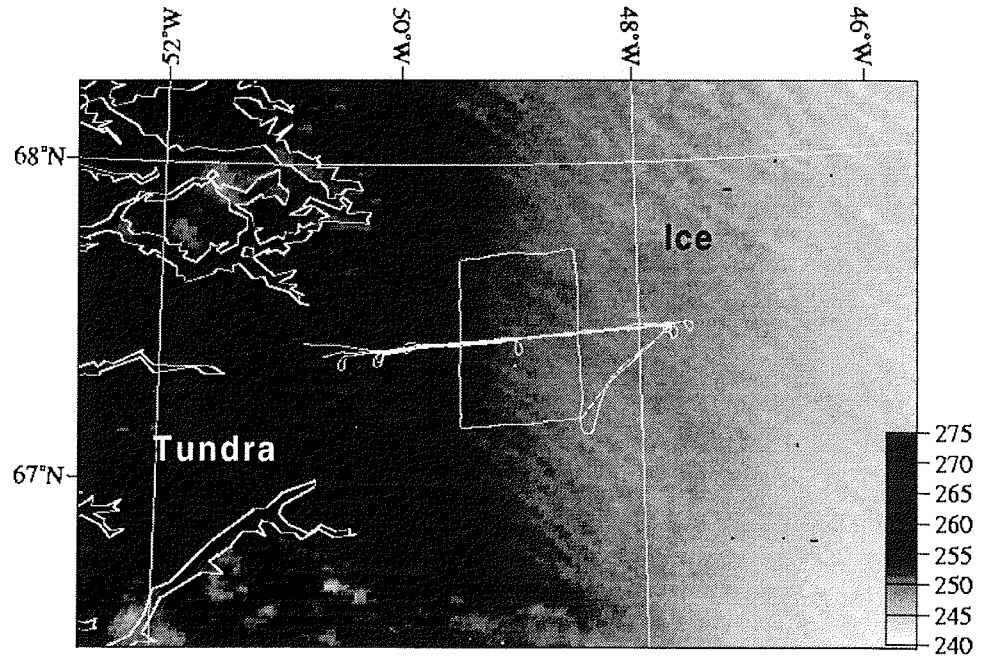

Fig.5.13b: HRPT infrared image for 2 May 1997, 06 UTC with the flight path superimposed.

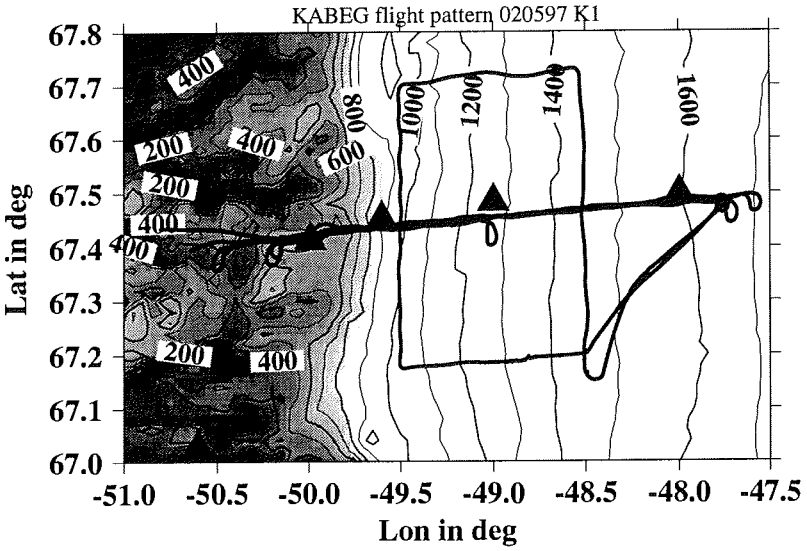

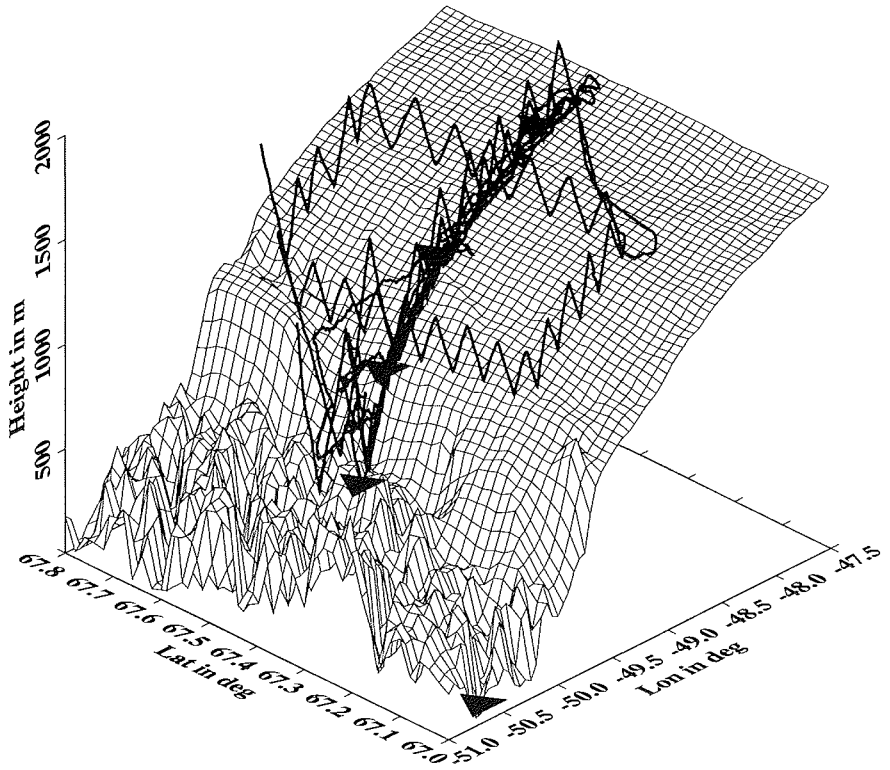

Fig.5.13 (continued): As Fig.5.5, but for the flight path KA5.

5.3.6 KA6 and KA7 11 May 1997

KA6 was the first flight over the valley region west of Kulusuk. A high pressure system extended over central Greenland and an area of relatively high pressure gradients was present near the coast of southeast Greenland. Over the area of K2 forecasted 10 m winds were around 10 m/s. One P cross-section and the cross-sections Q1, Q2 and Q3 were flown (see Fig.5.2 and Fig.515.a). Q4 was dropped, since the katabatic wind system was completely dissipated even at Q3. During the transfer flight from Kangerlussuaq to the measurement area K2 low-level Sc was observed over the ice, but except a few aircraft contrails no clouds were present during the flight at the east coast. The program K2 was flown a second time after refueling at Kulusuk. One P cross-section and aircraft temps in a box including Q1 and Q2 as well as low-level legs for Q1 and Q2 were flown in the KA7 flight. This flight took place in the dissipating katabatic wind system.

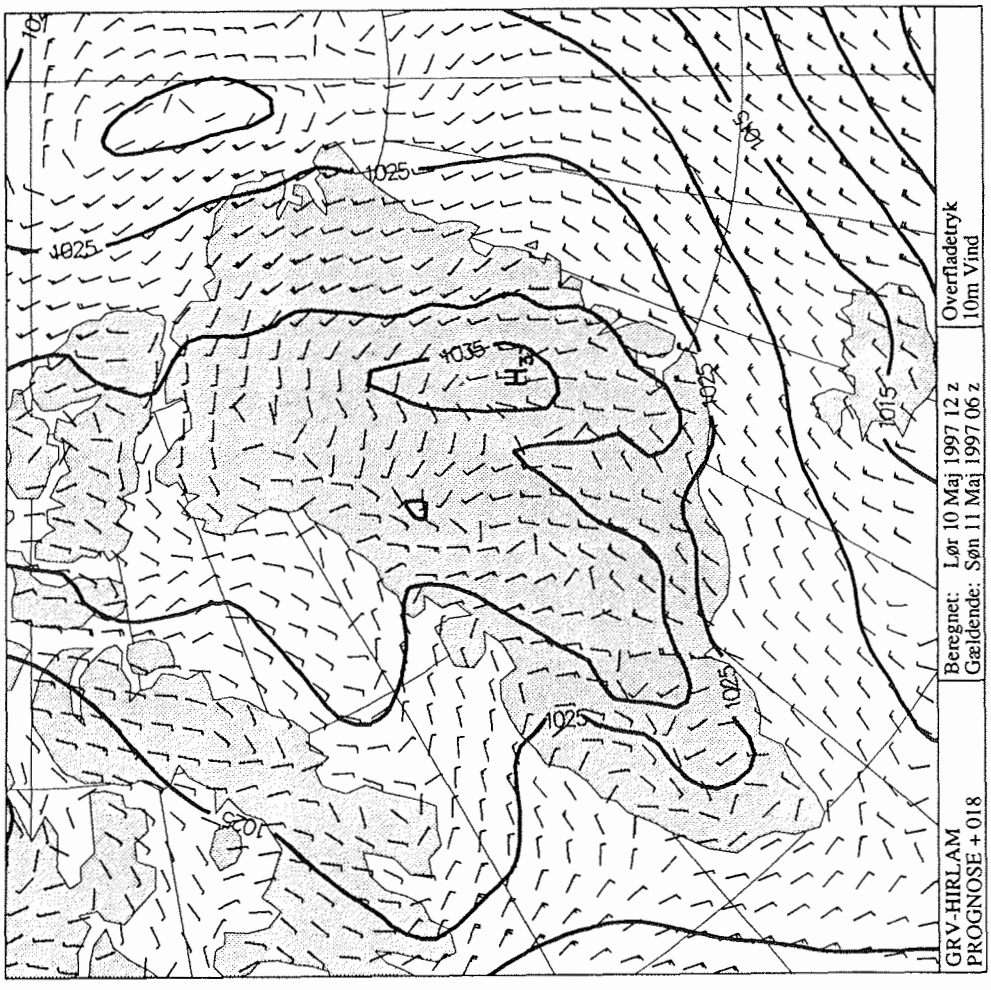

Fig.5.14a: As Fig.5.4a, but valid for 06 UTC 11 May 1997.

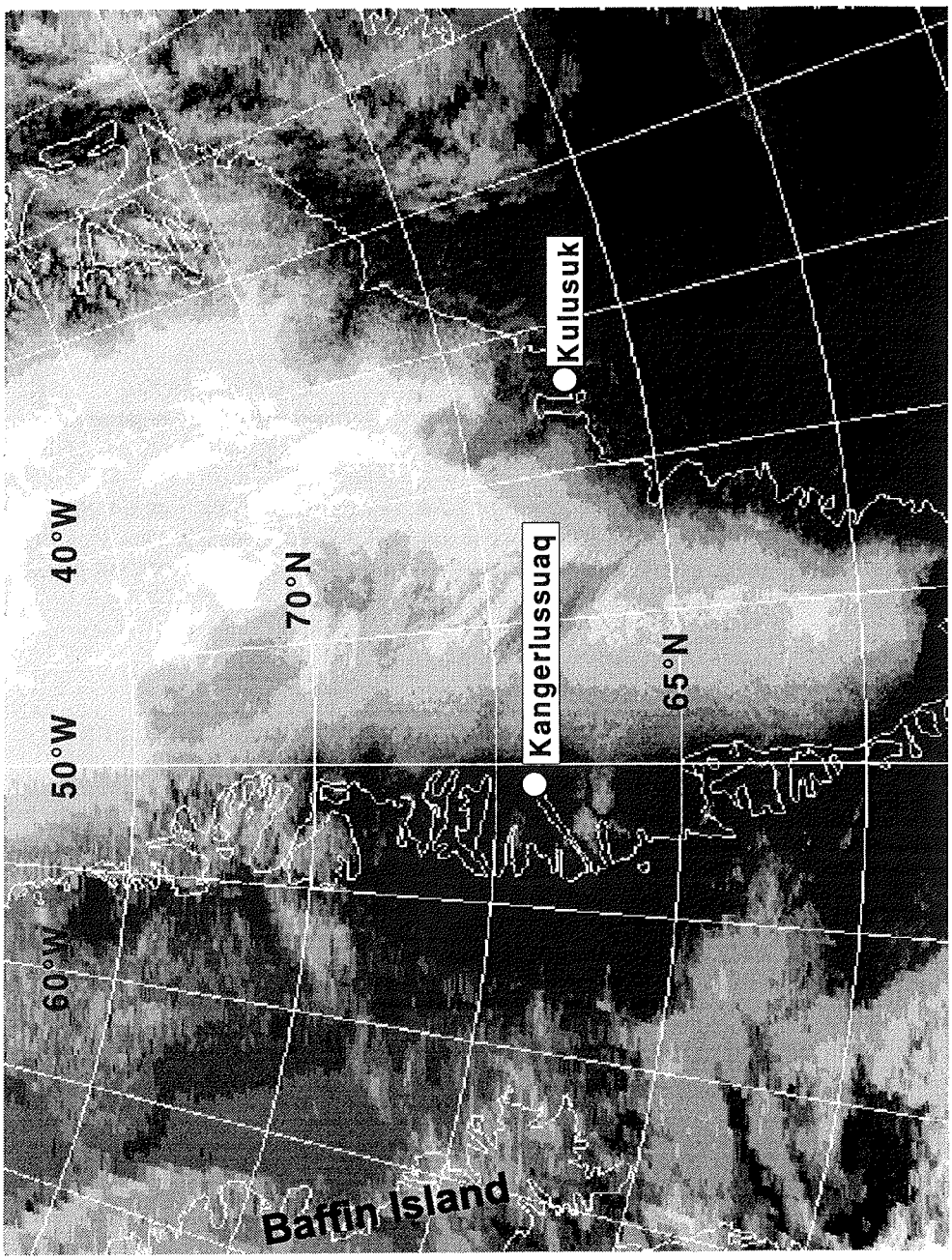

Fig.5.14b: GAC infrared image for 06 UTC 11 May 1997 (reduced resolution).

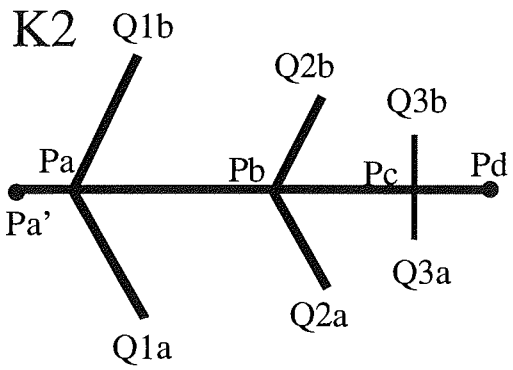

Way point coordinates	
Long.	Lat.
-50.708	67.013 Kan
-41.998	66.082 Pa'
-41.153	65.947 Pa
-40.387	65.673 Pb
-39.838	65.477 Pc
-39.265	65.268 Pd
-41.302	65.635 Q1a
-40.383	66.060 Q1b
-40.493	65.445 Q2a
-39.900	65.793 Q2b
-39.945	65.427 Q3a
-39.602	65.590 Q3b
-37.134	65.574 Kul

Fig.5.15a: Schematic plot of the flight pattern and a table with the geographic coordinates of the way points for KA6 on 11 May 1997.

A detailed description will only be given for KA6. During KA6 temps were flown down-slope between Pa' and Pd, and then cross-section Q3 two times with temps. This flight pattern was followed by a low-level profile along Pc-Pa. Q1 was flown with temps and a low-level profile, and Q2 was flown in the same way.

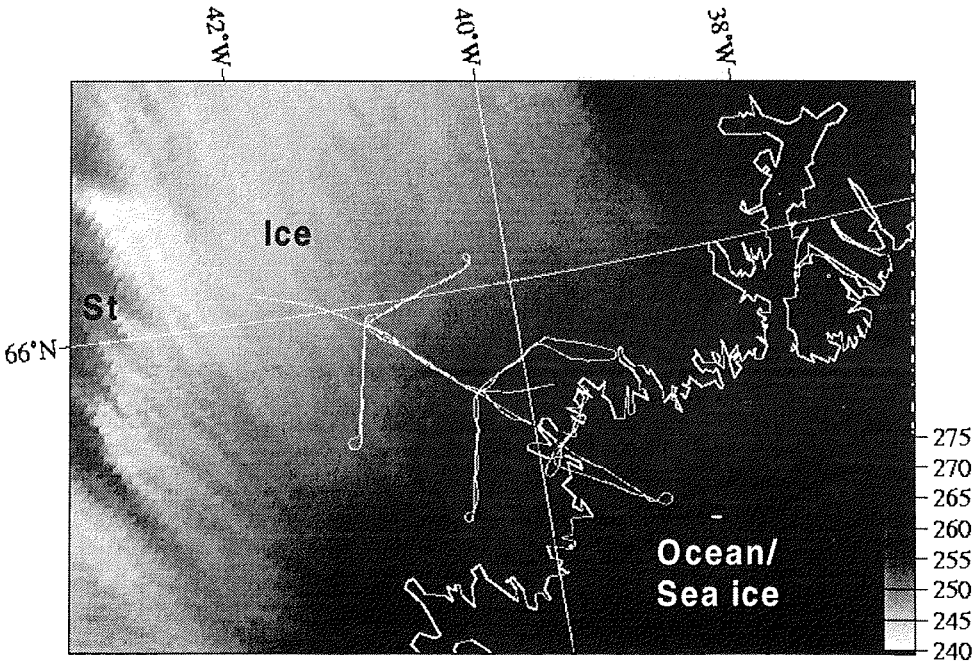

Fig.5.15b: HRPT infrared image for 11 May 1997, 06 UTC with the flight path superimposed.

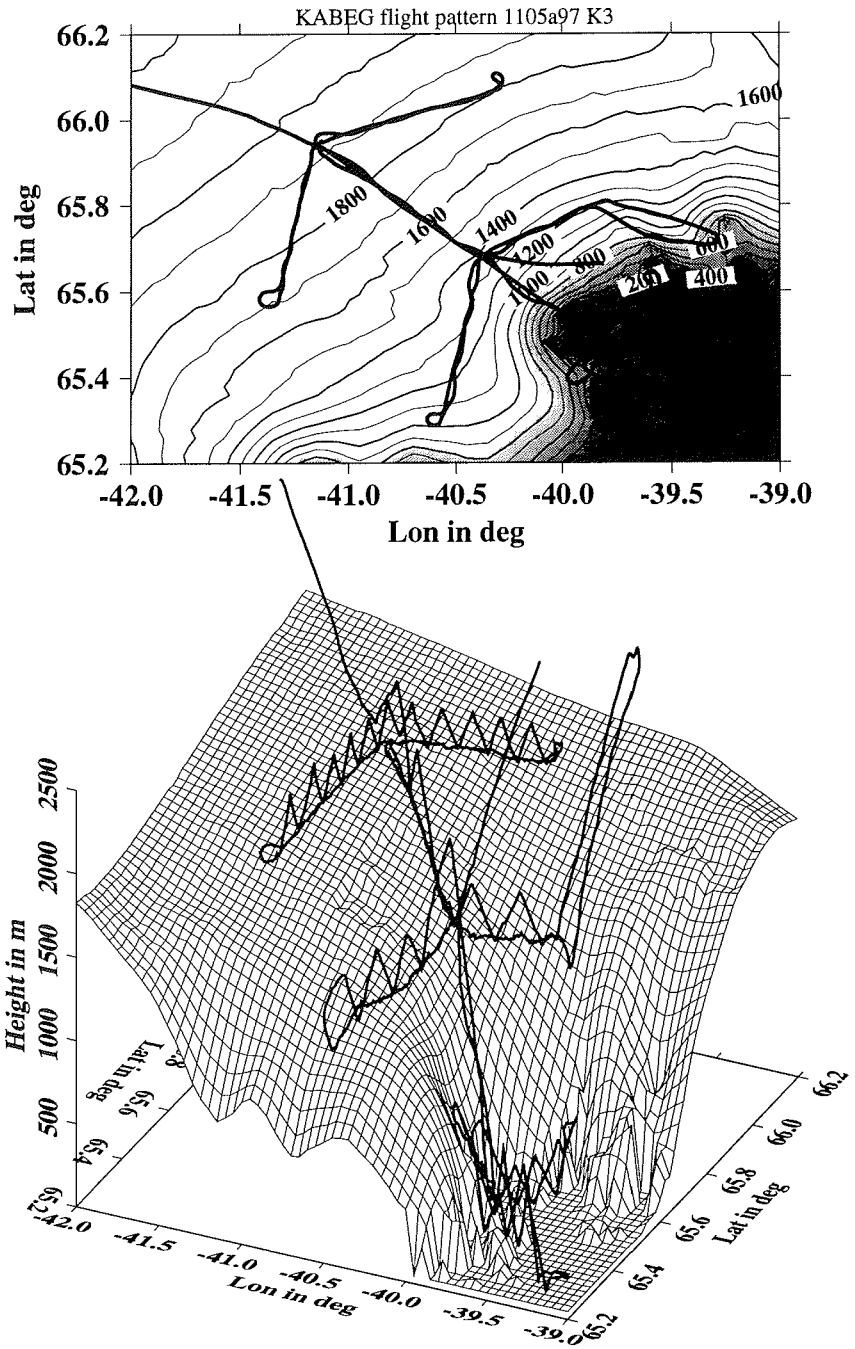

Fig.5.15 (continued): As Fig.5.5, but for the flight path KA6.

5.3.7 KA8 13 May 1997

The synoptic situation was characterized by a strong high pressure system over central Greenland leading to almost cloud-free conditions for the whole ice sheet. Over the area of of K1 forecasted 10 m winds were around 10 m/s. Intense winds and snow drift were observed during the flight; the cloud coverage was 3/8 Cs. Severe turbulence was encountered in the transition zone between the ice and the almost ice-free tundra. Two P cross-sections and aircraft temps in a box including Q1 and Q2 were flown. Flight legs at constant pressure levels were flown near the ice edge in order to investigate the dissipation of the katabatic wind in the transition zone ice/tundra. In addition, a third cross-section parallel to the ice edge was flown over the tundra (Q3).

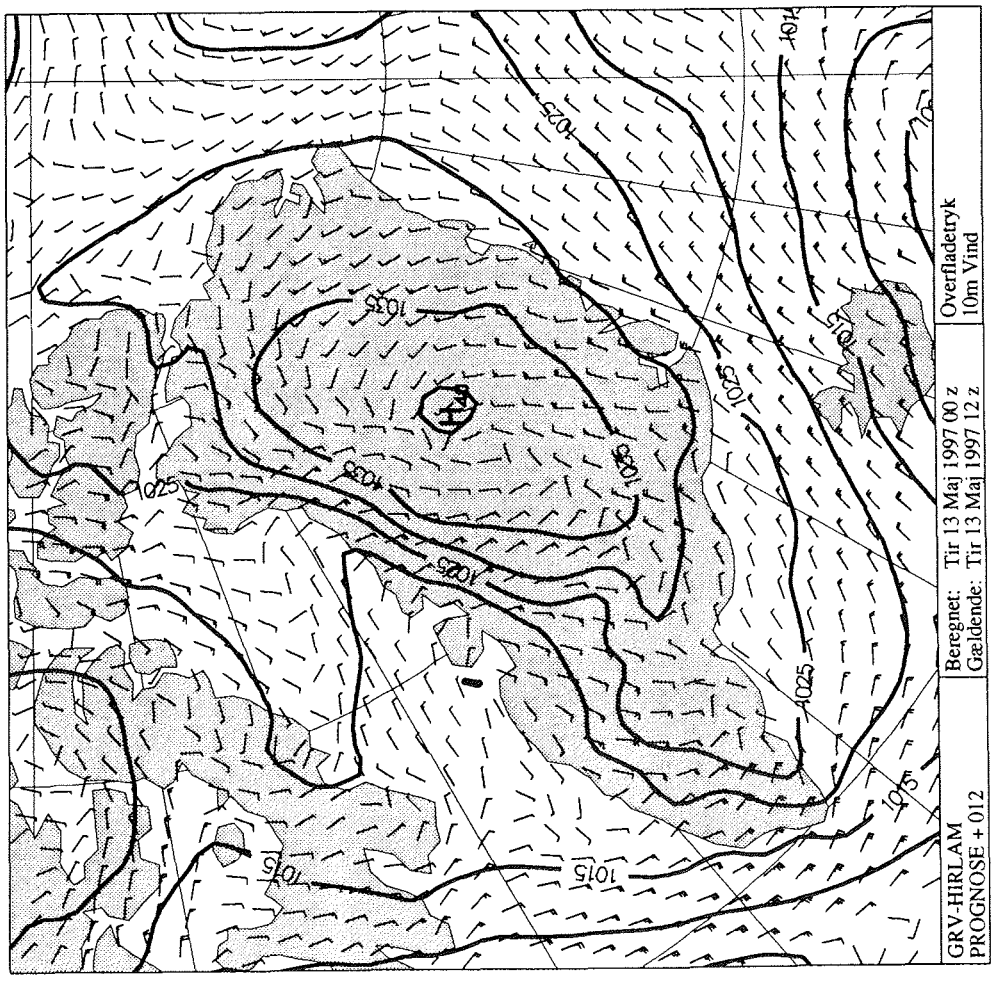

Fig.5.16a: As Fig.5.4a, but valid for 12 UTC 13 May 1997.

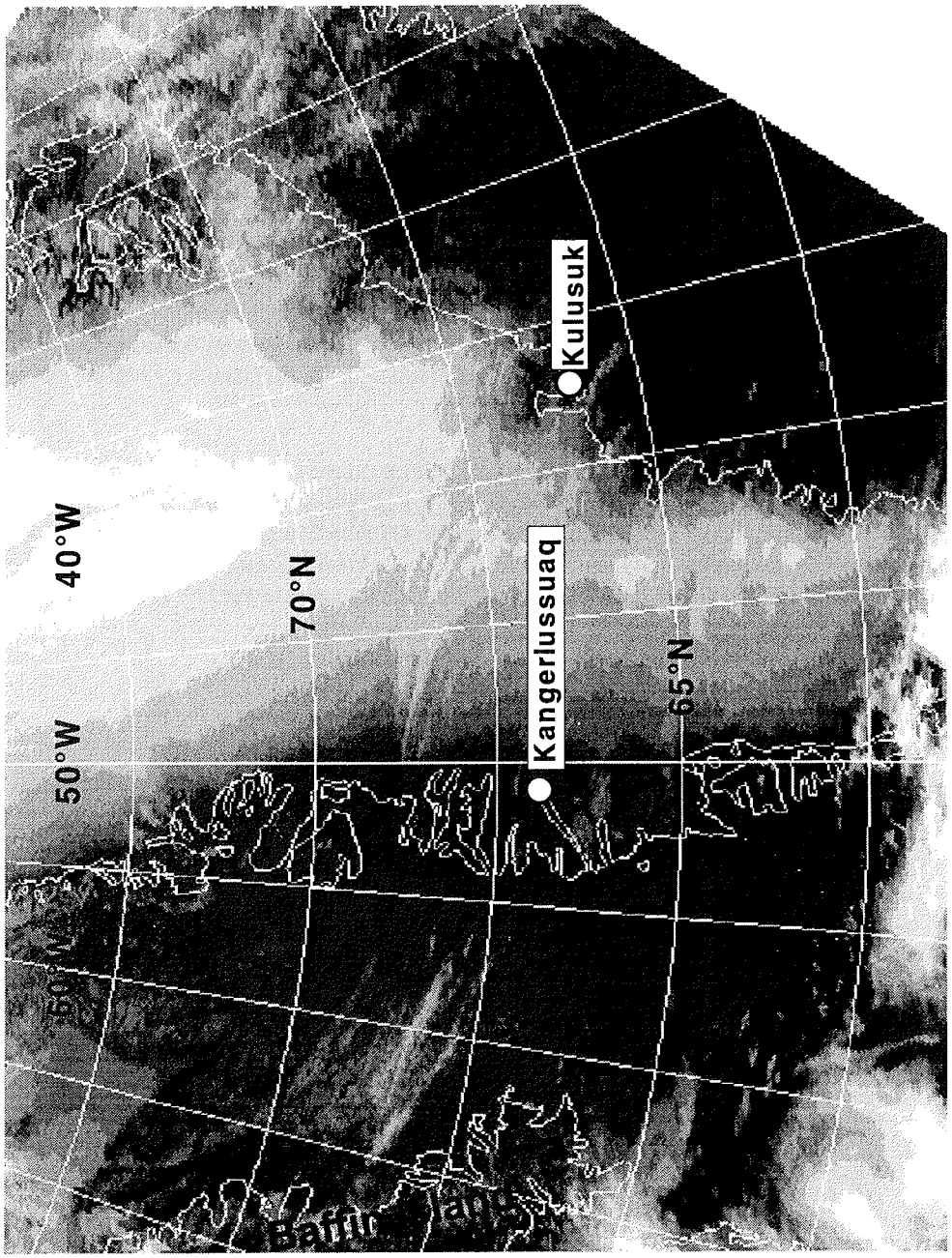

Fig.5.16b: GAC infrared image for 07 UTC 13 May 1997 (reduced resolution).

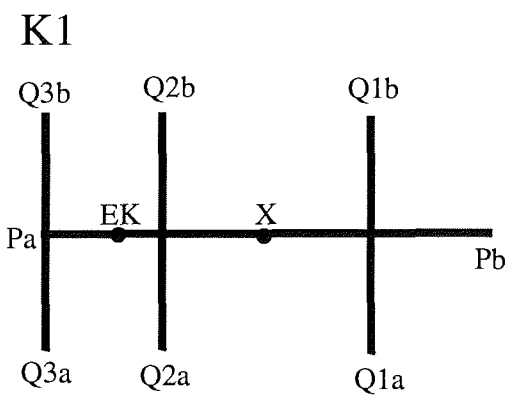

Way point coordinates		
Long.	Lat.	
-50.708	67.013	Kan
-50.090	67.420	Pa
-47.800	67.485	Pb
-48.500	67.200	Q1a
-48.500	67.730	Q1b
-49.500	67.170	Q2a
-49.500	67.710	Q2b
-50.100	67.140	Q3a
-50.100	67.710	Q3b
-49.200	67.450	X
-49.700	67.435	EK

Fig.5.17a: Schematic plot of the flight pattern and a table with the geographic coordinates of the way points for KA8 on 13 May 1997.

Cross-section P was flown with temps and four profiles, three of the latter were at constant SH over the ice and constant BH over the tundra. This flight pattern was followed by a second P cross-section with temps, then cross-section Q3 was flown by temps and a BH profile. After Q3, the box Q2a-Q2b-Q1b-Q1a-Q2a was flown by temps. At the end of the flight, the area near the ice edge between Pa and X was investigated by temps and four SH/BH profiles.

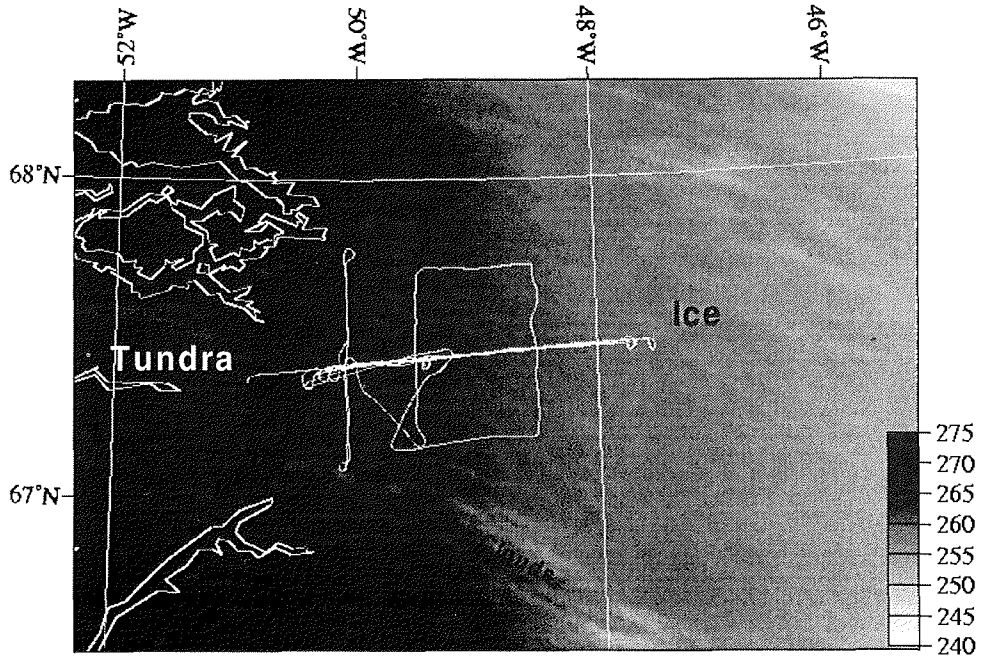

Fig.5.17b: HRPT infrared image for 13 May 1997, 07 UTC with the flight path superimposed.

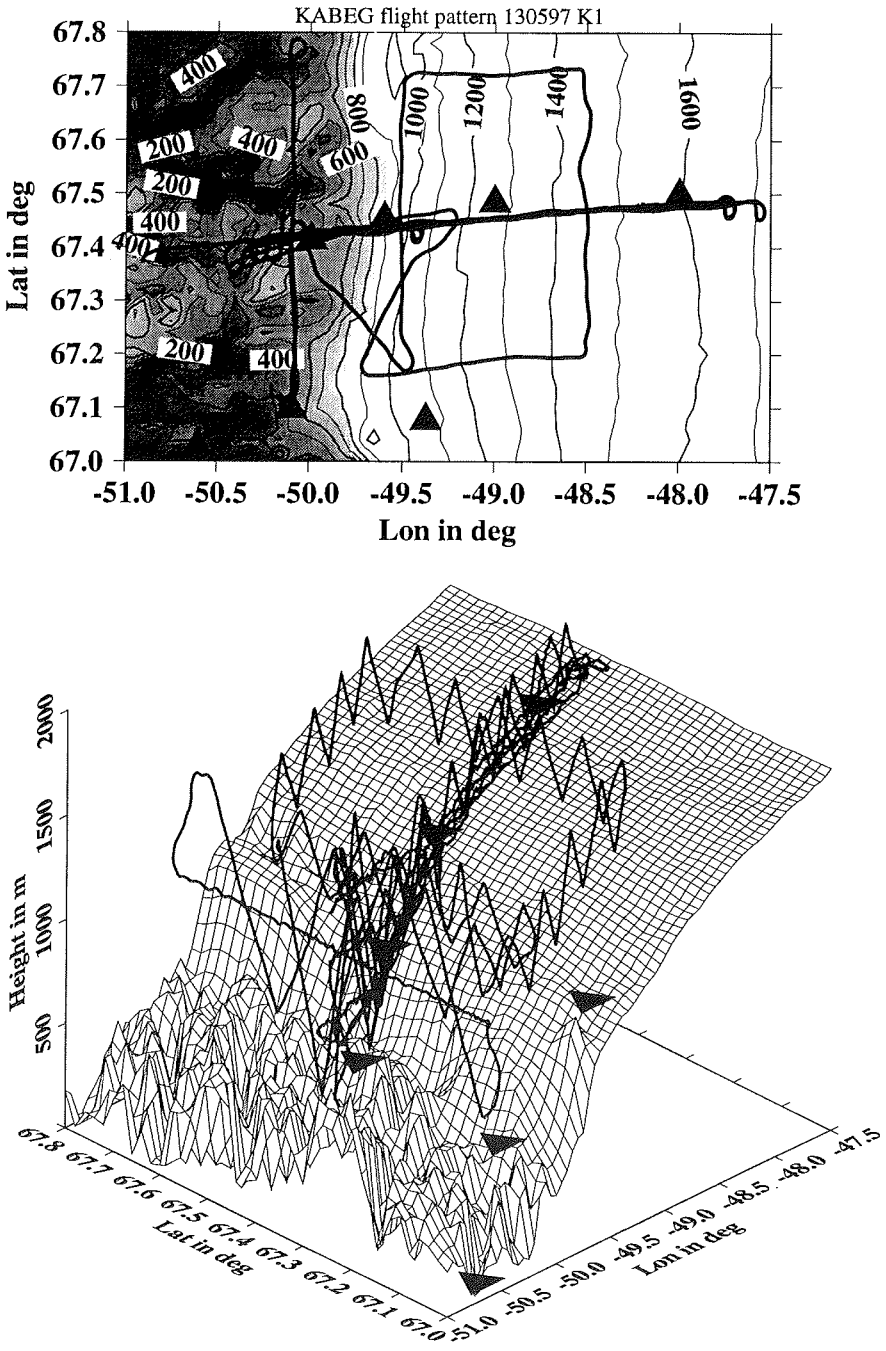

Fig.5.17 (continued): As Fig.5.5, but for the flight path KA8.

5.3.8 KA9 14 May 1997

This was the only flight for the program K3 over the valley region east of Ilulissat. A high pressure system lay over central Greenland, a weak cyclone was situated west of Disco Island. Over the area of K3 forecasted 10 m winds were only around 2.5 m/s. High-level clouds (3/8 Ci) were present over the ice, in some areas also low-level clouds (1/8 Sc) were observed.

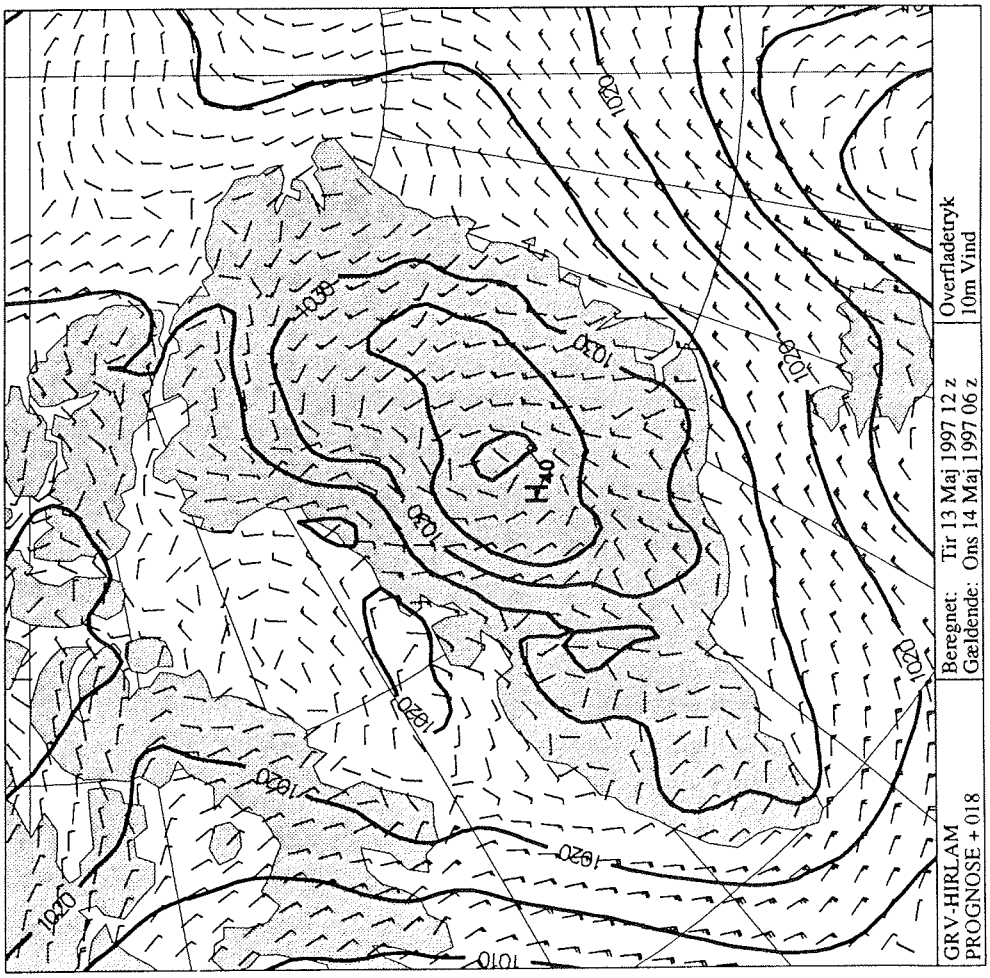

Fig.5.18a: As Fig.5.4a, but valid for 06 UTC 14 May 1997.

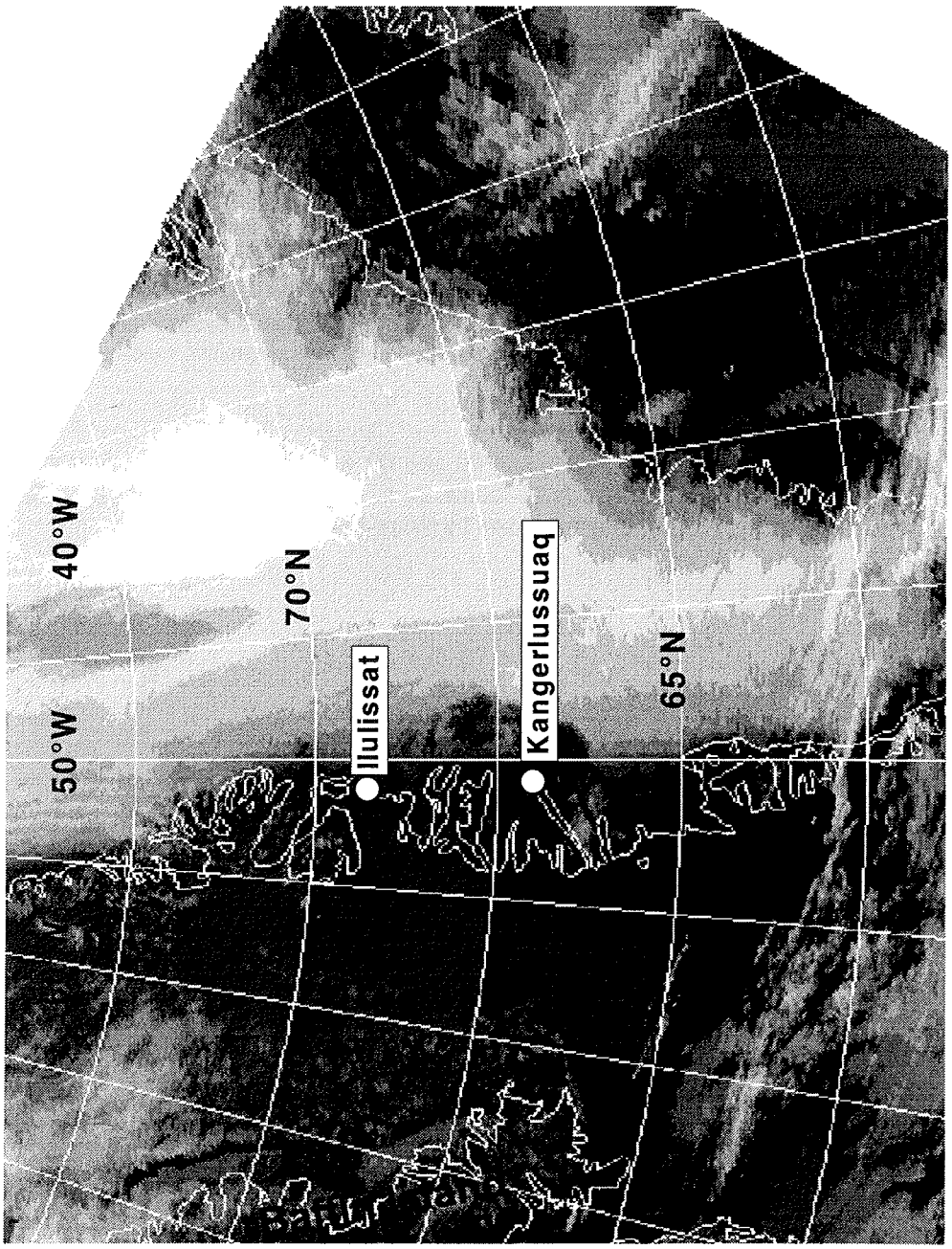

Fig.5.18b: GAC infrared image for 07 UTC 14 May 1997 (reduced resolution).

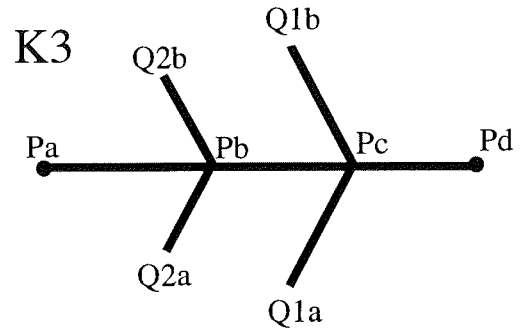

Way point coordinates		
Long.	Lat.	
-50.708	67.013	Kan
-50.167	69.183	Pa
-49.583	69.225	Pb
-48.833	69.293	Pc
-48.000	69.367	Pd
-48.833	69.031	Q1a
-48.305	69.572	Q1b
-49.567	69.115	Q2a
-49.867	69.353	Q2b
-51.062	69.245	Ilu

Fig.5.19a: Schematic plot of the flight pattern and a table with the geographic coordinates of the way points for KA9 on 14 May 1997.

One P cross-section and a box including Q1 and Q2 were flown as aircraft temps and constant level legs. The cross-section Pa-Pd was flown with temps and three profiles, then the box Q2a-Q2b-Q1b-Q1a-Q2a was flown by temps and two SH profiles.

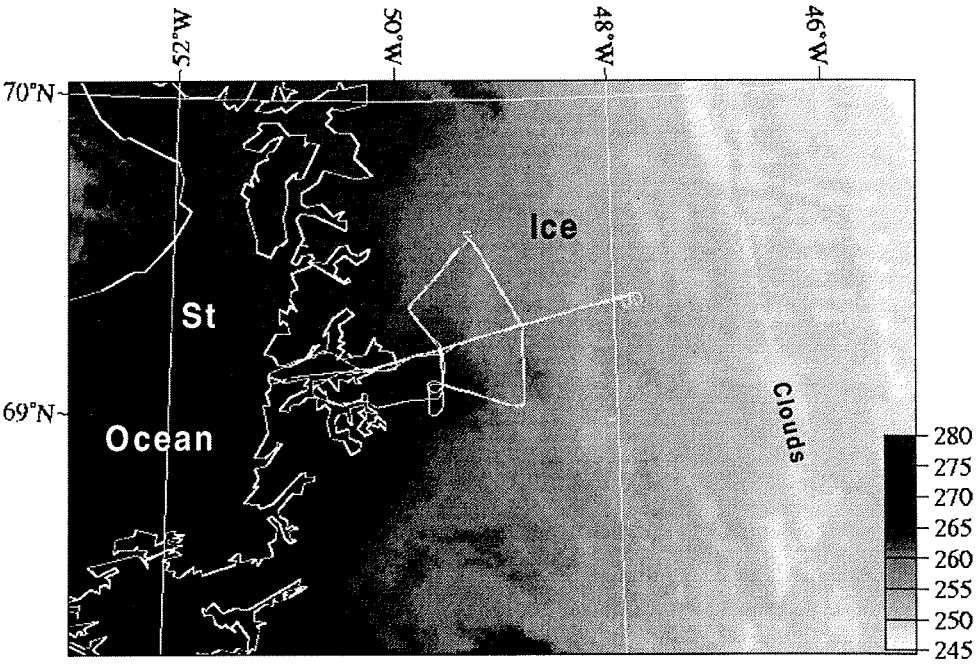

Fig.5.19b: HRPT infrared image for 14 May 1997, 07 UTC with the flight path superimposed.

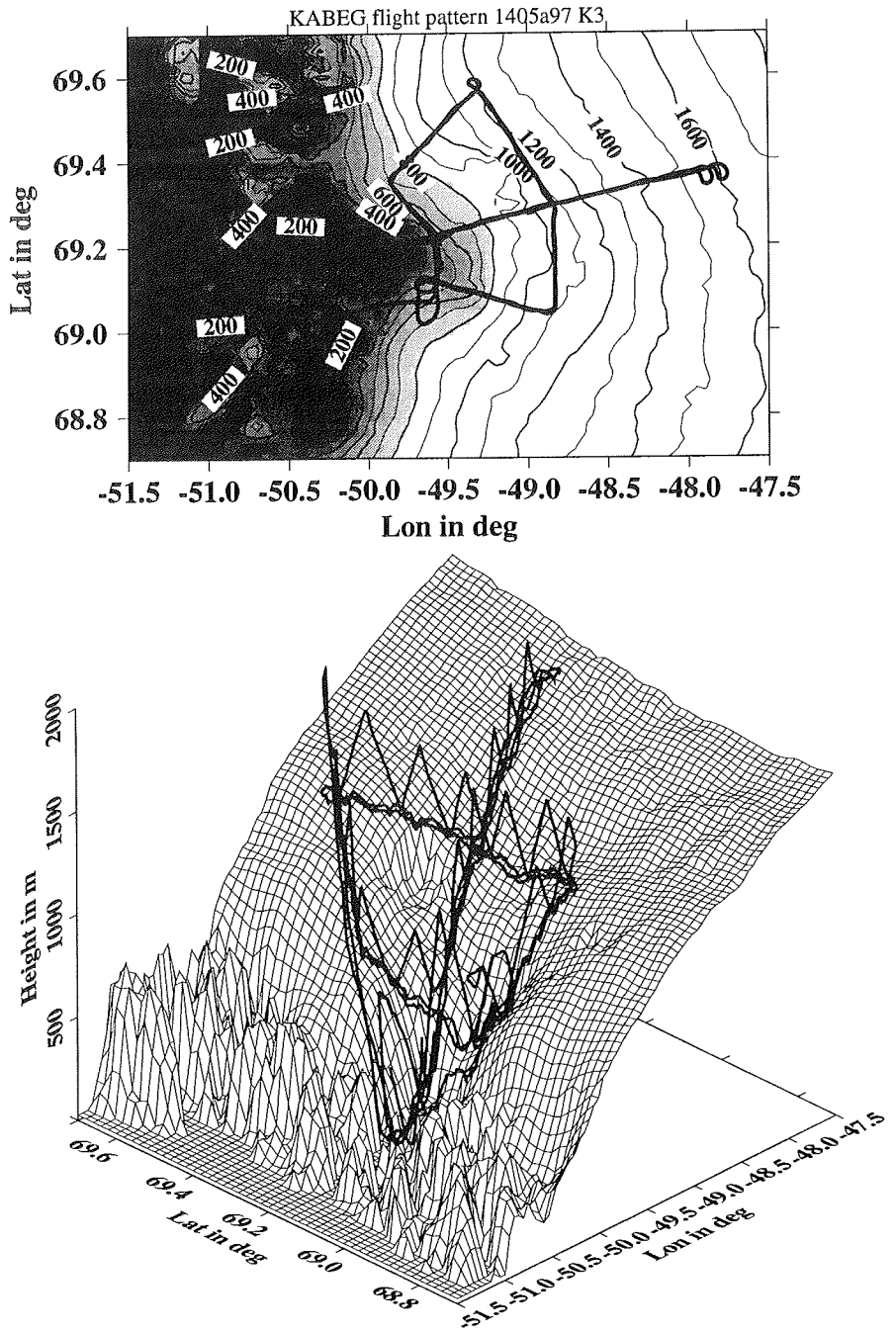

Fig.5.19 (continued): As Fig.5.5, but for the flight path KA9.

5.4 A brief description of the BLF flight missions

As for the katabatic wind flights, the synoptic situation is described using forecasts of the DMI operational model HIRLAM and AVHRR imagery. The sea ice analysis maps being closest to the BLF flights and plots of the ERS-derived wind vectors are also presented.

5.4.1 BLF1 15 April 1997

The synoptic situation was characterized by a high pressure system over Disco Island and a low over the southern Labrador Sea. Over the Davis Strait moderate pressure gradients were present. Forecasted 10 m winds were around 10 m/s from the north in that area. High-level clouds associated with the low can be seen over southern Greenland (Fig5.20b).

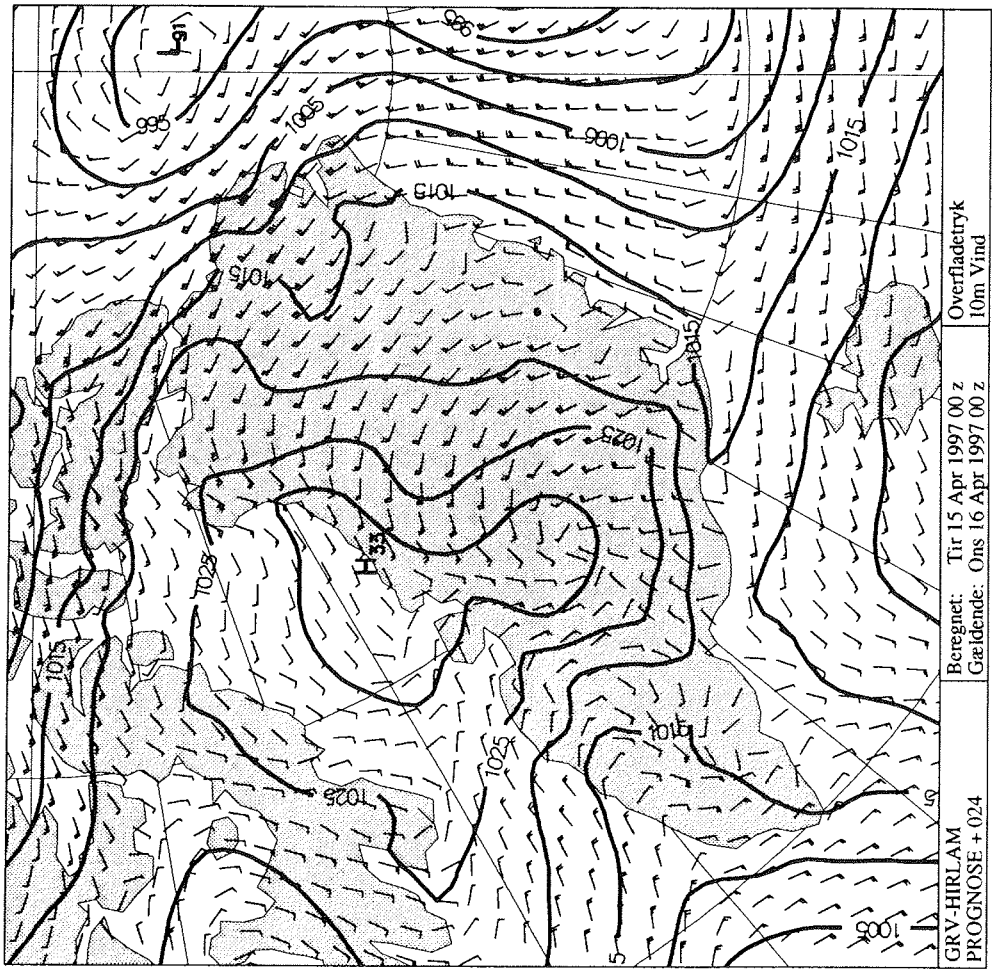

Fig.5.20a: As Fig.5.4a, but valid for 00 UTC 16 April 1997.

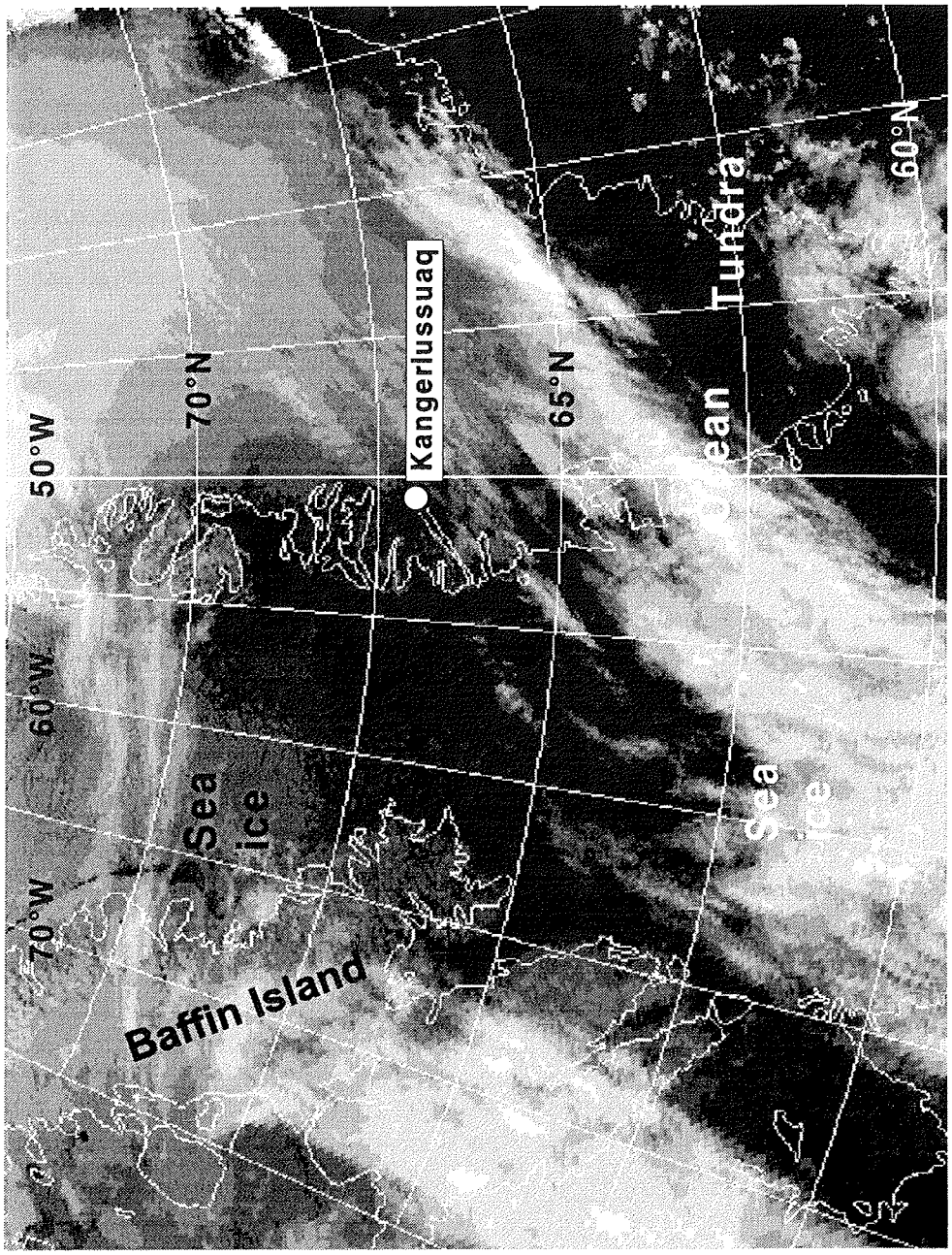

Fig.5.20b: GAC infrared image for 16 UTC 15 April 1997 (reduced resolution).

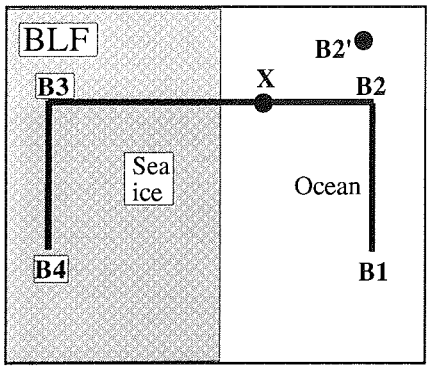

Way point coordinates		
Long.	Lat.	
-50.708	67.013	Kan
-54.117	65.415	B1
-54.117	65.775	B2
-55.872	65.775	B3
-55.872	65.415	B4
-54.067	65.954	B2'
-54.824	65.777	X

Fig.5.21a: Schematic plot of the flight pattern and a table with the geographic coordinates of the way points for BLF1 on 15 April 1997.

After the transfer flight a temp was made at B2', then the ice edge was searched and the points B1-B4 were defined. After a temp at B4, five GPS dropsondes were deployed successfully from a height of about 2000 m. Altogether five constant level legs along B1-B4 were flown (one above the ABL, one at the ABL height and three within the ABL). A cross-section with aircraft temps (B3-X) was performed at the end of the flight. Observed high-level cloud coverage was about 5/8 As, low-level cloud coverage was variing and consisted of Sc near the sea ice front. The observed sea ice coverage was up to 9/10.

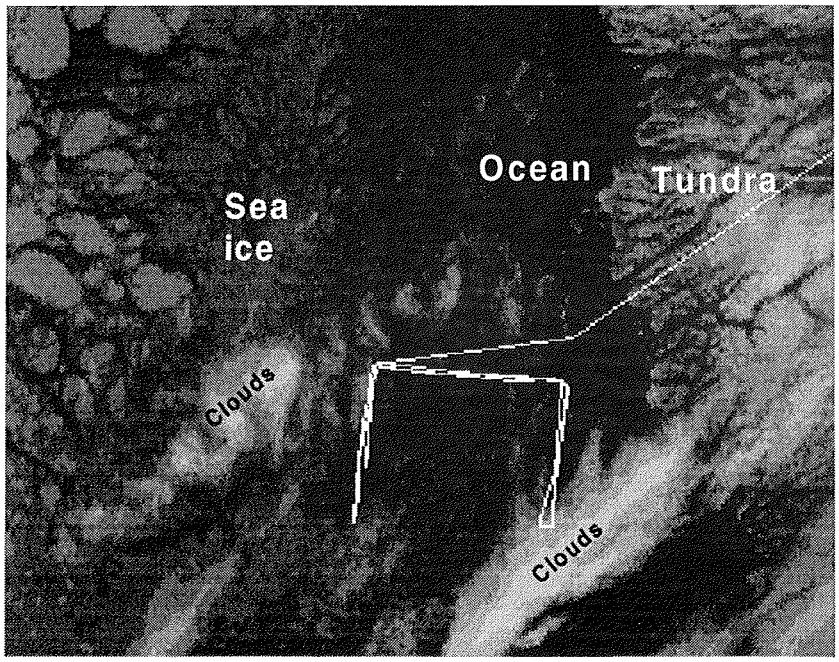

Fig.5.21b: HRPT infrared image for 15 April 1997, 16 UTC with the flight path superimposed.

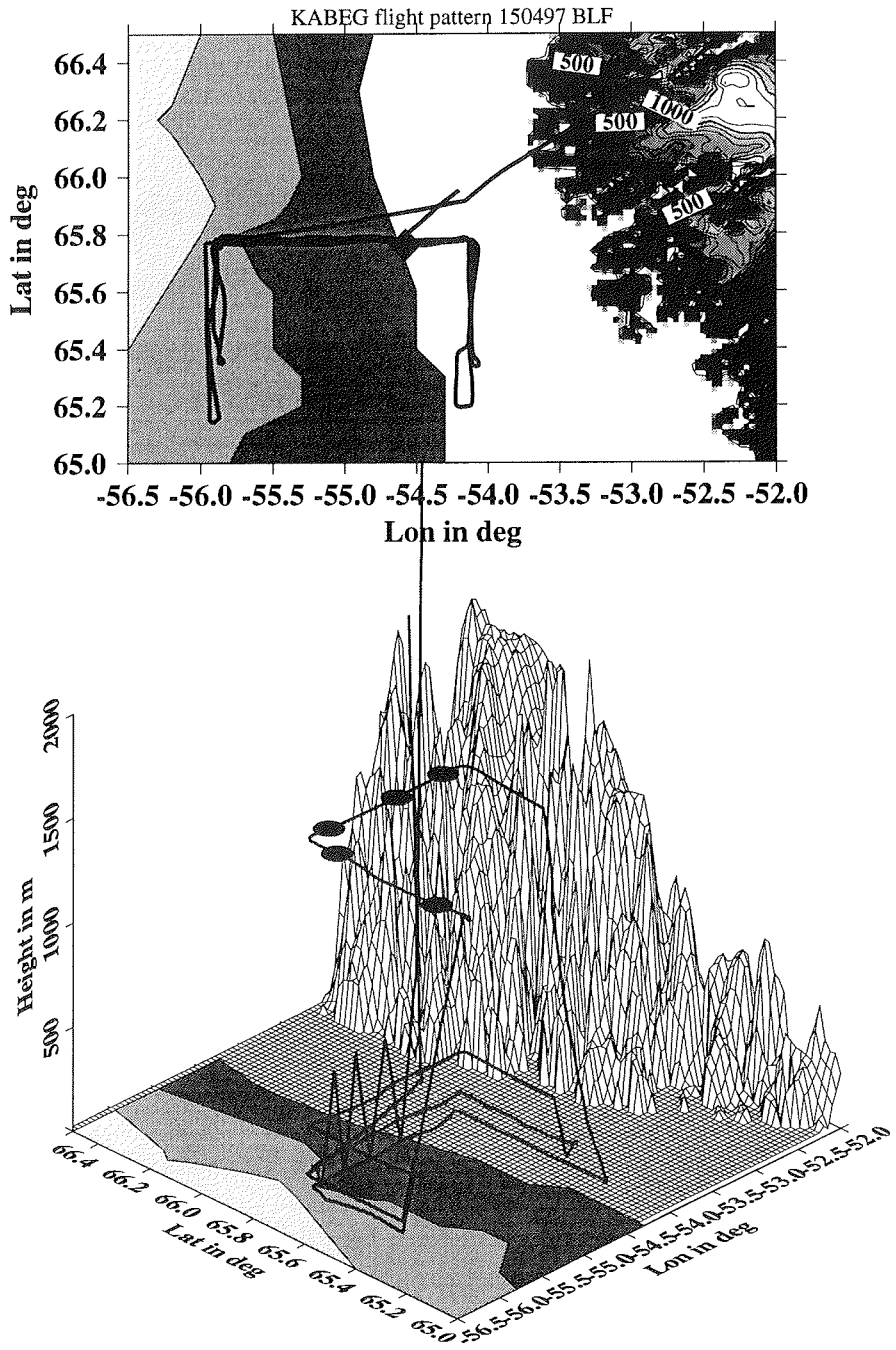

Fig.5.21 (continued): Flight path superimposed on a high-resolution topography as a 2D plot (upper panel, isolines every 100 m, areas lower than 1000 m shaded) as well as a 3D plot. The ice concentration from NOAA weekly ice maps is indicated (dark gray: 3-5/10, medium gray: 7-9/10, and light gray: 8-10/10). The diamond in the upper panel marks the observed ice margin during the flight; the circles in the lower panel mark the positions of dropsondes.

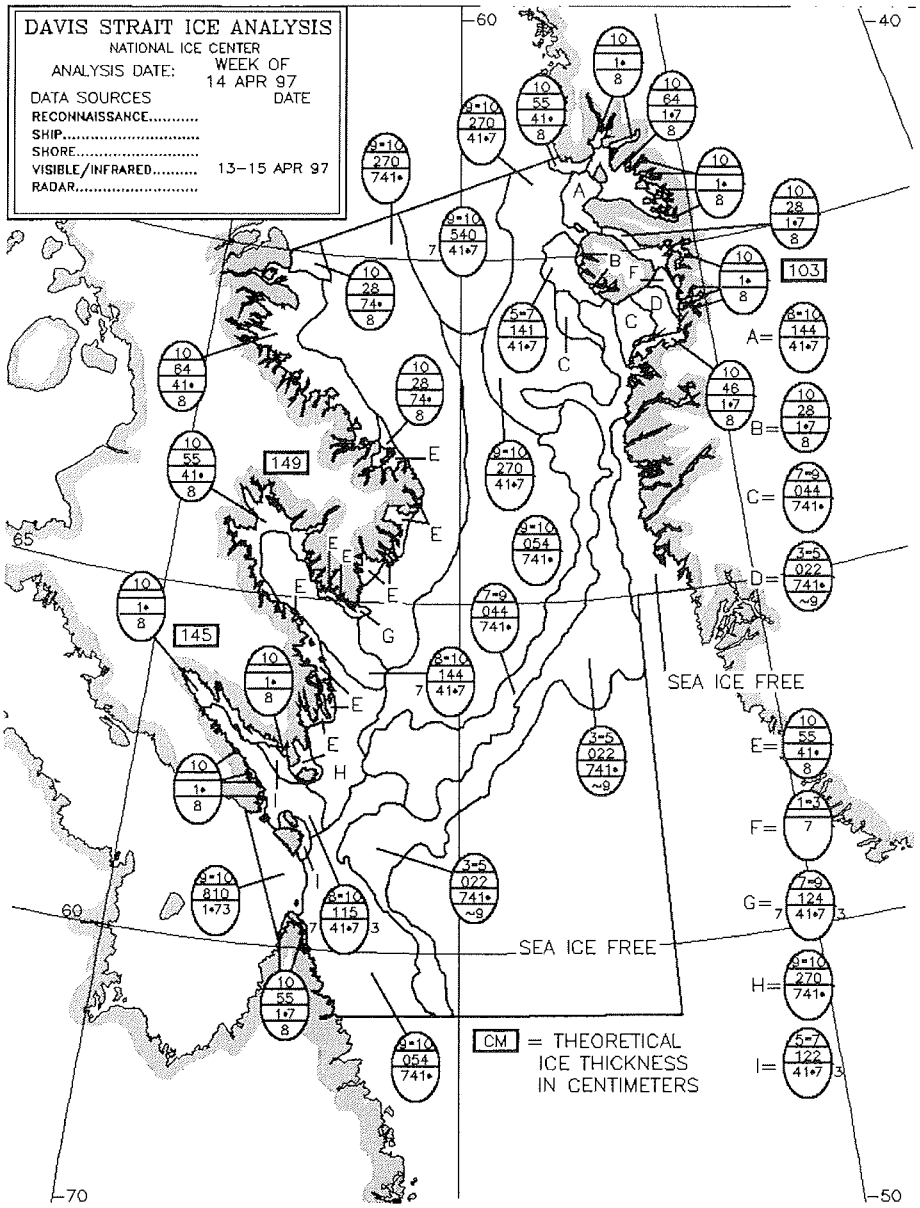

Fig.5.22: Sea ice map for the Davis Strait area from the NOAA National Ice Center valid for the week of 14 April 1997.

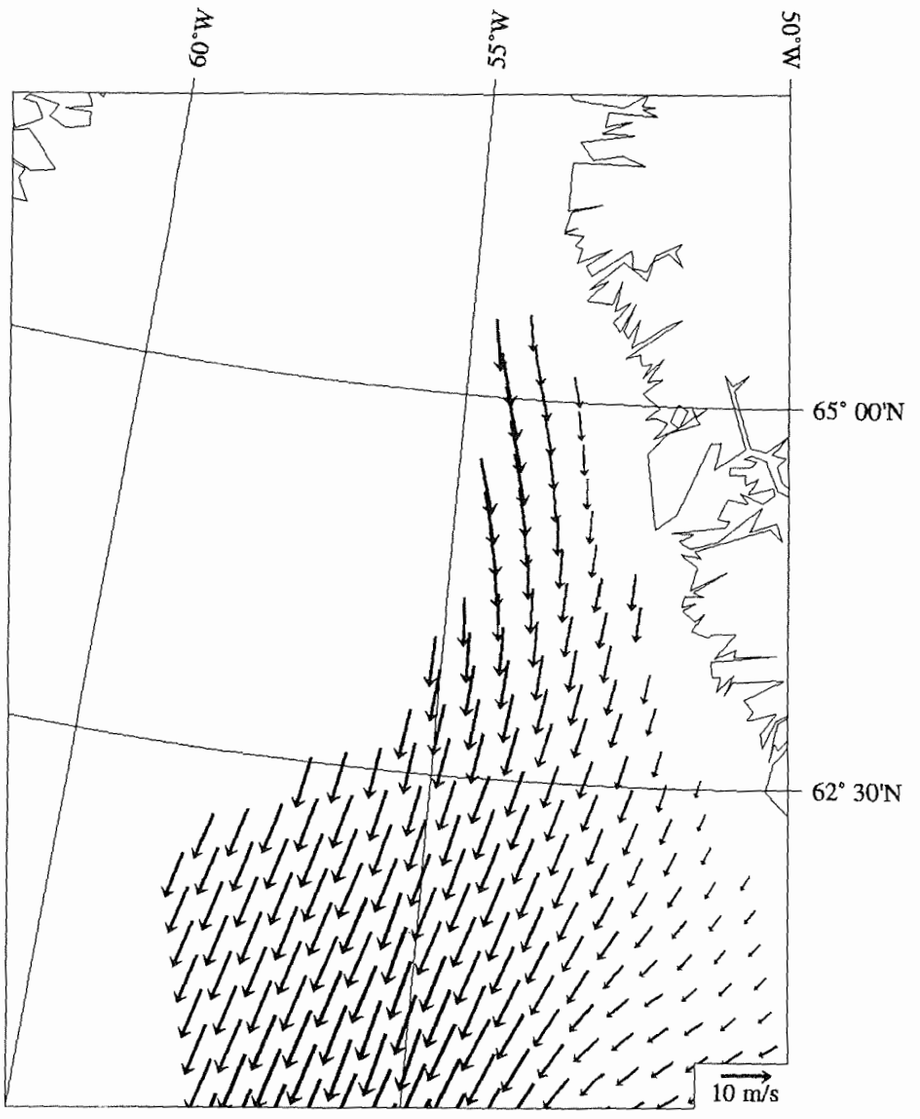

Fig.5.23: ERS-2 scatterometer wind vectors for the Davis Strait area for 0140 UTC 16 April 1997. A scaling vector is shown in the lower right corner. No wind retrievals are possible over the sea ice and near the sea ice margin. The strong cold air outbreak parallel to the sea ice edge at about 54°W is evident.

5.4.2 BLF2 19 April 1997

The synoptic situation was characterized by a high pressure system over Baffin Island, which caused the outflow of cold air at its eastern side. Forecasted 10 m winds were around 10 m/s from the north over the Davis Strait. The measuring area was northward of that of BLF1.

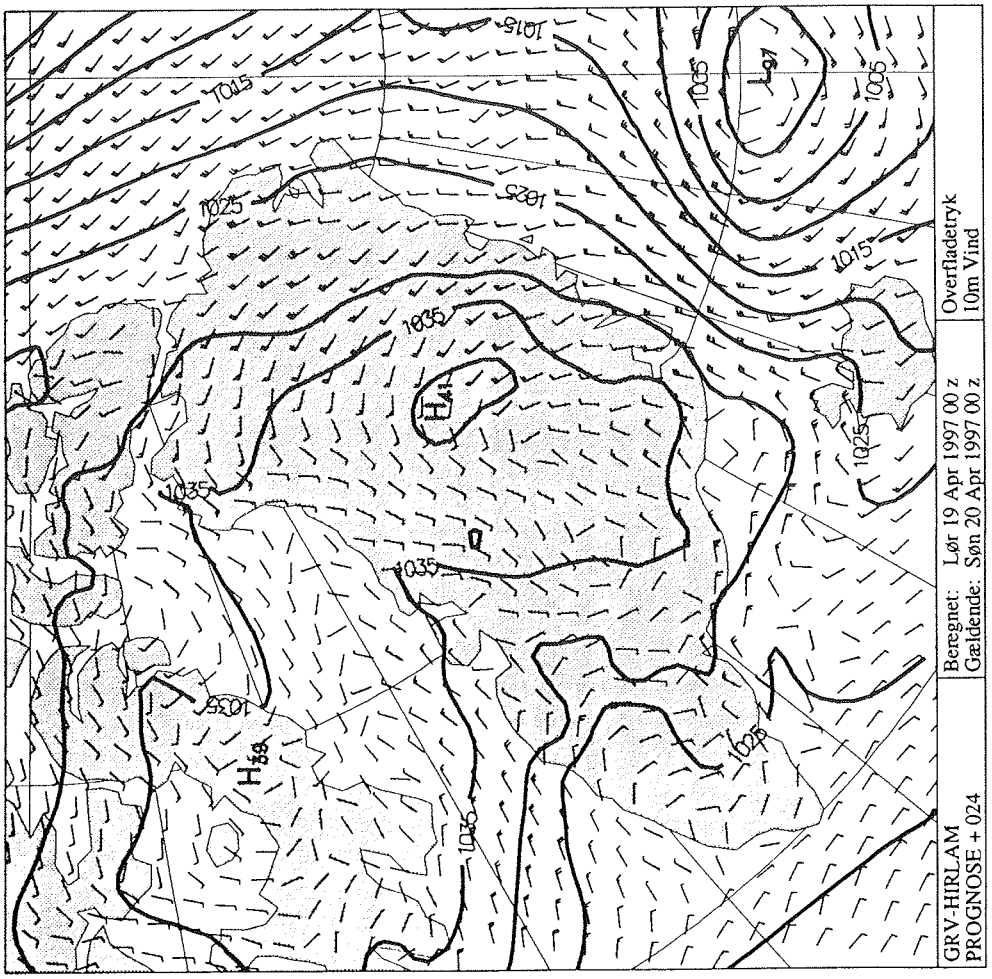

Fig.5.24a: As Fig.5.4a, but valid for 00 UTC 20 April 1997.

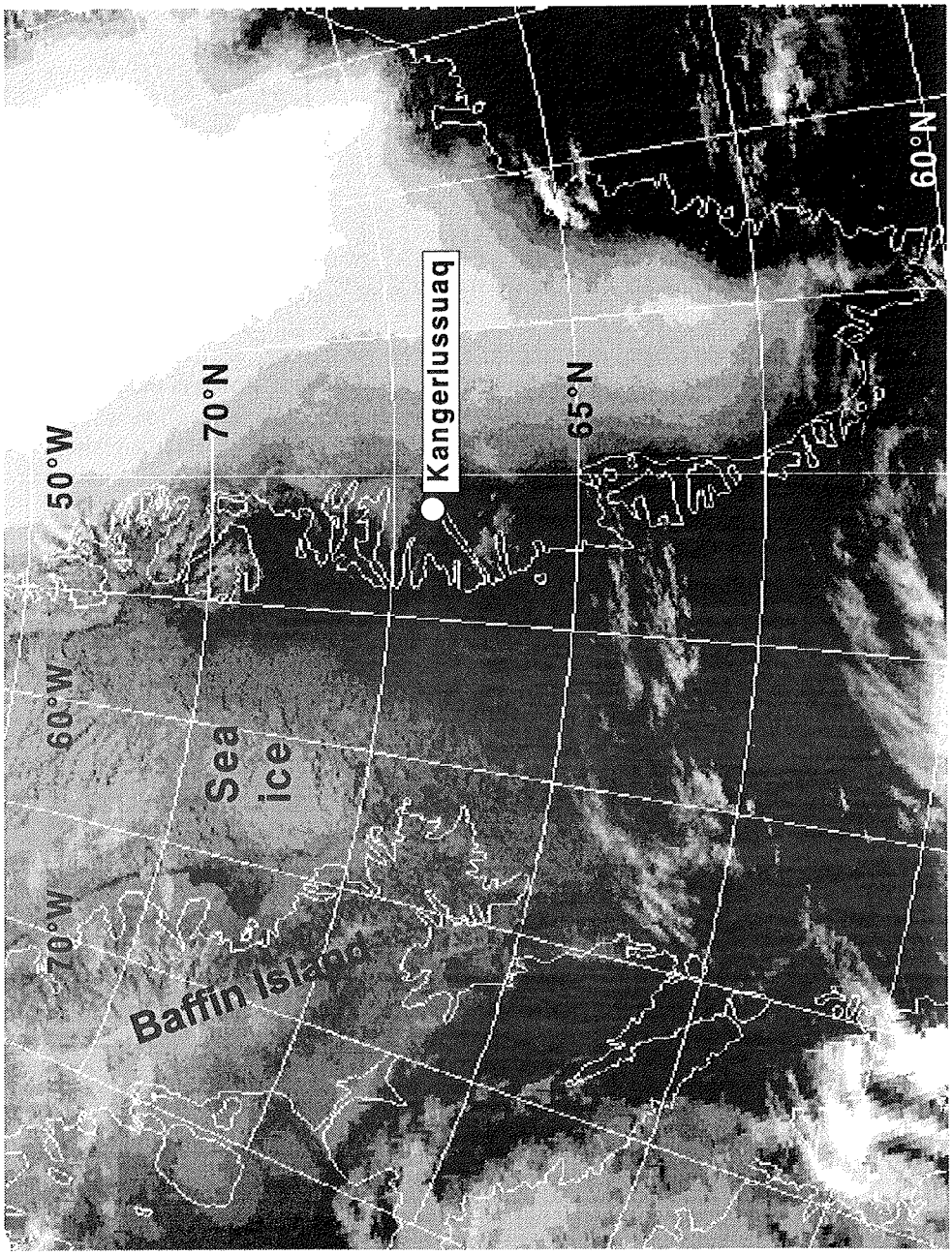

Fig.5.24b: GAC infrared image for 16 UTC 19 April 1997 (reduced resolution).

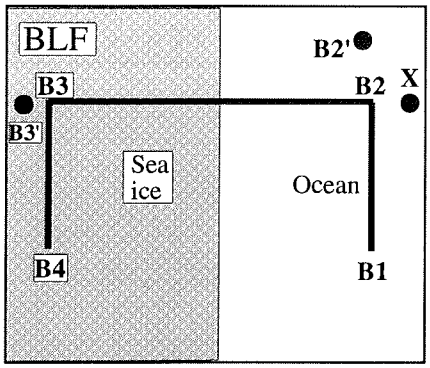

Way point coordinates		
Long.	Lat.	
-50.708	67.013	Kan
-54.003	66.839	B2'
-56.954	66.764	B3'
-54.520	66.417	B1
-54.558	66.778	B2
-56.412	66.782	B3
-56.436	66.418	B4
-54.224	66.801	X

Fig.5.25a: As Fig.5.21a, but for BLF2 on 19 April 1997.

After the transfer flight a temp was made at B2', then the ice edge was searched on the leg B2'-B3' and the points B1-B4 were defined. The full pattern was flown in temps, followed by three constant level legs along B1-B4 within the ABL. A cross-section with aircraft temps (B3-X) was performed at the end of the flight. Only low-level cloud coverage with Sc roll clouds were found near the sea ice front. The observed sea ice coverage was up to 9/10, which agrees with the sea ice map.

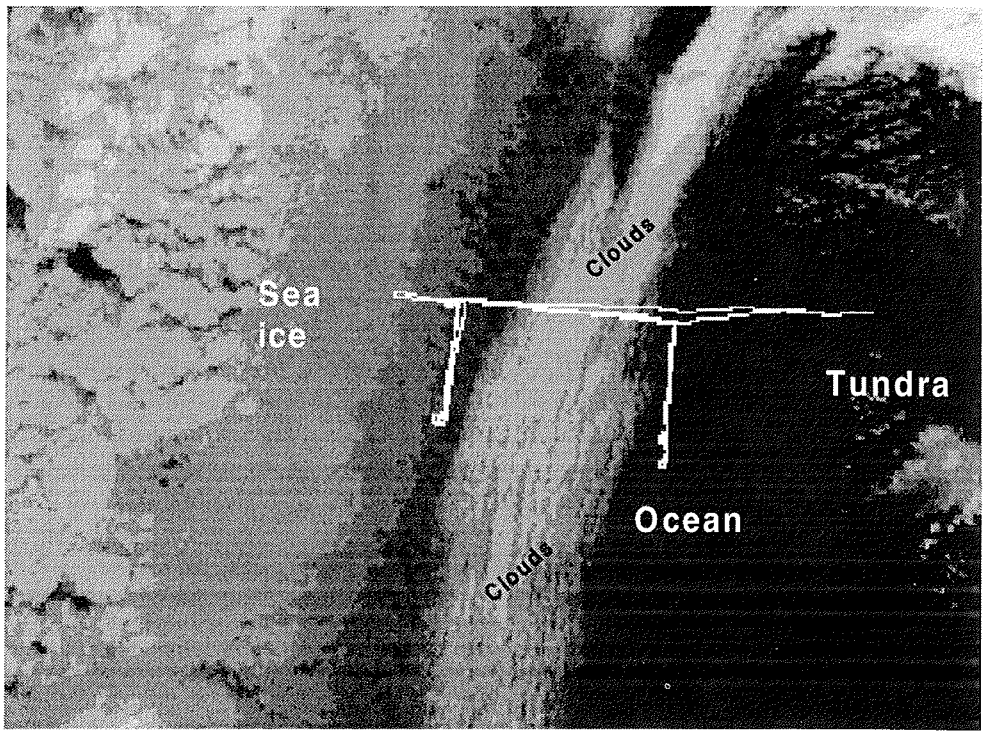

Fig.5.25b: HRPT infrared image for 19 April 1997, 16 UTC with the flight path superimposed.

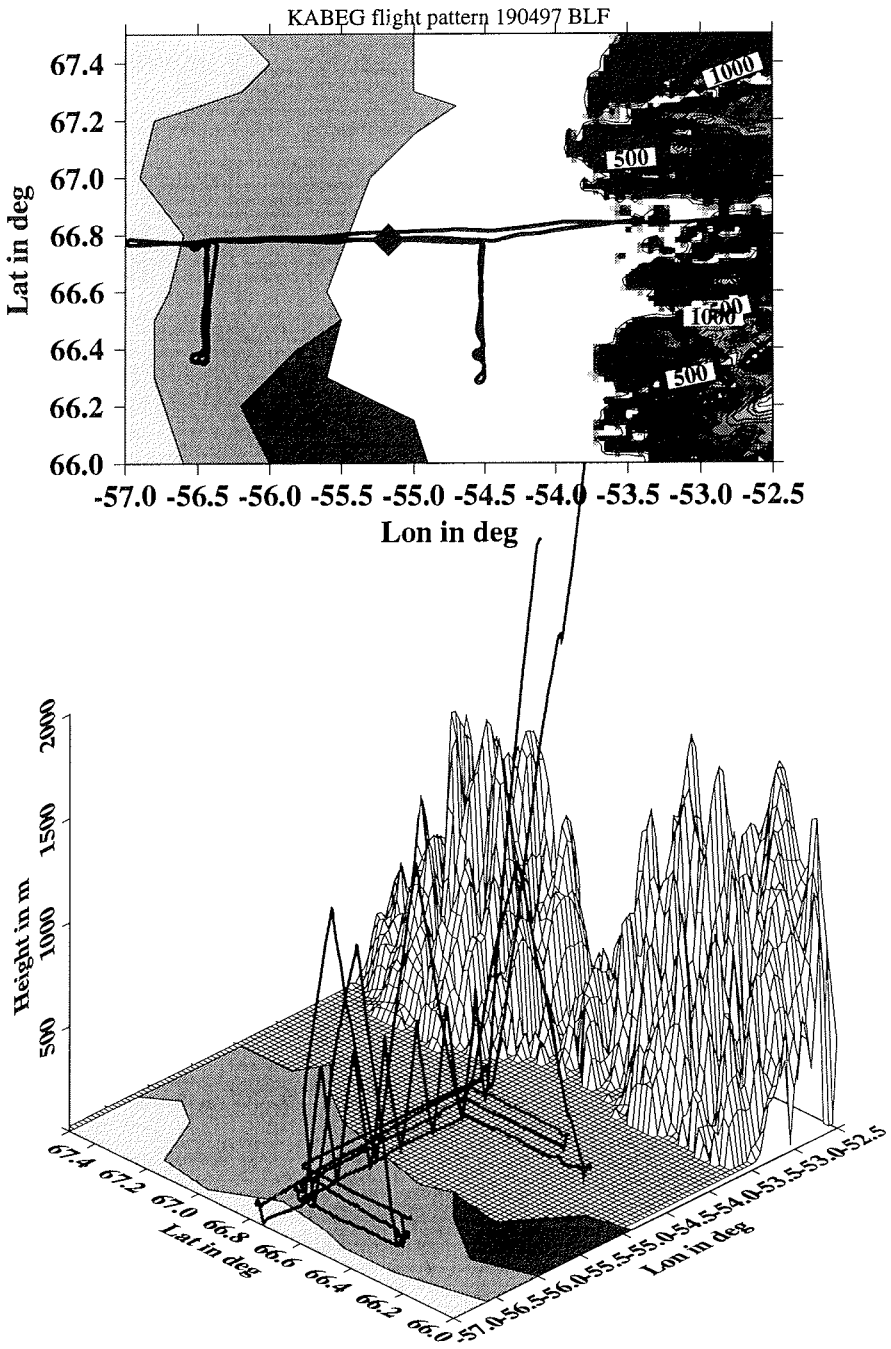

Fig.5.25 (continued): As Fig.5.21, but for BLF2. The ice concentration from NOAA weekly ice maps is indicated (dark gray: 1-3/10, medium gray: 5-7/10, and light gray: 9-10/10).

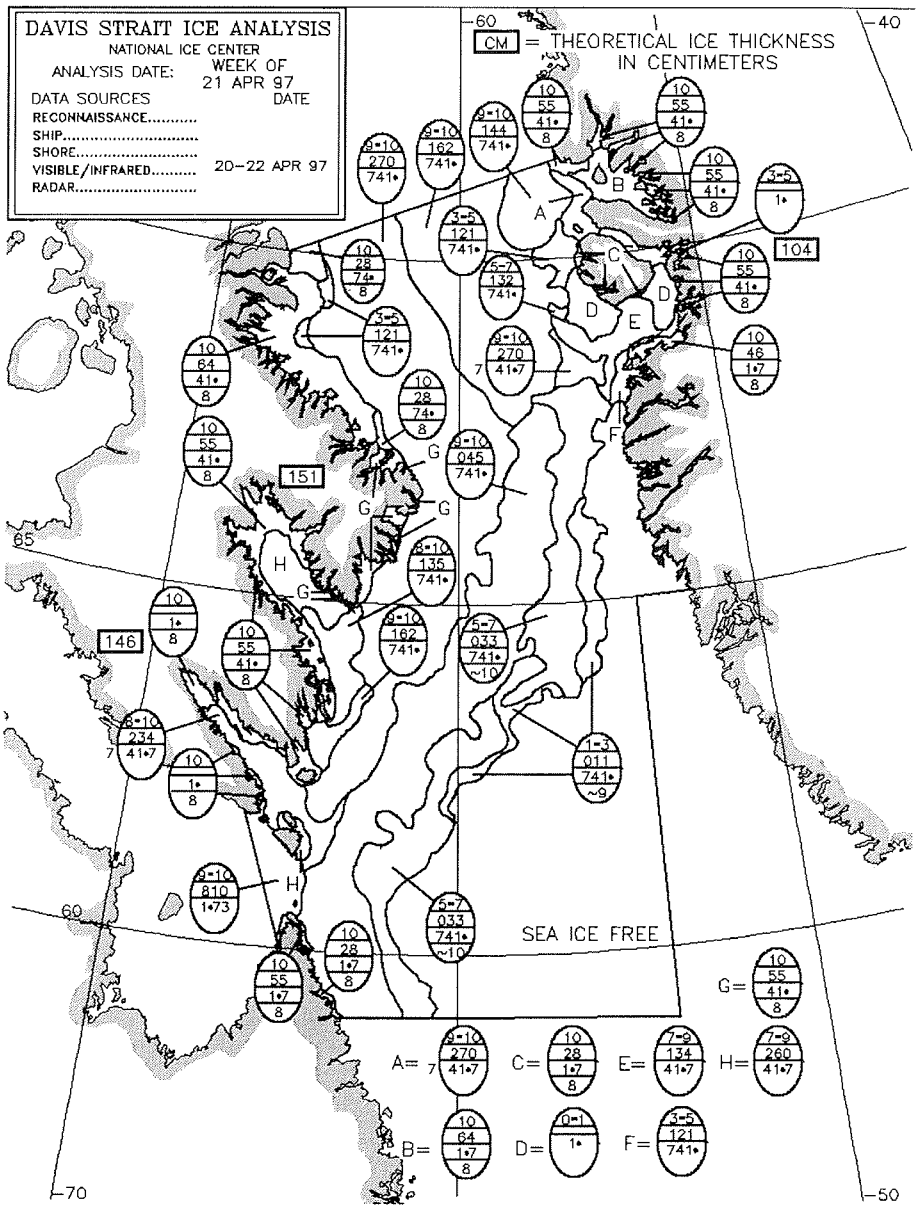

Fig.5.26: Sea ice map for the Davis Strait area from the NOAA National Ice Center valid for the week of 21 April 1997.

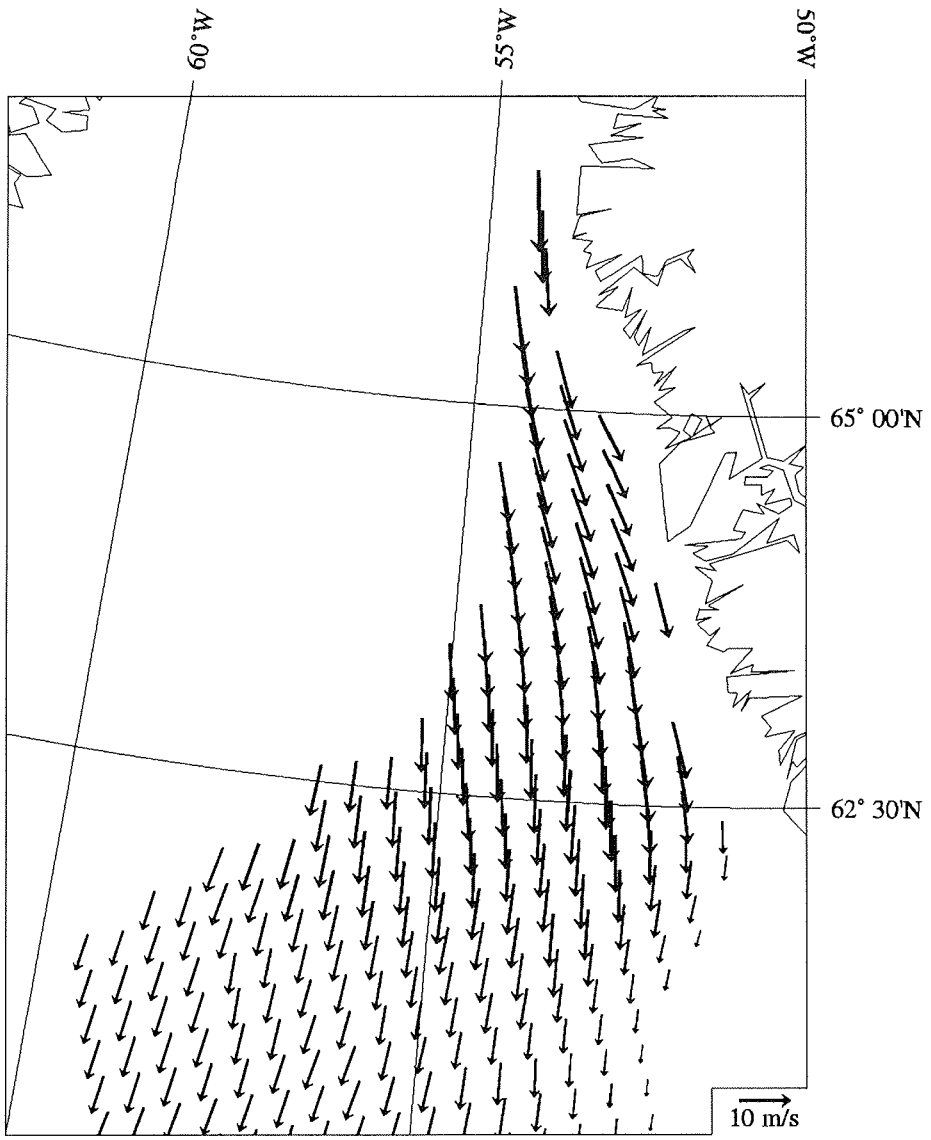

Fig.5.27: As Fig.5.23, but for ERS-2 scatterometer wind vectors for the Davis Strait area for 0140 UTC 19 April 1997. As on 16 April, a strong cold air outbreak parallel to the sea ice edge at about 54°W is present.

5.4.3 BLF3 24 April 1997

The synoptic situation was similar to that of BLF2. Again a high pressure system over Baffin Island and eastern Canada caused the outflow of cold air from the north over the Davis Strait. Forecasted 10 m winds were around 10 m/s. The measuring area was westward of that of BLF1. An extended area of low-level Sc clouds over the Davis Strait can be seen on the satellite image.

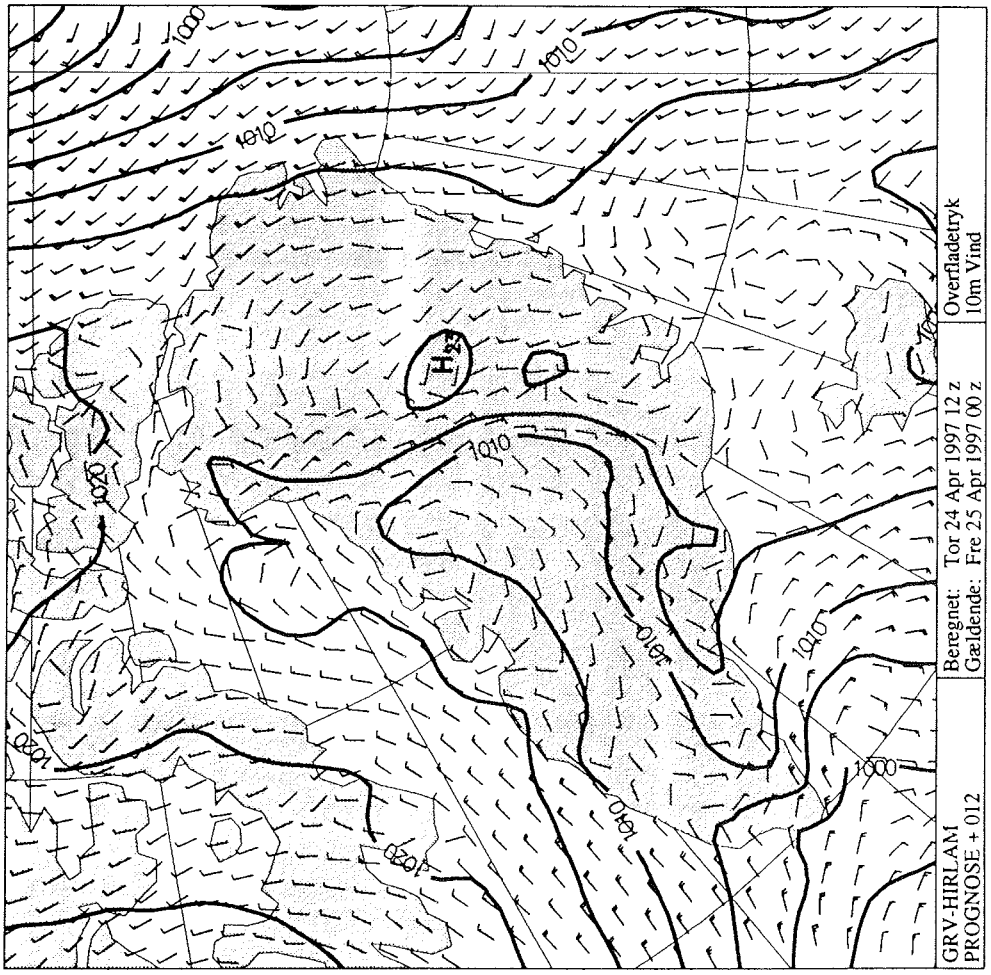

Fig.5.28a: As Fig.5.4a, but valid for 00 UTC 25 April 1997.

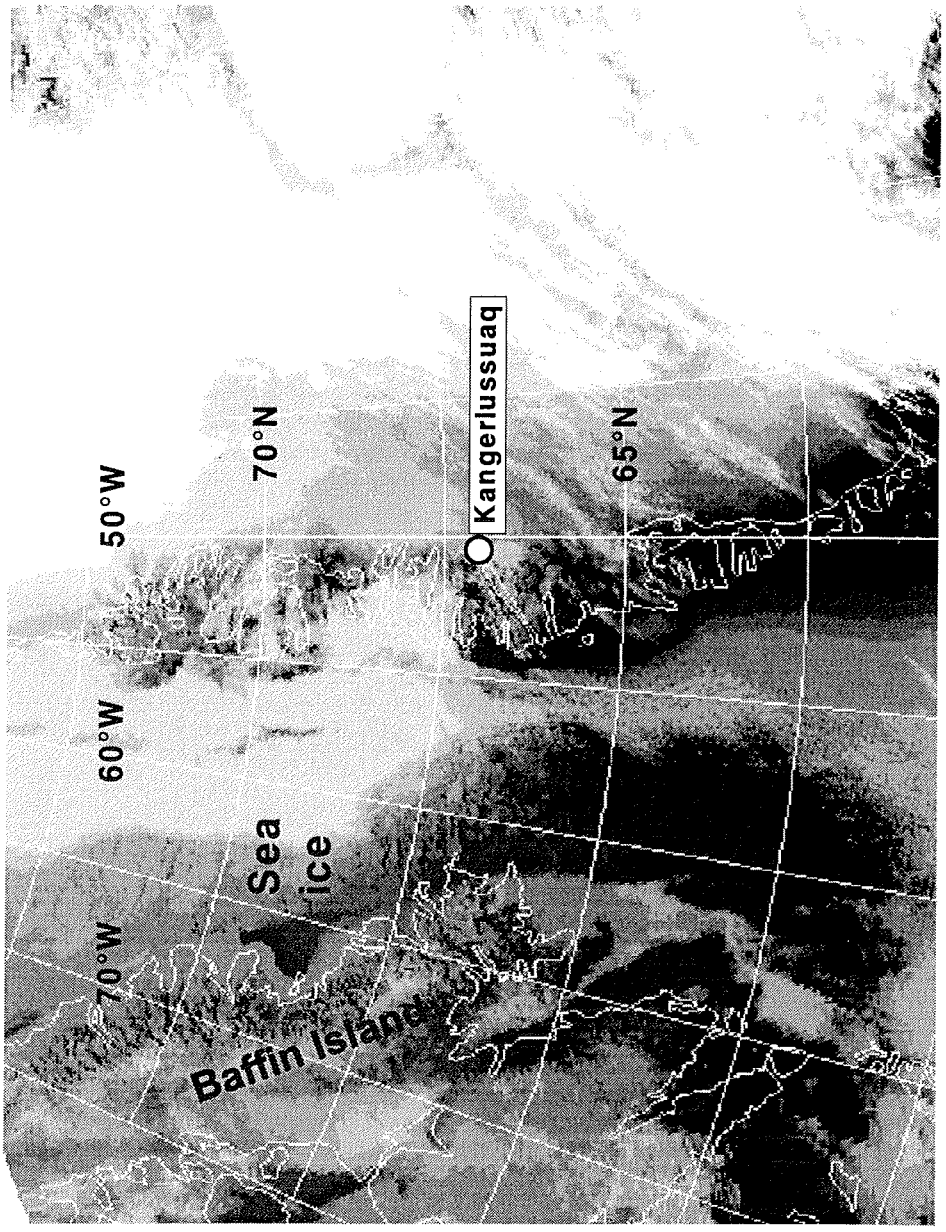

Fig.5.28b: GAC infrared image for 16 UTC 24 April 1997 (reduced resolution).

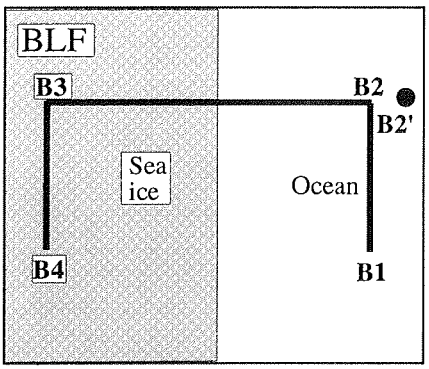

Way point coordinates

Long.	Lat.	
-50.708	67.013	Kan
-54.008	65.980	B2'
-57.006	65.637	B4
-57.016	66.000	B3
-55.179	66.001	B2
-55.141	65.636	B1

Fig.5.29a: As Fig.5.21a, but for BLF3 on 24 April 1997.

After the transfer flight a temp was made at B2', then the ice edge was searched and the points B1-B4 were defined. Because low-level Sc clouds streets with snow showers were encountered near the sea ice front, there was a risk of icing of the sensors when flying temps. Therefore, two constant level legs were first flown along B1-B4 within the ABL. Then a cross-section with aircraft temps (B2-B3) was performed without icing conditions. Three additional constant level legs were flown, one above and two within the ABL. The observed sea ice coverage was up to 8/10.

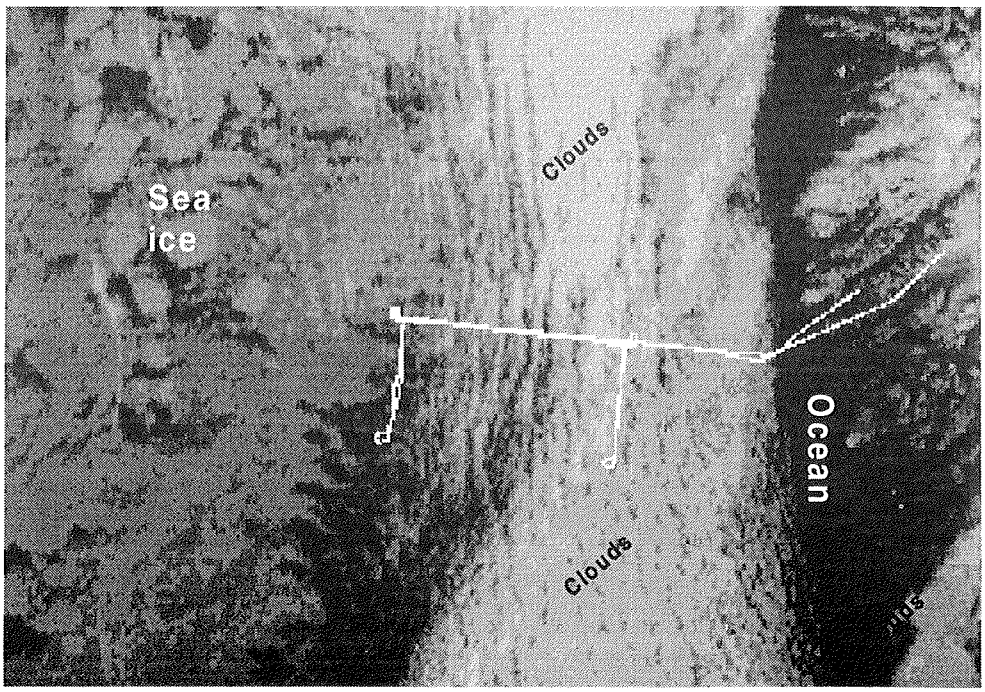

Fig.5.29b: HRPT infrared image for 24 April 1997, 16 UTC with the flight path superimposed.

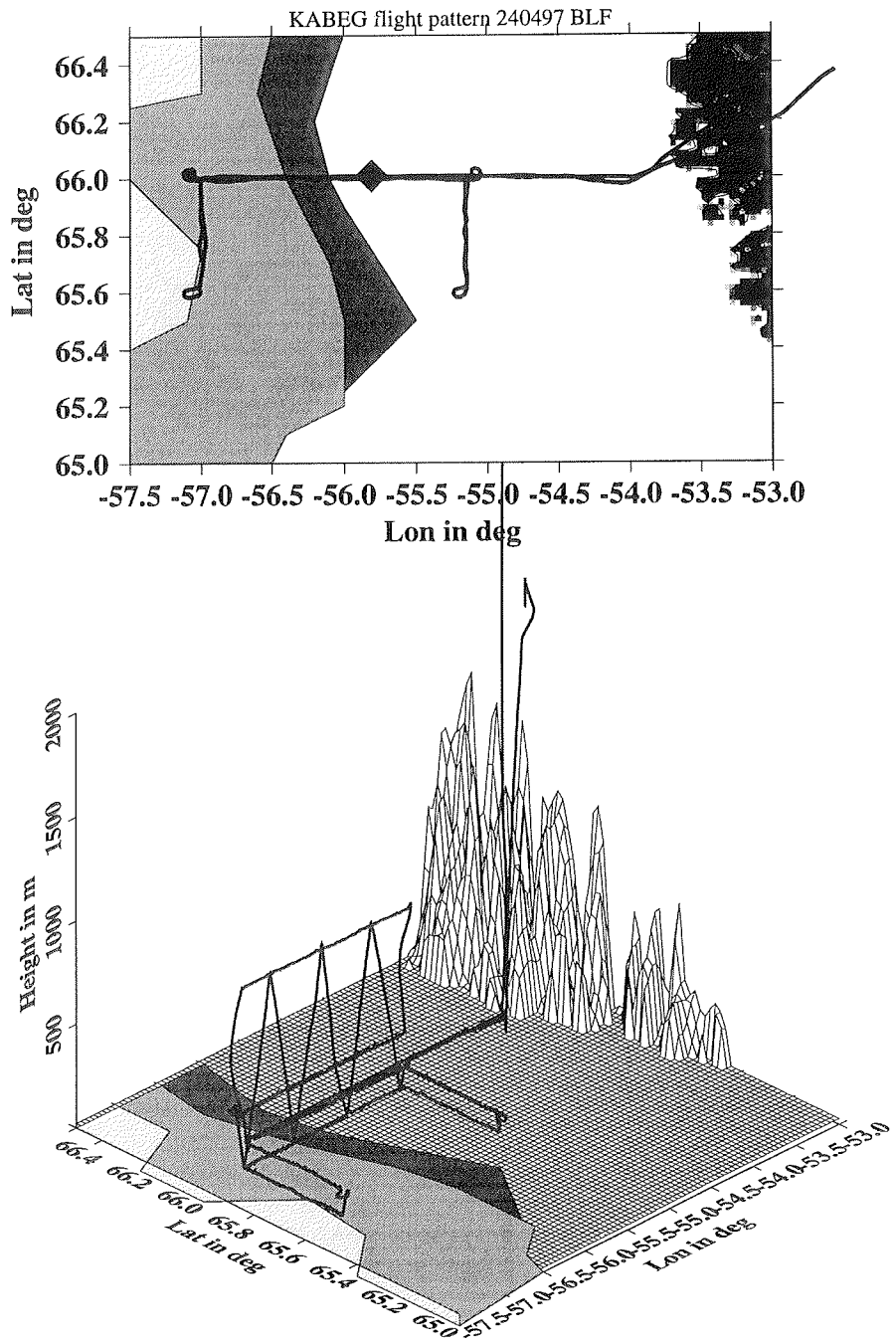

Fig.5.29 (continued): As Fig.5.21, but for BLF3. The ice concentration from NOAA weekly ice maps is indicated (dark gray: 1-3/10, medium gray: 7-9/10, and light gray: 9-10/10).

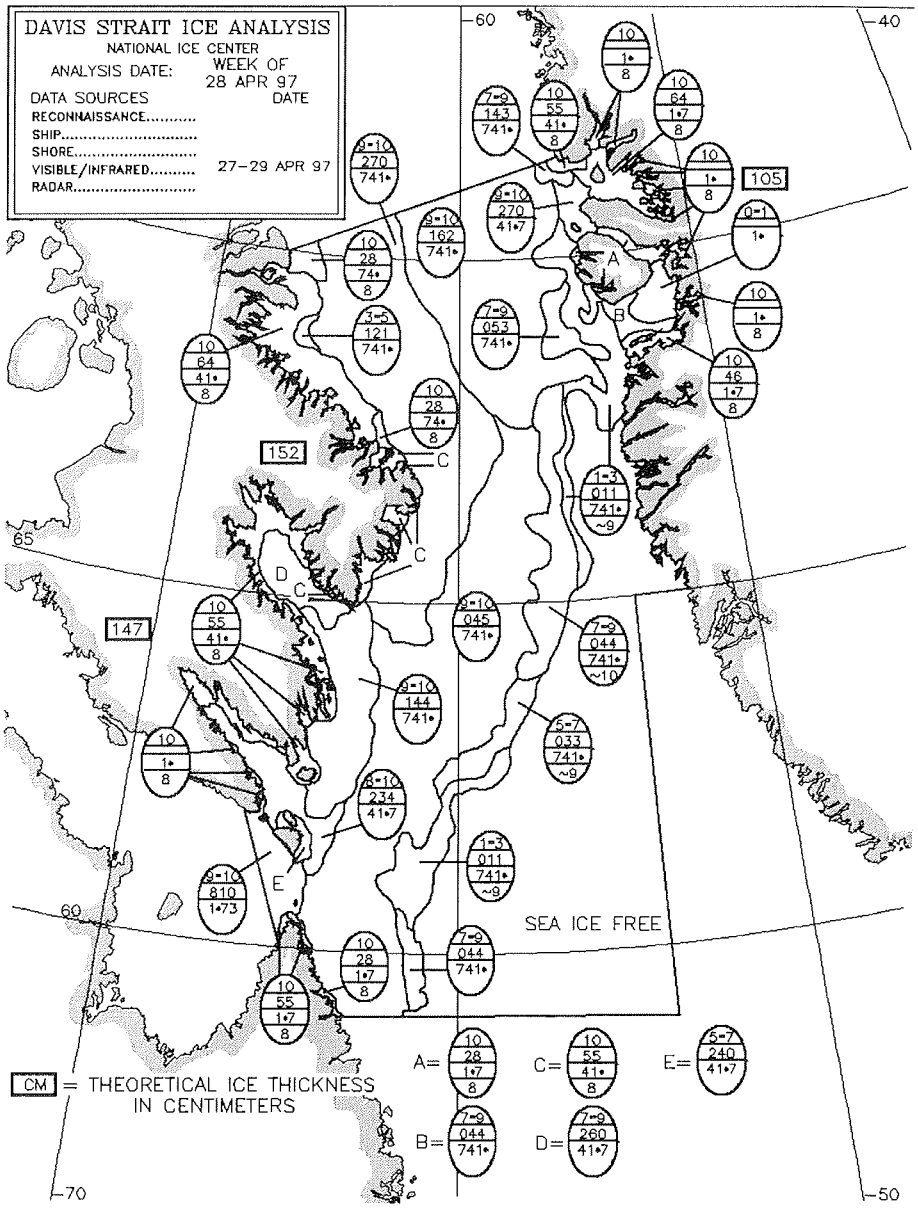

Fig.5.30: Sea ice map for the Davis Strait area from the NOAA National Ice Center valid for the week of 28 April 1997. North of 65°N the ice margin is found further westwards compared to two weeks before..

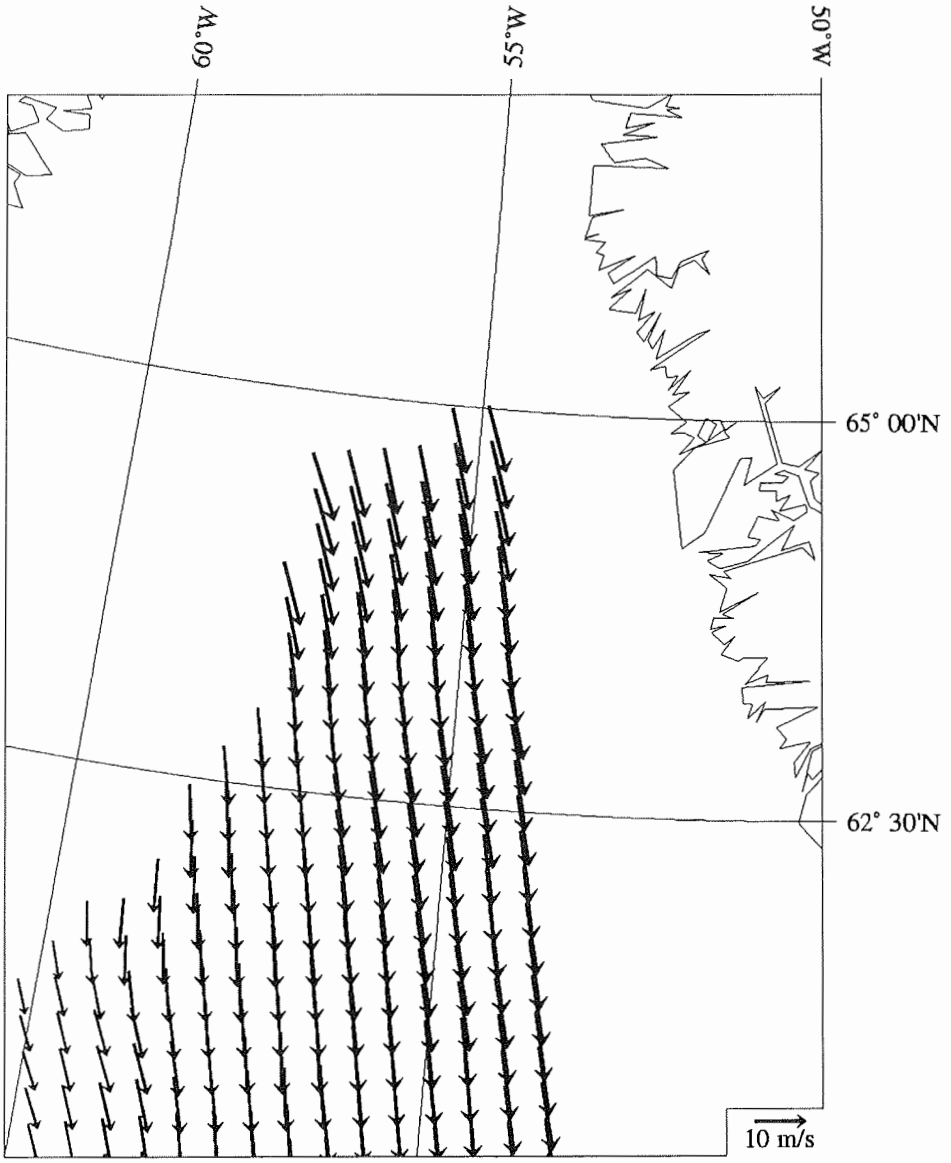

Fig.5.31: As Fig.5.23, but for ERS-2 scatterometer wind vectors for the Davis Strait area for 0140 UTC 25 April 1997. A scaling vector is shown in the lower right corner.

6. First results of the katabatic wind flight missions

6.1 18 April 1997

This was the first of the KABEG katabatic wind flights. The case represents an example of the katabatic wind system under weak synoptic forcing. Fig.6.1 shows vertical profiles for two aircraft temps over the ice at distances of about 25 km (Tpm) and 70 km (Tpo) from the edge of the inland ice (flown along the line Pa-Pb, see Section 5). The profiles are plotted against the METEOPOD radar height (i.e. above the surface). The lowest points for the profiles correspond to barometric heights of about 1300 and 1600 m, respectively. The profiles were flown between 0730 and 0745 UTC, which is about 3 hours later than the local solar time (LST) and just before sunrise. A pronounced surface inversion of about 8K/150m is present in the lowest 200 m. A low-level jet (LLJ) at a height of 60-90 m with wind speeds of about 15 m/s is found in both profiles. The wind direction changes from 135° near the surface (i.e. 45° relative to the slope) to 180° above the LLJ (i.e. perpendicular to the slope) for the Tpo profile. For the lower Tpm profile the LLJ is shallower and wind speeds decrease to 2 m/s at heights of 200-400 m above the surface. The wind direction in this weak wind layer turns to westerly and northwesterly directions. Therefore, the wind speed anomaly associated with the katabatic wind is about 10 m/s.

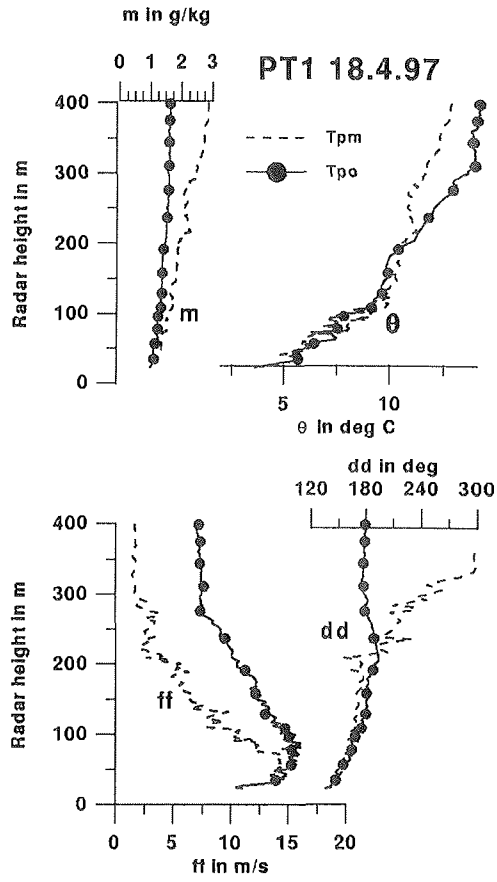

Fig.6.1: Aircraft temps on 18 April over the ice along the line P. Upper panels show mixing ratio (m) and potential temperature (θ), lower panels display wind speed (ff) and wind direction (dd). For details see text.

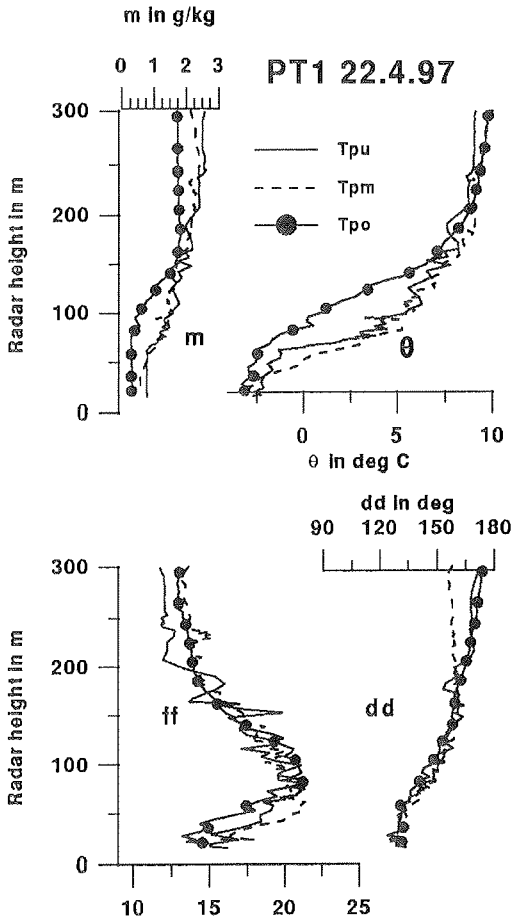

Fig.6.2: As Fig.6.1, but for 22 April.

6.2 22 April 1997

This case represents an example of the katabatic wind system under strong synoptic forcing. At that time most of the tundra area was snow covered and near-surface temperatures were relatively low (see Section 4). Fig.6.2 shows vertical profiles for three aircraft temps over the ice at distances of about 10 km (Tpu), 25 km (Tpm) and 75 km (Tpo) from the edge of the inland ice. The lowest points for the three profiles correspond to baro metric heights of 1100, 1300 and 1500 m, respectively. The profiles were flown between 0725 and 0745 UTC. A well-developed katabatic wind system can be seen in the wind speed profile. A LLJ with more than 22 m/s is found at a height of about 100 m. Compared to the case of 18 April the wind speed at heights above 200 m is much higher (13 m/s), which reflects the strong synoptic wind from southerly directions. The profiles of the potential temperature show a strong surface inversion of more than 10K/100m. In contrast to 18 April, the boundary layer structure is also obvious in the humidity profiles, since the real temperatures in the lowest layers are -11°C and -16°C for the Tpu and the Tpo profiles, respectively (being about 7°C cooler compared to 18 April). The three profiles show only little variation with respect to the wind speed profile along the flight leg Pa-Pb.

One of the scientific goals of KABEG is to investigate the 3D structure of the katabatic wind system. Therefore, studies of the variation of the katabatic wind system perpendicular to the gradient of the topography (i.e. approximately north-south) along the lines Q1 and Q2 (Fig.5.1) are of particular interest. Fig.6.3 shows three profiles along Q1, which were flown around 0930 UTC, i.e. about 2 h later than the temps shown in Fig.6.2. Temp Ta is the southernmost point of Q1, temp Tm lies over the line P and temp Te is the northernmost point of Q1. The lowest points for the three profiles correspond to barometric heights of about 1500 m. The surface inversion and the low-level jet are again well developed, but significant differences are present. An increase in wind speed of several m/s is found with the northernmost profile revealing the highest values. These

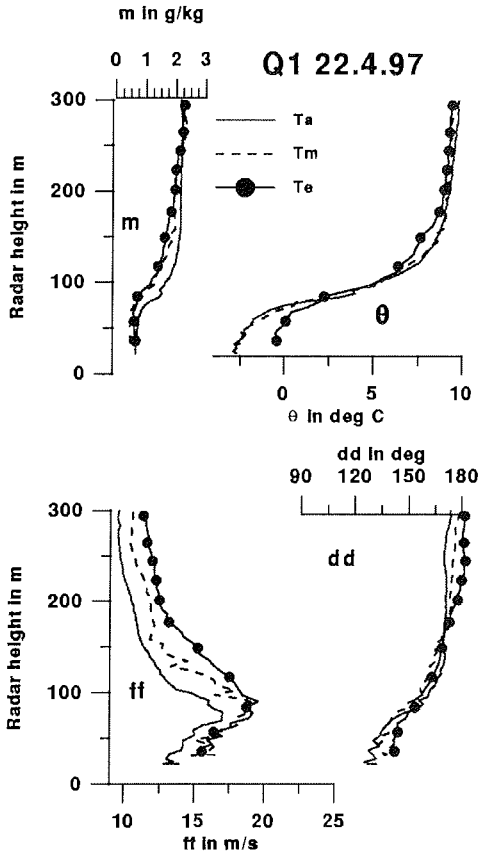

Fig.6.3: As Fig.6.2, but along the line Q1.

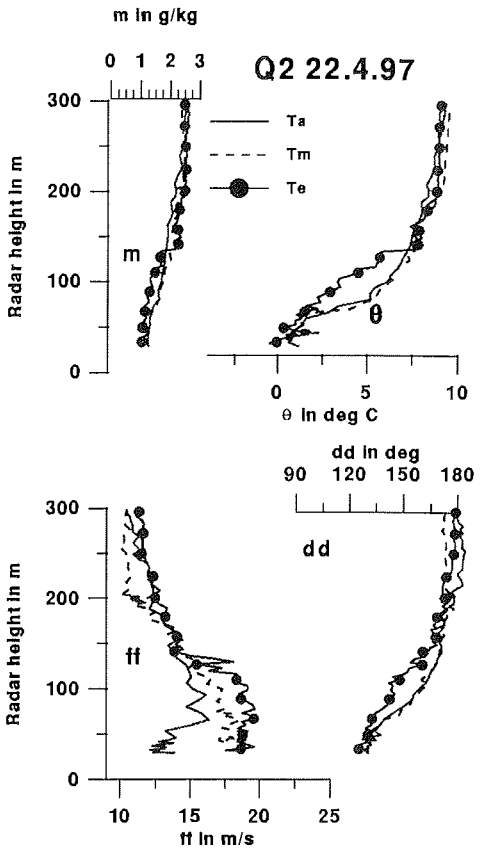

Fig.6.4: As Fig.6.2, but along the line Q2.

gradients (particularly in the wind speed) are also present along the line Q2 (Fig.6.3, see Fig.5.1 for the position of Q2). While for temp Ta at the southernmost point of Q2 wind speeds of 8 m/s are found at the lowest levels, the wind increases along Q2 and reaches values of up to 18 m/s at the northernmost point of Q2. This effect is also discussed in the next section.

6.3 13 May 1997

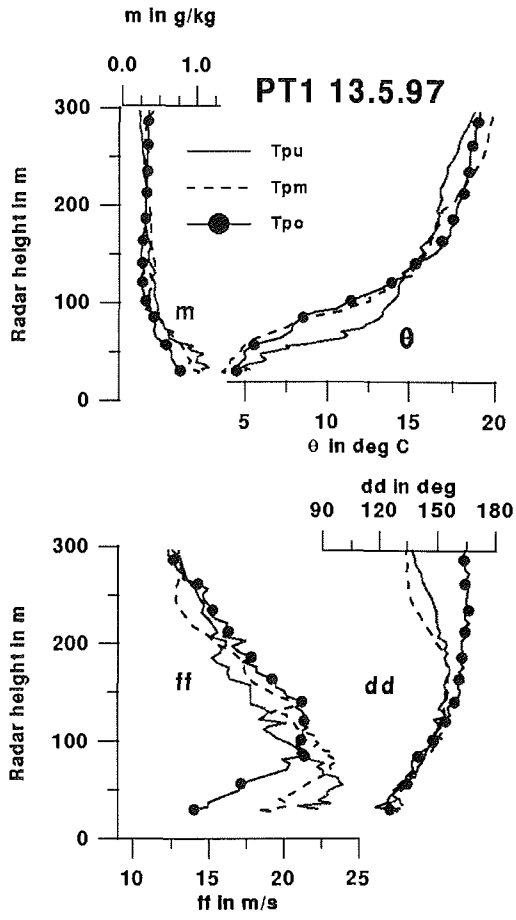

Fig.6.5: As Fig.6.2, but for the flight 13 May.

This case represents again an example of the katabatic wind system under strong synoptic forcing. But, in contrast to 22 April most of the tundra area was snow-free and near-surface temperatures were relatively high (cf. Section 4). Fig.6.5 shows vertical profiles for three aircraft temps over the ice at approximately the same locations as for 22 April. The profiles were flown between 0625 and 0645 UTC, which is again around local sunrise. Like on 22 April the profiles show a strong surface inversion of more than 10K/100m, but temperatures are considerably higher (real temperatures near the surface were -4°C and -9°C for the Tpu and Tpo temps, respectively). The LLJ is even more pronounced than on 22 April and wind speeds reach almost 25 m/s. The three profiles show a distinct variation along the flight leg. An acceleration of the wind close to the ice edge is found in the lower layers, which leads to a sharper wind maximum closer to the ice edge. Like on 22 April, the boundary layer structure is also present in the humidity profiles, but in this case the humidities above the stable boundary layer are extremely low (around 0.3 g/kg), while the evaporation at the surface and in the drifting snow leads to values around 1.0 g/kg at low levels.

Again, the variation of the katabatic wind system perpendicular to the gradient of the topography is studied along the lines Q1 and Q2 (see Fig.5.1). Fig.6.6 shows three profiles Ta, Tm and Te along Q1, which were flown around 1010 UTC, i.e. about 3 h later than the temps shown in Fig.6.5. The surface inversion and the low-level jet are again well developed and the katabatic wind system can be regarded to be homogeneous perpendicular to the gradient of the topography for this situation. In contrast, the profiles along Q2 (flown around 950 UTC) show significant differences perpendicular to the gradient of the topography. While for temp Ta at the southernmost point of Q2 wind speeds of 15 m/s were found at the lowest levels, the wind increases along Q2 and reaches values of up to 25 m/s at the northernmost point of Q2.

A cross-section of the wind speed and the potential temperature interpolated from the aircraft temps and constant level flights along the line P is shown in Fig.6.8. Unlike the

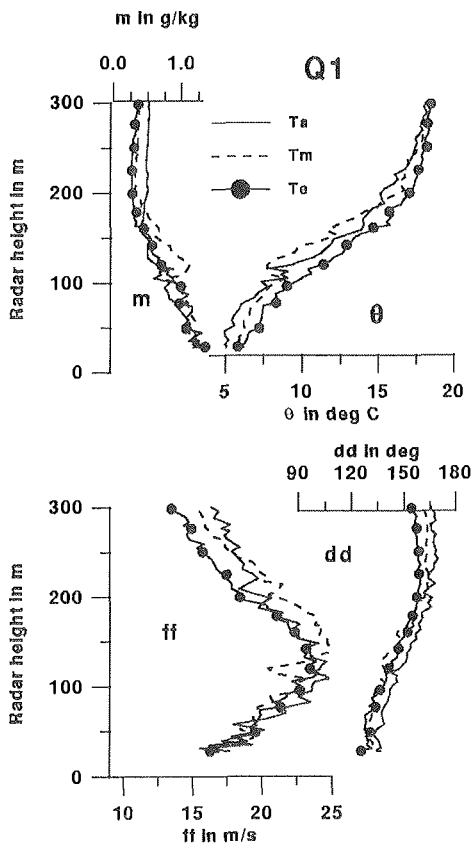

Fig.6.6: As Fig.6.5, but along Q1

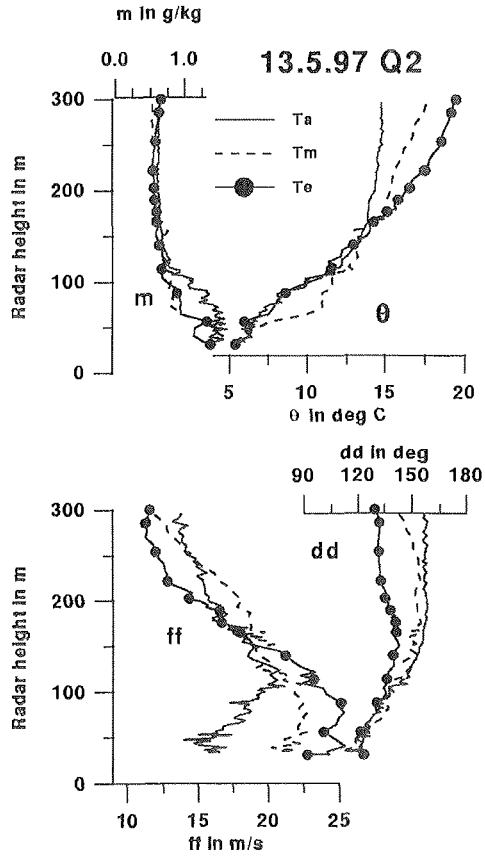

Fig.6.7: As Fig.6.6, but along Q2.

profiles shown before, the vertical coordinate is the barometric height. The topography calculated as the difference between barometric height and radar height from the lowest constant level flight is displayed in black (the variations over the ice do not correspond to real topography structures, since deviations of the aircraft position from the horizontal cause a variation in the radar height when flying over the sloped terrain). The shallow stable layer over the ice sheet is evident, which is associated with high downslope wind speeds. At the ice edge (horizontal coordinate +20 km) a strong wind convergence is present. Strong up- and downdrafts and severe turbulence were encountered at this convergence zone during the flight.

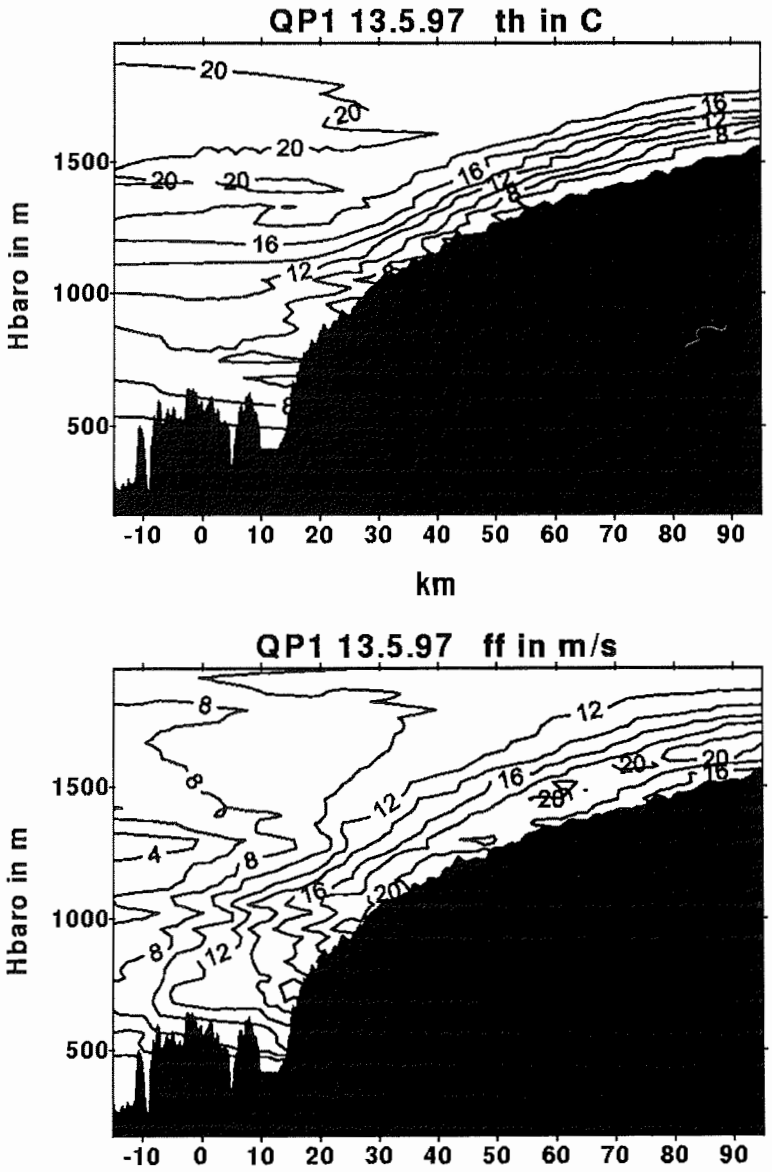

Fig.6.8: Cross-section along P for 13 May 1997, 630 UTC. Upper panel: potential temperature (in °C); lower panel: wind speed (in m/s).

6.4 Concluding remarks

A total of 9 katabatic wind flights were performed during KABEG. While the three flights for the programs K2 and K3 took place on two days, the flights for K1 were made under quite different synoptic situations and surface conditions (see Tab.5.2). The first results presented in the previous sections rely on the quicklook data (1 Hz data sampled from the 120 Hz raw data) of the aircraft data set. This data gives a first insight into the structures of the katabatic wind system, but a detailed investigation using the full data set for the computation of turbulent fluxes, boundary layer budget etc. will remain a challeging task for the future.

The dependance of the 3D structure of the katabatic wind system on synoptic forcing and boundary conditions over the ice and the tundra seems to be quite complex. The fact that profiles perpendicular to the gradient of the topography yielded significant differences may be surprising, since previous studies using data from the GIMEX experiment (Van den Broeke et al., 1994), which was performed in the same area, have argued that the katabatic wind system can be regarded as being two-dimensional for the interpretation of measurements as well as for numerical simulations (e.g. Gallée and Duynkerke, 1997). However, a closer inspection of the topography reveals a slight valley-like structure in the area of the aircraft measurements of K1. This may explain in part the observed variations of the boundary layer structure in an area, which - at a first view- seems to be a region of almost homogeneous topography in the north-south direction.

7. First results of the BLF flight missions

7.1 15 April 1997

This was the first of the KABEG BLF flights and it took place during an cold air outbreak over the Davis Strait under conditions of low-level flow parallel to the sea ice edge wind speeds of about 20 m/s. The different structure of the boundary layer over the open water and over the sea ice is illustrated by the two aircraft temps shown in Fig.7.1 (1 Hz data sampled from the 120 Hz raw data). The solid line without symbols represents the METEOPOD data on 15 April over the ocean (1630 UTC), the line with triangles the METEOPOD over the sea ice (1715 UTC). Over the open water the profile of the potential temperature shows values of about -9 °C in the well-mixed lowest 400 m and a well pronounced inversion being coincident with a marked decrease in specific humidity. The wind vector reflects the turbulent structure of the boundary layer with mean values of about 20 m/s and northerly directions. Above the inversion, the wind speed decreases and the wind turns to a direction of 20°. The profiles over the sea ice reflect the marked temperature contrast associated with the BLF. The boundary layer height over the sea ice is about 100 m lower than over the open water, and the temperatures are about 5 K lower, corresponding to a horizontal temperature gradient of about 10K/100km, which is almost twice as large as that observed by Shaw et al. (1991). A large difference in the wind speed profile can also be noticed.

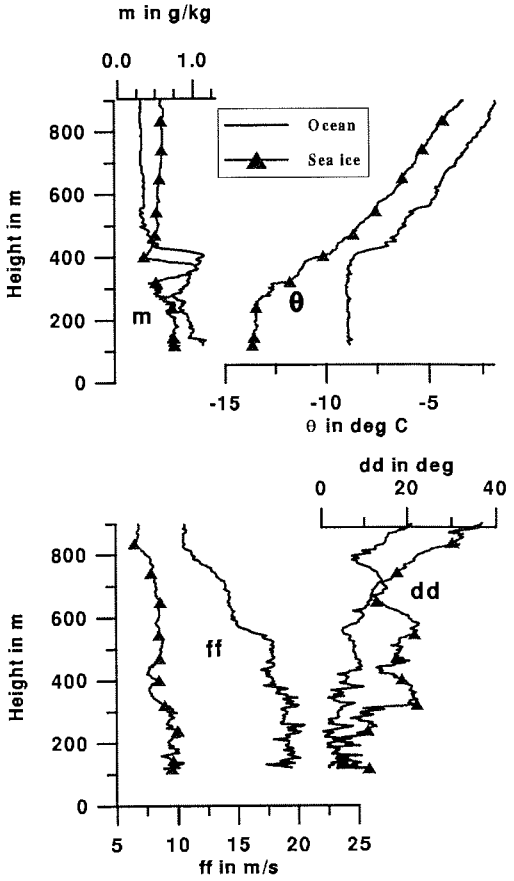

Fig.7.1. Vertical profiles of mixing ratio (m), potential temperature (θ), wind speed (ff) and direction (dd) over the Davis Strait for 1630UTC and 17.15 UTC 15 April (lines without symbols: open water; lines with triangles: sea ice).

The aircraft temp over the sea ice at 1715 UTC allows a comparison with the GPS dropsonde deployed a few minutes later at about the same location. Fig.7.2 displays the same aircraft data as Fig.7.1, but for the comparison with the dropsonde pressure was chosen as the vertical coordinate, since this is the primary height information from the

dropsonde (1 Hz data). The potential temperature profiles agree very well and indicate the strong stability of the inversion above the shallow boundary layer. Larger differences occur for the humidity profiles. While the dropsonde profile shows high specific humidities in the boundary layer and a marked decrease at the capping inversion, the humidity profile from the Lyman-α sensor (line with triangles) shows a different behaviour. The Lyman-α profile reveals an unexpected peak at the top of the boundary layer and lower humidity values in the mixed layer. The latter can be attributed to the coupling of the fast Lyman-α data with the data of the slow humicap humidity sensor, which is necessary due to the drift of the Lyman-α sensor, but results in often too low values of the coupled data. This is illustrated by the profile of the METEOPOD dew point mirror data (line with circles), with are significantly higher than the coupled Lyman-α data. The peak at the inversion is also present, but is smeared out due to the slower response of the dew point mirror during the ascent of the aircraft. Therefore, a re-evaluation of the aircraft humidity data seems to be necessary.

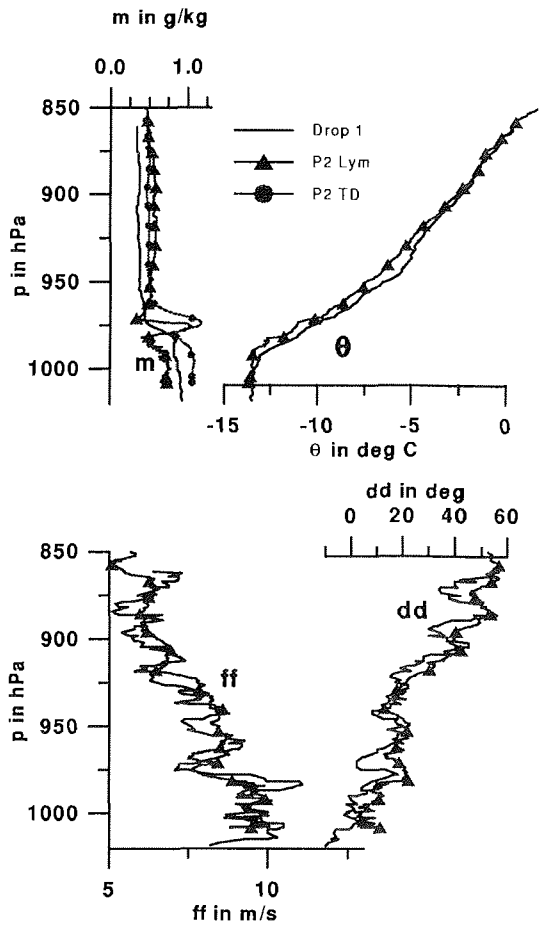

Fig.7.2. Comparison of the vertical profiles of mixing ratio (m), potential temperature (θ), wind speed (ff) and direction (dd) from METEOPOD and dropsonde data over the sea ice (lines without symbols: dropsonde; lines with symbols: METEOPOD, see text).

An interesting question was the quality of the wind data from the GPS dropsonde. The comparison of the curves in Fig.7.2 shows relative good agreement between the dropsonde and the METEOPOD data both for the wind speed and the wind direction. A comparison of details is difficult, because turbulent fluctuations are included in the aircraft data on the one hand, while errors due to the parachute oscillations are present in the dropsonde data on the other hand. The tests prior to KABEG showed that the latter errors were around 1 m/s, which is larger than the error expected from the GPS. In summary, the comparison shows that the dropsonde profiles of all parameters are able to represent the mean boundary layer structure in the same way as the aircraft temps with respect to mean quantities.

The gradients in the boundary layer structure normal to the sea ice front are shown in Fig.7.3, where the GPS dropsonde profiles for the sondes 3 (over the sea ice), sonde 5 (at the sea ice idge) and sonde 6 over the ocean are displayed. The BLF structure can be seen as a pronounced increase in inversion height from the sea ice to the open water, which is associated with a marked increase in the wind speed. Relatively weak winds are present at heights above 800 m. Apart from the baroclinicity in the boundary layer a superimposed baroclinicity is also present for layers above the capping inversion (cf. also Fig.7.1). It should be noted that the length of the cross-section is about 80 km.

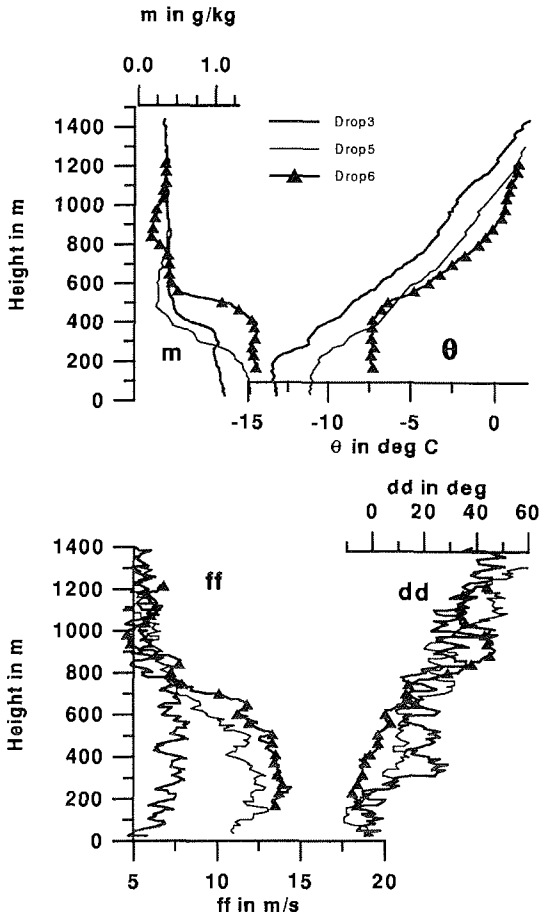

Fig.7.3. As Fig.7.1, but for the dropsonde data of sonde 3 over the sea ice (thick lines), sonde 5 at the sea ice edge (thin lines) and sonde 6 over the open water (lines with symbols).

7.2 Concluding remarks

A total of 3 BLF flights were performed during KABEG. Only during April the conditions were favourate for the BLF program, while temperatures were too high during May for establishing a strong air-sea temperature contrast. The three flights were made during similar low-level flow conditions, but under different synoptic situations with respect to the flow above the boundary layer (see Tab.5.1). As for the katabatic wind flights, the quicklook data gives a first insight into the main structures, but a detailed investigation with the goal of obtaining a full boundary layer budget will be left for future work.

8. Abbreviations

A1-A4	MIUB AWS on the ice sheet during KABEG
ACE	Arctic Cyclone Experiment
AVHRR	Advanced Very High Resolution Radiometer
AWI	Alfred-Wegener-Institut für Polar- und Meeresforschung
AWS	automatic weather station
BAS	British Antarctic Survey
BH	barometric flight height
BLF	boundary layer front
BLF1-3	BLF flight missions during KABEG
CEAREX	Coordinated Eastern Arctic Experiment
DLR	Deutsches Zentrum für Luft- und Raumfahrt
DMI	Danish Meteorological Institute
ECMWF	European Centre for Medium Range Weather Forecasts
ERS	European Remote Sensing Satellite
ERS-SCAT	ERS scatterometer
GAC	Global Area Coverage AVHRR data
GIMEX	Greenland Ice Margin Experiment
GHRC	Global Hydrology Resource Center
GPS	global positioning system
HRPT	High Resolution Picture Transmission
IFREMER	Institut Français de Recherche pour l'Exploitation de la Mer (Brest, France)
IMAU	Institute for Marine and Atmospheric Research (Universität Utrecht)
IR	infrared
IWV	Integrated Water Vapour
K1,2,3	katabatic wind flight programs near Kangerlussuaq, Angmassalik, Ilulissat
KA1-9	katabatic wind flight missions during KABEG
KABEG	**Ka**tabatic wind and **B**oundary layer front **E**xperiment around **G**reenland
KUL	Kulusuk
LAM25 (50)	Limited-area model with horizontal resolution of 25 km (50 km)
LLJ	low-level jet
MFH	minimum flight height
MIUB	Meteorologisches Institut der Universität Bonn
MIZEX	Marginal Ice Zone Experiment
MSFC	Marshall Space Flight Center (Alabama, USA)
MW	Microwave
NESDIS	National Environmental Satellite and Data Information Services (NOAA)
NOAA	National Oceanic and Atmospheric Administration
NORLAM	NORwegian Limited Area Model
REFLEX	Radiation and Eddy Flux Experiment
S	tundra AWS near Kangerlussuaq
SH	flight height relative to the surface
SSM/I	Special Sensor Microwave/Imager
U1-U2	IMAU AWS on the ice sheet near Kangerlussuaq
VIS	visible

9. References

Ball, F.K., 1960: Winds on the ice slopes of Antarctica. *Antarctic Meteorology, Proceedings of the Symposium,* Pergamon Press, 9-16.

BAS, SPRI, WCMC, 1993: Antarctic digital database. Published by Scientific Committee on Antarctic Research, Cambridge, UK.

Bromwich, D.H., 1989: An extraordinary katabatic wind regime at Terra Nova Bay, Antarctica. *Mon. Wea. Rev. 117,* 688-695.

Bromwich, D.H., Du, Y., Parish, T.R., 1994: Numerical simulation of winter katabatic winds from West Antarctica crossing Siple Coast and the Ross Ice Shelf. *Mon. Wea. Rev. 122,* 1417-1435.

Bromwich, D.H., Du, Y., Hines, K.M., 1996: Wintertime surface winds over the Greenland ice sheet. *Mon. Wea. Rev. 124,* 1941-1947.

Brümmer, B., Rump, B., Kruspe, G., 1992: A cold air outbreak near Spitzbergen in springtime - boundary-layer modification and cloud development. *Boundary Layer Meteorol. 61,* 13-46.

Douglas, M.W., Shapiro, M.A., Fedor, L.S., Saukkonen, L., 1995: Research aircraft observations of a polar low at the East-Greenland ice-edge. *Mon. Wea. Rev. 123,* 5-15.

Ekholm, S., 1996: A full coverage, high-resolution, topographic model of Greenland computed from a variety of digital elevation data, J. Geophys. Res., B10, 21,961-21,972.

Engels, R., Heinemann, G., 1996: Three-dimensional structures of summertime Antarctic meso-scale cyclones: Part II: Numerical simulations with a limited area model. *Global Atmosphere-Ocean System* 4, 181-208.

Fairall, C.W., Markson, R., 1987: Mesoscale variations in surface stress, heat fluxes, and drag coefficient in the marginal ice zone of the Greenland Sea. *J. Geophys. Res. 92,* 6921-6932.

Fett, R.W., 1989: Polar low development associated with boundary layer fronts in the Greenland, Norwegian and Barents Seas. In: *Polar and Arctic lows* (Eds. P.F. Twitchell, E.A. Rasmussen and K.L. Davidson), A. Deepak Publishing, 421pp.

Gallée H., and Duynkerke, P.G. 1997: Air-snow interactions and the surface energy and mass balance over the melting zone of west Greenland during the Greenland Ice Margin Experiment. *J. of Geophys. Res.,* 102, 13813-13824

Gosink, J., 1982: Measurements of the katabatic winds between Dome C and Dumont d'Urville. *Pageoph.,* 120, 503-526.

Hartmann, J., Kottmeier, Ch., Wamser, Ch., 1992: Radiation and eddy flux experiment 1991 (REFLEX I). *Reports on Polar Research 105,* Alfred-Wegener-Institute for Polar Research, Bremerhaven, FRG, 72pp.

Heinemann, G., 1995: Polare Mesozyklonen. Habilitationsschrift, Meteorologisches Institut der Universität Bonn, 156pp.

Heinemann, G., 1996a: Katabatic wind systems over polar ice sheets. *Proceedings 6th Workshop on mass balance of the Greenland ice sheet and related topics, 22-23 January 1996,* Copenhagen, Denmark. Published by The Geological Survey of Greenland, Copenhagen, Report No. 53, 39-43.

Heinemann, G., 1996b: On the development of wintertime meso-scale cyclones near the sea ice front in the Arctic and Antarctic. *Global Atmosphere-Ocean System* 4, 89-123.

Heinemann, G., 1997: Idealized simulations of the Antarctic katabatic wind system with a three-dimensional meso-scale model. *J. of Geophys. Res.,* 102, 13825-13834.

Hines, K.M., Bromwich, D.H., Parish, T.R., 1995: A mesoscale modeling study of the atmospheric circulation of high southern latitudes. *Mon. Wea. Rev. 123,* 1146-1165

Johannessen, O.M., 1987: Introduction: Summer marginal ice zone experiments during 1983 and 1984 in Fram Strait and the Greenland Sea. *J. Geophys. Res. 92,* 6716-6718.

Kellner, G., Wamser, Ch., Brown, R.A., 1987: An observation of the planetary boundary layer in the marginal ice zone. *J. Geophys. Res. 92,* 6955-6965.

Kottmeier, Ch., 1994: Radiation and eddy flux experiment (REFLEX II). *Reports on Polar Research 133,* Alfred-Wegener-Institute for Polar Research, Bremerhaven, FRG, 62pp.

Meesters, A., 1994: Dependence of the energy balance of the Greenland ice sheet on climatic change: Influence of the katabatic wind and tundra. *Quart. J. Roy. Meteorol. Soc. 120,* 491-517.

Oerlemans, J., Vugts, H., 1993: A meteorological experiment in the ablation zone of the Greenland ice sheet. *Bull. Am. Meteorol. Soc. 74,* 355-365.

Parish, T.R., Bromwich, D.H., 1989: Instrumented aircraft observations of the katabatic wind regime near Terra Nova Bay. Mon. Wea. Rev. 117, 1570-1585.

Phee, M.G., Maykut, G.A., Morison, J.H., 1987: Dynamics and thermodynamics of the ice/upper ocean system in the marginal ice zone of the Greenland Sea. *J. Geophys. Res. 92,* 7017-7031.

Phillpot, H., 1997: Some observationally-identified meteorological features of East Antarctica. Meteorological Study No.42, Bureau of Meteoroloy, Canberra, Australia,

275pp.

Putnins, P., 1970: The climate of Greenland. In: *Climates of the polar regions (Ed. S. Orvig), World Survey of Climatology 14,* 3-113.

Rasmussen, L., 1989: Greenland winds and satellite imagery. Vejret, Danish Meteorological Society, 32-37.

Schwerdtfeger, W., 1984: Weather and climate of the Antarctic. Elsevier Science Publishers, 261pp.

Shapiro, M.A., Fedor, L.S., 1989: A case study of an ice edge boundary layer front and polar low development over the Norwegian and Barents Seas. In: *Polar and Arctic lows* (Eds. P.F. Twitchell, E.A. Rasmussen and K.L. Davidson), A. Deepak Publishing, 421pp.

Shaw, W.J., Pauley, R.L., Gobel, T.M., Radke, L.F., 1991: A case study of atmospheric boundary layer mean structure for flow parallel to the ice edge: Aircraft observations from CEAREX. *J. Geophys. Res. 96,* 4691-4708.

Sorbjan, Z., Kodama, Y., Wendler, G., 1986: Observational study of the atmospheric boundary layer over Antarctica. *J. Clim. Appl. Meteorol. 25,* 641-651.

Van den Broeke, M.R., Duynkerke, P.G., Oerlemans, J., 1994: The observed katabatic flow at the edge of the Greenland ice sheet during GIMEX-91. *Global and Planetary Change 9,* 3-15.

Wendler, G., 1990: Strong gravity flow observed along the slope of eastern Antarctica. *Meteorol. Atmos. Phys. 43,* 127-135.

Appendix: Pictures of KABEG (made by C. Drüe and G. Heinemann)

Fig.A1: Research aircraft POLAR2 at Kangerlussuaq

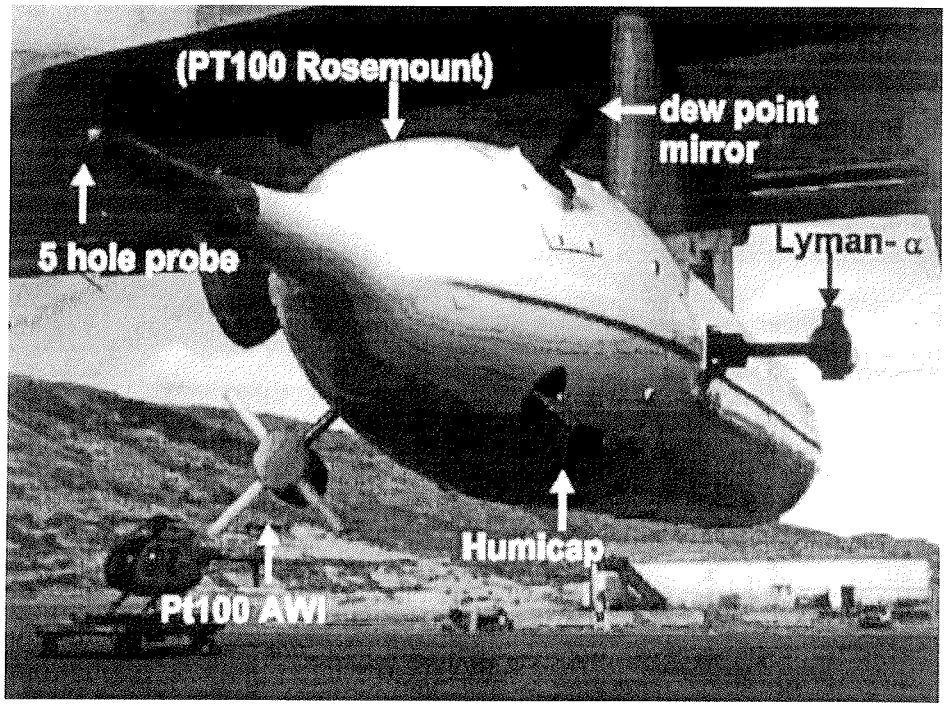

Fig.A2: Turbulence measuring device METEOPOD. Some sensors are indicated.

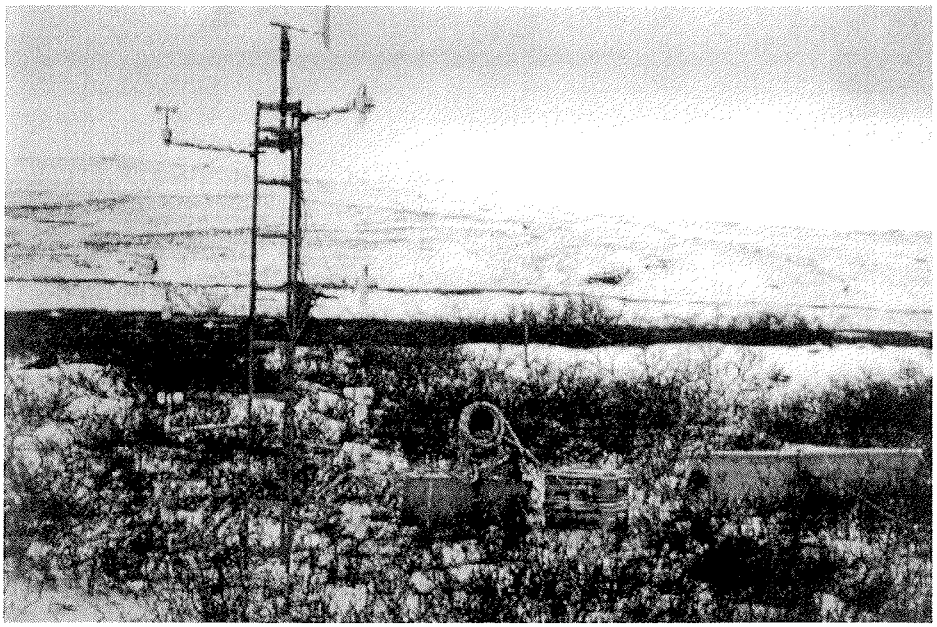

Fig.A3: Surface station S near Kangerlussuaq in April

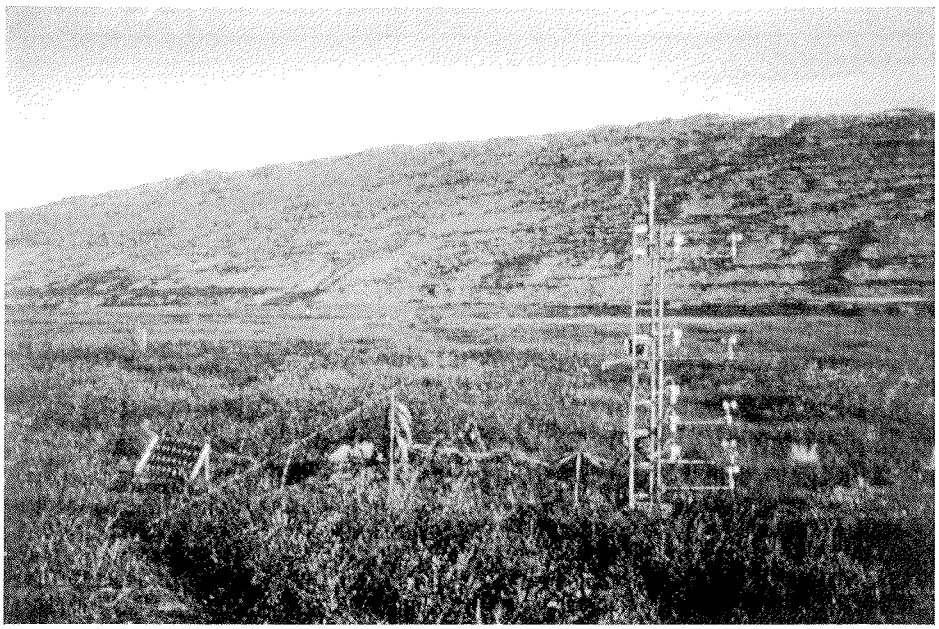

Fig.A4: Surface station S near Kangerlussuaq in May

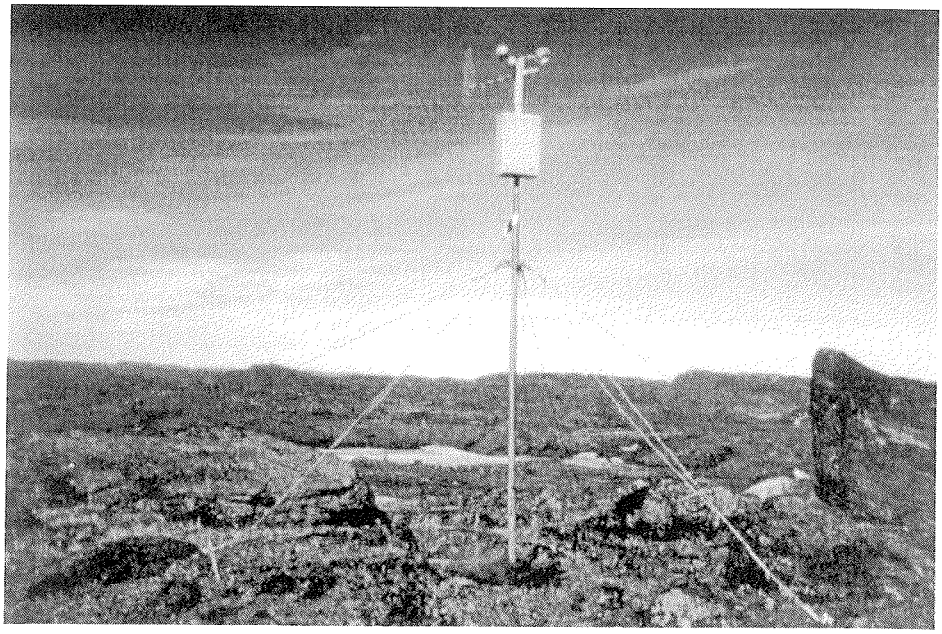

Fig.A5: AWS A1 in May on the tundra

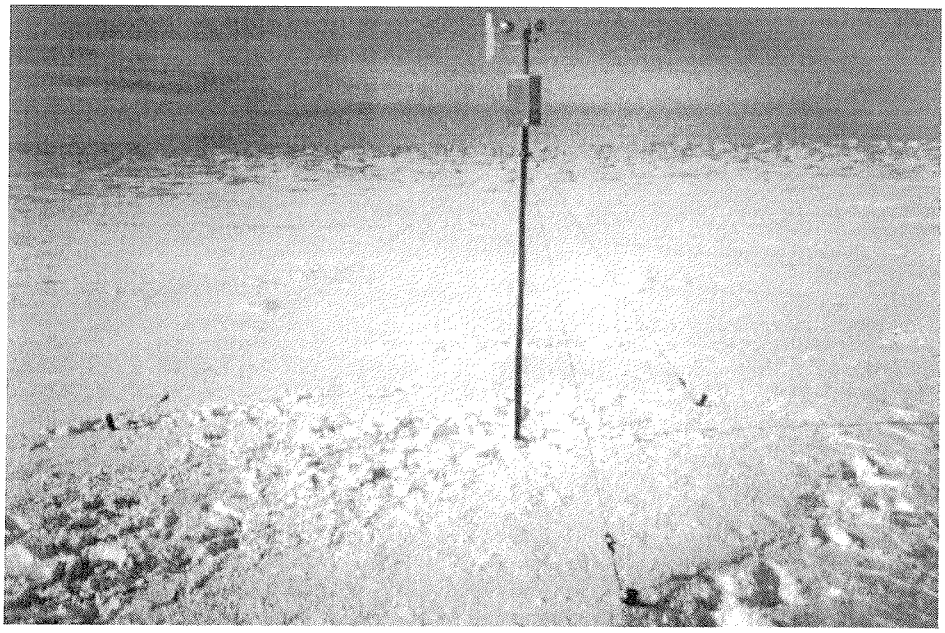

Fig.A6: AWS A2 on the inland ice

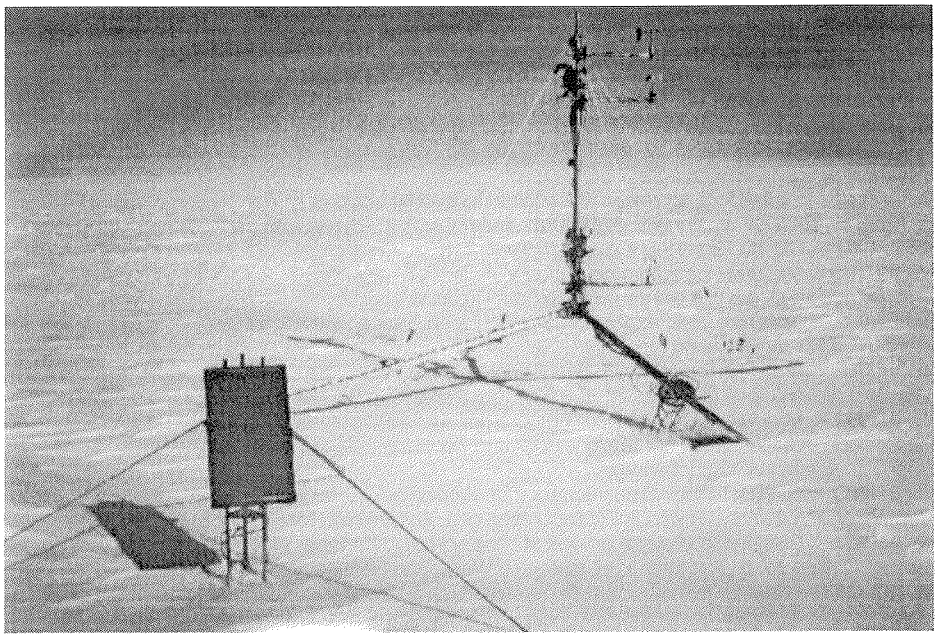

Fig.A7: AWS A3 on the inland ice

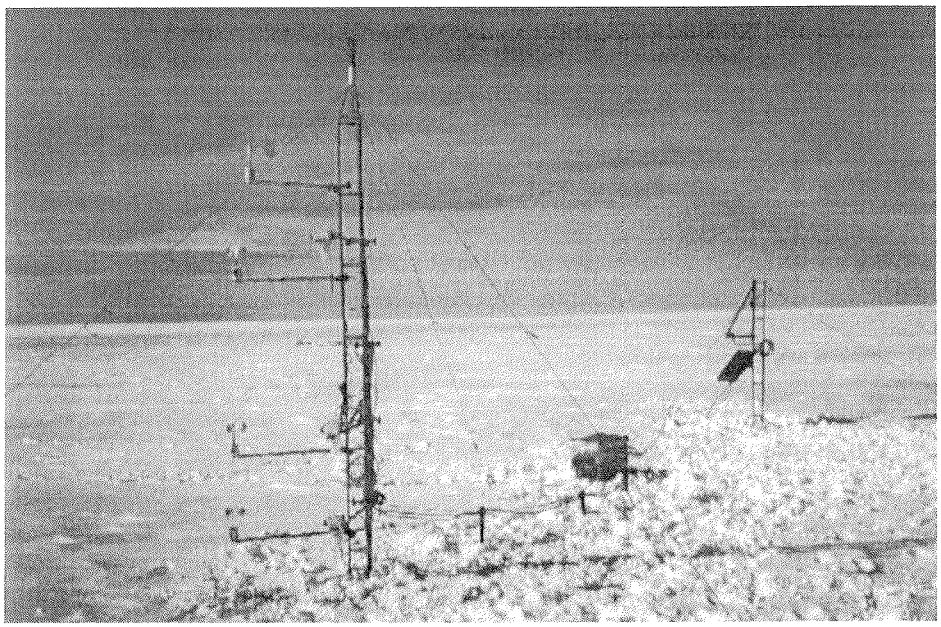

Fig.A8: AWS A4 on the inland ice

Folgende Hefte der Reihe „Berichte zur Polarforschung" sind bisher erschienen:

* **Sonderheft Nr. 1/1981** – „Die Antarktis und ihr Lebensraum",
Eine Einführung für Besucher – Herausgegeben im Auftrag von SCAR
Heft Nr. 1/1982 – „Die Filchner-Schelfeis-Expedition 1980/81",
zusammengestellt von Heinz Kohnen
* **Heft Nr. 2/1982** – „Deutsche Antarktis-Expedition 1980/81 mit FS 'Meteor'",
First International BIOMASS Experiment (FIBEX) – Liste der Zooplankton- und Mikronektonnetzfänge
zusammengestellt von Norbert Klages
Heft Nr. 3/1982 – „Digitale und analoge Krill-Echolot-Rohdatenerfassung an Bord des Forschungsschiffes 'Meteor'" (im Rahmen von FIBEX 1980/81, Fahrtabschnitt ANT III), von Bodo Morgenstern
Heft Nr. 4/1982 – „Filchner-Schelfeis-Expedition 1980/81",
Liste der Planktonfänge und Lichtstärkemessungen
zusammengestellt von Gerd Hubold und H. Eberhard Drescher
* **Heft Nr. 5/1982** – „Joint Biological Expedition on RRS 'John Biscoe', February 1982",
by G. Hempel and R. B. Heywood
* **Heft Nr. 6/1982** – „Antarktis-Expedition 1981/82 (Unternehmen 'Eiswarte')",
zusammengestellt von Gode Gravenhorst
Heft Nr. 7/1982 – „Marin-Biologisches Begleitprogramm zur Standorterkundung 1979/80 mit MS 'Polarsirkel' (Pre-Site Survey)" – Stationslisten der Mikronekton- und Zooplanktonfänge sowie der Bodenfischerei
zusammengestellt von R. Schneppenheim
Heft Nr. 8/1983 – „The Post-Fibex Data Interpretation Workshop",
by D. L. Cram and J.-C. Freytag with the collaboration of J. W. Schmidt, M. Mall, R. Kresse, T. Schwinghammer
* **Heft Nr. 9/1983** – „Distribution of some groups of zooplankton in the inner Weddell Sea in summer 1979/80",
by I. Hempel, G. Hubold, B. Kaczmaruk, R. Keller, R. Weigmann-Haass
Heft Nr. 10/1983 – „Fluor im antarktischen Ökosystem" – DFG-Symposium November 1982
zusammengestellt von Dieter Adelung
Heft Nr. 11/1983 – „Joint Biological Expedition on RRS 'John Biscoe', February 1982 (II)",
Data of micronecton and zooplankton hauls, by Uwe Piatkowski
Heft Nr. 12/1983 – „Das biologische Programm der ANTARKTIS-I-Expedition 1983 mit FS 'Polarstern'",
Stationslisten der Plankton-, Benthos- und Grundschleppnetzfänge und Liste der Probennahme an Robben und Vögeln, von H. E. Drescher, G. Hubold, U. Piatkowski, J. Plötz und J. Voß
* **Heft Nr. 13/1983** – „Die Antarktis-Expedition von MS 'Polarbjörn' 1982/83" (Sommerkampagne zur Atka-Bucht und zu den Kraul-Bergen), zusammengestellt von Heinz Kohnen
* **Sonderheft Nr. 2/1983** – „Die erste Antarktis-Expedition von FS 'Polarstern' (Kapstadt, 20. Januar 1983 – Rio de Janeiro, 25. März 1983)", Bericht des Fahrtleiters Prof. Dr. Gotthilf Hempel
Sonderheft Nr. 3/1983 – „Sicherheit und Überleben bei Polarexpeditionen",
zusammengestellt von Heinz Kohnen
* **Heft Nr. 14/1983** – „Die erste Antarktis-Expedition (ANTARKTIS I) von FS 'Polarstern' 1982/83",
herausgegeben von Gotthilf Hempel
Sonderheft Nr. 4/1983 – „On the Biology of Krill *Euphausia superba*" – Proceedings of the Seminar and Report of the Krill Ecology Group, Bremerhaven 12.-16. May 1983, edited by S. B. Schnack
Heft Nr. 15/1983 – „German Antarctic Expedition 1980/81 with FRV 'Walther Herwig' and RV 'Meteor'" – First International BIOMASS Experiment (FIBEX) – Data of micronekton and zooplankton hauls
by Uwe Piatkowski and Norbert Klages
Sonderheft Nr. 5/1984 – „The observatories of the Georg von Neumayer Station", by Ernst Augstein
Heft Nr. 16/1984 – „FIBEX cruise zooplankton data",
by U. Piatkowski, I. Hempel and S. Rakusa-Suszczewski
Heft Nr. 17/1984 – „Fahrtbericht (cruise report) der 'Polarstern'-Reise ARKTIS I, 1983",
von E. Augstein, G. Hempel und J. Thiede
Heft Nr. 18/1984 – „Die Expedition ANTARKTIS II mit FS 'Polarstern' 1983/84",
Bericht von den Fahrtabschnitten 1, 2 und 3, herausgegeben von D. Fütterer
Heft Nr. 19/1984 – „Die Expedition ANTARKTIS II mit FS 'Polarstern' 1983/84",
Bericht vom Fahrtabschnitt 4, Punta Arenas-Kapstadt (Ant-II/4), herausgegeben von H. Kohnen
Heft Nr. 20/1984 – „Die Expedition ARKTIS II des FS 'Polarstern' 1984, mit Beiträgen des FS 'Valdivia' und des Forschungsflugzeuges 'Falcon 20' zum Marginal Ice Zone Experiment 1984 (MIZEX)",
von E. Augstein, G. Hempel, J. Schwarz, J. Thiede und W. Weigel
Heft Nr. 21/1985 – „Euphausiid larvae in plankton samples from the vicinity of the Antarctic Peninsula, February 1982", by Sigrid Marschall and Elke Mizdalski

Heft Nr. 22/1985 – „Maps of the geographical distribution of macrozooplankton in the Atlantic sector of the Southern Ocean", by Uwe Piatkowski
Heft Nr. 23/1985 – „Untersuchungen zur Funktionsmorphologie und Nahrungsaufnahme der Larven des Antarktischen Krills *Euphausia superba* Dana", von Hans-Peter Marschall
Heft Nr. 24/1985 – „Untersuchungen zum Periglazial auf der König-Georg-Insel Südshetlandinseln/ Antarktika. Deutsche physiogeographische Forschungen in der Antarktis. – Bericht über die Kampagne 1983/84", von Dietrich Barsch, Wolf-Dieter Blümel, Wolfgang Flügel, Roland Mäusbacher, Gerhard Stäblein, Wolfgang Zick
* **Heft Nr. 25/1985** – „Die Expedition ANTARKTIS III mit FS 'Polarstern' 1984/85", herausgegeben von Gotthilf Hempel
* **Heft Nr. 26/1985** – „The Southern Ocean"; A survey of oceanographic and marine meteorological research work by Hellmer et al.
Heft Nr. 27/1986 – „Spätpleistozäne Sedimentationsprozesse am antarktischen Kontinentalhang vor Kapp Norvegia, östliche Weddell-See", von Hannes Grobe
Heft Nr. 28/1986 – „Die Expedition ARKTIS III mit 'Polarstern' 1985", mit Beiträgen der Fahrtteilnehmer, herausgegeben von Rainer Gersonde
* **Heft Nr. 29/1986** – „5 Jahre Schwerpunktprogramm 'Antarktisforschung' der Deutschen Forschungsgemeinschaft." Rückblick und Ausblick. Zusammengestellt von Gotthilf Hempel, Sprecher des Schwerpunktprogramms
Heft Nr. 30/1986 – „The Meteorological Data of the Georg-von-Neumayer-Station for 1981 and 1982", by Marianne Gube and Friedrich Obleitner
Heft Nr. 31/1986 – „Zur Biologie der Jugendstadien der Notothenioidei (Pisces) an der Antarktischen Halbinsel", von A. Kellermann
Heft Nr. 32/1986 – „Die Expedition ANTARKTIS-IV mit FS 'Polarstern' 1985/86", mit Beiträgen der Fahrtteilnehmer, herausgegeben von Dieter Fütterer
Heft Nr. 33/1987 – „Die Expedition ANTARKTIS-IV mit FS 'Polarstern' 1985/86 – Bericht zu den Fahrtabschnitten ANT-IV/3-4", von Dieter Karl Fütterer
Heft Nr. 34/1987 – „Zoogeographische Untersuchungen und Gemeinschaftsanalysen an antarktischem Makroplankton", von U. Piatkowski
Heft Nr. 35/1987 – „Zur Verbreitung des Meso- und Makrozooplanktons in Oberflächenwasser der Weddell See (Antarktis)", von E. Boysen-Ennen
Heft Nr. 36/1987 – „Zur Nahrungs- und Bewegungsphysiologie von *Salpa thompsoni* und *Salpa fusiformis*", von M. Reinke
Heft Nr. 37/1987 – „The Eastern Weddell Sea Drifting Buoy Data Set of the Winter Weddell Sea Project (WWSP) 1986", by Heinrich Hoeber und Marianne Gube-Lehnhardt
Heft Nr. 38/1987 – „The Meteorological Data of the Georg von Neumayer Station for 1983 and 1984", by M. Gube-Lenhardt
Heft Nr. 39/1987 – „Die Winter-Expedition mit FS 'Polarstern' in die Antarktis (ANT V/1-3)", herausgegeben von Sigrid Schnack-Schiel
Heft Nr. 40/1987 – „Weather and Synoptic Situation during Winter Weddell Sea Project 1986 (ANT V/2) July 16 – September 10, 1986", by Werner Rabe
Heft Nr. 41/1988 – „Zur Verbreitung und Ökologie der Seegurken im Weddellmeer (Antarktis)", von Julian Gutt
Heft Nr. 42/1988 – „The zooplankton community in the deep bathyal and abyssal zones of the eastern North Atlantic", by Werner Beckmann
Heft Nr. 43/1988 – „Scientific cruise report of Arctic Expedition ARK IV/3", Wissenschaftlicher Fahrtbericht der Arktis-Expedition ARK IV/3, compiled by Jörn Thiede
Heft Nr. 44/1988 – „Data Report for FV 'Polarstem' Cruise ARK IV/1, 1987 to the Arctic and Polar Fronts", by Hans-Jürgen Hirche
Heft Nr. 45/1988 – „Zoogeographie und Gemeinschaftsanalyse des Makrozoobenthos des Weddellmeeres (Antarktis)", von Joachim Voß
Heft Nr. 46/1988 – „Meteorological and Oceanographic Data of the Winter-Weddell-Sea Project 1986 (ANT V/3)", by Eberhard Fahrbach
Heft Nr. 47/1988 – „Verteilung und Herkunft glazial-mariner Gerölle am Antarktischen Kontinentalrand des östlichen Weddellmeeres", von Wolfgang Oskierski
Heft Nr. 48/1988 – „Variationen des Erdmagnetfeldes an der GvN-Station", von Arnold Brodscholl
* **Heft Nr. 49/1988** – „Zur Bedeutung der Lipide im antarktischen Zooplankton", von Wilhelm Hagen
Heft Nr. 50/1988 – „Die gezeitenbedingte Dynamik des Ekström-Schelfeises, Antarktis", von Wolfgang Kobarg
Heft Nr. 51/1988 – „Ökomorphologie nototheniider Fische aus dem Weddellmeer, Antarktis", von Werner Ekau
Heft Nr. 52/1988 – „Zusammensetzung der Bodenfauna in der westlichen Fram-Straße", von Dieter Piepenburg
* **Heft Nr. 53/1988** – „Untersuchungen zur Ökologie des Phytoplanktons im südöstichen Weddellmeer (Antarktis) im Jan./Febr. 1985", von Eva-Maria Nöthig

Heft Nr. 54/1988 – „Die Fischfauna des östlichen und südlichen Weddellmeeres: geographische Verbreitung, Nahrung und trophische Stellung der Fischarten", von Wiebke Schwarzbach
Heft Nr. 55/1988 – „Weight and length data of zooplankton in the Weddell Sea in austral spring 1986 (ANT V/3)", by Elke Mizdalski
Heft Nr. 56/1989 – „Scientific cruise report of Arctic expeditions ARK IV/1, 2 & 3", by G. Krause, J. Meincke und J. Thiede
Heft Nr. 57/1989 – „Die Expedition ANTARKTIS V mit FS 'Polarstern' 1986/87", Bericht von den Fahrtabschnitten ANT V/4-5 von H. Miller und H. Oerter
* **Heft Nr. 58/1989** – „Die Expedition ANTARKTIS VI mit FS 'Polarstern' 1987/88", von D. K. Fütterer
Heft Nr. 59/1989 – „Die Expedition ARKTIS V/1a, 1b und 2 mit FS 'Polarstern' 1988", von M. Spindler
Heft Nr. 60/1989 – „Ein zweidimensionales Modell zur thermohalinen Zirkulation unter dem Schelfeis", von H. H. Hellmer
Heft Nr. 61/1989 – „Die Vulkanite im westlichen und mittleren Neuschwabenland, Vestfjella und Ahlmannryggen, Antarktika", von M. Peters
* **Heft-Nr. 62/1989** – „The Expedition ANTARKTIS VII/1 and 2 (EPOS I) of RV 'Polarstern' in 1988/89", by I. Hempel
Heft Nr. 63/1989 – „Die Eisalgenflora des Weddellmeeres (Antarktis): Artenzusammensetzung und Biomasse, sowie Ökophysiologie ausgewählter Arten", von Annette Bartsch
Heft Nr. 64/1989 – „Meteorological Data of the G.-v.-Neumayer-Station (Antarctica)", by L. Helmes
Heft Nr. 65/1989 – „Expedition Antarktis VII/3 in 1988/89", by I. Hempel, P. H. Schalk, V. Smetacek
Heft Nr. 66/1989 – „Geomorphologisch-glaziologische Detailkartierung des arid-hochpolaren Borgmassivet, Neuschwabenland, Antarktika", von Karsten Brunk
Heft-Nr. 67/1990 – „Identification key and catalogue of larval Antarctic fishes", edited by Adolf Kellermann
Heft-Nr. 68/1990 – „The Expediton Antarktis VII/4 (Epos leg 3) and VII/5 of RV 'Polarstern' in 1989", edited by W. Arntz, W. Ernst, I. Hempel
Heft-Nr. 69/1990 – „Abhängigkeiten elastischer und rheologischer Eigenschaften des Meereises vom Eisgefüge", von Harald Hellmann
Heft-Nr. 70/1990 – „Die beschalten benthischen Mollusken (Gastropoda und Bivalvia) des Weddellmeeres, Antarktis", von Stefan Hain
Heft-Nr. 71/1990 – „Sedimentologie und Paläomagnetik an Sedimenten der Maudkuppe (Nordöstliches Weddellmeer)", von Dieter Cordes
Heft-Nr. 72/1990 – „Distribution and abundance of planktonic copepods (Crustacea) in the Weddell Sea in summer 1980/81", by F. Kurbjeweit and S. Ali-Khan
Heft-Nr. 73/1990 – „Zur Frühdiagenese von organischem Kohlenstoff und Opal in Sedimenten des südlichen und östlichen Weddellmeeres", von M. Schlüter
Heft-Nr. 74/1991 – „Expeditionen ANTARKTIS-VIII/3 und VIII/4 mit FS 'Polarstern' 1989", von Rainer Gersonde und Gotthilf Hempel
Heft-Nr. 75/1991 – „Quartäre Sedimentationsprozesse am Kontinentalhang des Süd-Orkney-Plateaus im nordwestlichen Weddelmeer (Antarktis)", von Sigrun Grünig
Heft-Nr. 76/1991 – „Ergebnisse der faunistischen Arbeiten in Benthal von King George Island (Südshetlandinseln, Antarktis)", Martin Rauschert
Heft-Nr. 77/1991 – „Verteilung von Mikroplankton-Organismen nordwestlich der Antarktischen Halbinsel unter dem Einfluß sich ändernder Umweltbedingungen in Herbst", von Heinz Klöser
Heft-Nr. 78/1991 – „Hochauflösende Magnetostratigraphie spätquartärer Sedimente arktischer Meeresgebiete", von Norbert R. Nowaczyk
Heft-Nr. 79/1991 – „Ökophysiologische Untersuchungen zur Salinitäts- und Temperaturtoleranz antarktischer Grünalgen unter besonderer Berücksichtigung des ß-Dimethylsulfoniumpropionat (DMSP) – Stoffwechsels", von Ulf Karsten
Heft-Nr. 80/1991 – „Die Expedition ARKTIS VII/1 mit FS 'POLARSTERN' 1990", herausgegeben von Jörn Thiede und Gotthilf Hempel
Heft-Nr. 81/1991 – „Paläoglaziologie und Paläozeanographie im Spätquartär am Kontinentalrand des südlichen Weddellmeeres, Antarktis", von Martin Melles
Heft-Nr. 82/1991 – „Quantifizierung von Meereiseigenschaften: Automatische Bildanalyse von Dünnschnitten und Parametrisierung von Chlorophyll- und Salzgehaltsverteilungen", von Hajo Eicken
Heft-Nr. 83/1991 – „Das Fließen von Schelfeisen – numerische Simulationen mit der Methode der finiten Differenzen", von Jürgen Determann
Heft-Nr. 84/1991 – Die Expedition ANTARKTIS VIII/1-2, 1989 mit der Winter Weddell Gyre Study der Forschungsschiffe 'Polarstern' und 'Akademik Fedorov' ", von Ernst Augstein, Nicolai Bagriantsev und Hans Werner Schenke
Heft-Nr. 85/1991 – „Zur Entstehung von Unterwassereis und das Wachstum und die Energiebilanz des Meereises in der Atka Bucht, Antarktis", von Josef Kipfstuhl

Heft-Nr. 86/1991 – „Die Expedition ANTARKTIS-VIII mit FS 'Polarstern' 1989/90. Bericht vom Fahrtabschnitt ANT-VIII/5", herausgegeben von Heinz Miller und Hans Oerter
Heft-Nr. 87/1991 – „Scientific cruise reports of Arctic expeditions ARK-VI/1-4 of RV 'Polarstern' in 1989", edited by G. Krause, J. Meincke & H. J. Schwarz
Heft-Nr. 88/1991 – „Zur Lebensgeschichte dominanter Copepodenarten *(Calanus finmarchicus, C. glacialis, C. hyperboreus, Metridia longa)* in der Framstraße", von Sabine Diel
Heft-Nr. 89/1991 – „Detaillierte seismische Untersuchungen am östlichen Kontinentalrand des Weddell-Meeres vor Kapp Norvegia, Antarktis", von Norbert E. Kaul
Heft-Nr. 90/1991 – „Die Expedition ANTARKTIS VIII mit FS 'Polarstern' 1989/90. Bericht von Fahrtabschnitten ANT VIII/6-7", herausgegeben von Dieter Karl Fütterer und Otto Schrems
Heft-Nr. 91/1991 – „Blood physiology and ecological consequences in Weddell Sea fishes (Antarctica)", by Andreas Kunzmann.
Heft-Nr. 92/1991 – „Zur sommerlichen Verteilung des Mesozooplanktons im Nansen-Becken, Nordpolarmeer", von Nicolai Mumm.
Heft-Nr. 93/1991 – Die Expedition ARKTIS VII mit FS 'Polarstern' 1990. Bericht von Fahrtabschnitten ARK VII/2", herausgegeben vom Gunther Krause.
Heft-Nr. 94/1991 – „Die Entwicklung des Phytoplanktons im östlichen Weddellmeer (Antarktis) beim Übergang vom Spätwinter zum Frühjahr", von Renate Scharek.
Heft-Nr. 95/1991 – „Radioisotopenstratigraphie, Sedimentologie und Geochemie jungquartärer Sedimente des östlichen Arktischen Ozeans", von Horst Bohrmann.
Heft-Nr. 96/1991 – „Holozäne Sedimentationsentwicklung im Scoresby Sund, Ost-Grönland", von Peter Marienfeld
Heft-Nr. 97/1991 – „Strukturelle Entwicklung und Abkühlungsgeschichte der Heimefrontfjella (Westliches Dronning Maud Land / Antarktika)", von Joachim Jacobs
Heft-Nr. 98/1991 – „Zur Besiedlungsgeschichte des antarktischen Schelfes am Beispiel der Isopoda (Crustacea, Malacostraca)", von Angelika Brandt
Heft-Nr. 99/1992 – „The Antarctic ice sheet and environmental change: a three-dimensional modelling study", by Philippe Huybrechts
* **Heft-Nr. 100/1992** – „Die Expeditionen ANTARKTIS IX/1-4 des Forschungsschiffes 'Polarstern' 1990/91", herausgegeben von Ulrich Bathmann, Meinhard Schulz-Baldes, Eberhard Fahrbach, Victor Smetacek und Hans-Wolfgang Hubberten
Heft-Nr. 101/1992 – „Wechselbeziehungen zwischen Spurenmetallkonzentrationen (Cd, Cu, Pb, Zn) im Meerwasser und in Zooplanktonorganismen (Copepoda) der Arktis und des Atlantiks", von Christa Pohl
Heft-Nr. 102/1992 – „Physiologie und Ultrastruktur der antarktischen Grünalge *Prasiola crispa* ssp. *antarctica* unter osmotischem Streß und Austrocknung", von Andreas Jacob
Heft-Nr. 103/1992 – „Zur Ökologie der Fische im Weddellmeer", von Gerd Hubold
Heft-Nr. 104/1992 – „Mehrkanalige adaptive Filter für die Unterdrückung von multiplen Reflexionen in Verbindung mit der freien Oberfläche in marinen Seismogrammen", von Andreas Rosenberger
Heft-Nr. 105/1992 – „Radiation and Eddy Flux Experiment 1991 *(REFLEX I)*", von Jörg Hartmann, Christoph Kottmeier und Christian Wamser
Heft-Nr. 106/1992 – „Ostracoden im Epipelagial vor der Antarktischen Halbinsel - ein Beitrag zur Systematik sowie zur Verbreitung und Populationsstruktur unter Berücksichtigung der Saisonalität", von Rüdiger Kock
Heft-Nr. 107/1992 – „ARCTIC '91: Die Expedition ARK-VIII/3 mit FS 'Polarstern' 1991", herausgegeben von Dieter K. Fütterer
Heft-Nr. 108/1992 – „Dehnungsbeben an einer Störungszone im Ekström-Schelfeis nördlich der Georg-von-Neumayer Station, Antarktis. - Eine Untersuchung mit seismologischen und geodätischen Methoden", von Uwe Nixdorf
Heft-Nr. 109/1992 – „Spätquartäre Sedimentation am Kontinentalrand des südöstlichen Weddellmeeres, Antarktis", von Michael Weber
Heft-Nr. 110/1992 – „Sedimentfazies und Bodenwasserstrom am Kontinentalhang des nordwestlichen Weddellmeeres", von Isa Brehme
Heft-Nr. 111/1992 – „Die Lebensbedingungen in den Solekanälchen des antarktischen Meereises", von Jürgen Weissenberger
Heft-Nr. 112/1992 – „Zur Taxonomie von rezenten benthischen Foraminiferen aus dem Nansen Becken, Arktischer Ozean", von Jutta Wollenburg
Heft-Nr. 113/1992 – „Die Expedition ARKTIS VIII/1 mit FS 'Polarstern' 1991", herausgegeben von Gerhard Kattner
* **Heft-Nr. 114/1992** – „Die Gründungsphase deutscher Polarforschung, 1865-1875", von Reinhard A. Krause
Heft-Nr. 115/1992 – „Scientific Cruise Report of the 1991 Arctic Expedition ARK VIII/2 of RV "Polarstern" (EPOS II)", by Eike Rachor

Heft-Nr. 116/1992 – „The Meteorological Data of the Georg-von-Neumayer-Station (Antarctica) for 1988, 1989, 1990 and 1991", by Gert König-Langlo

Heft-Nr. 117/1992 – „Petrogenese des metamorphen Grundgebirges der zentralen Heimefrontfjella (westliches Dronning Maud Land / Antarktis)", von Peter Schulze

Heft-Nr. 118/1993 – „Die mafischen Gänge der Shackleton Range / Antarktika: Petrographie, Geochemie, Isotopengeochemie und Paläomagnetik", von Rüdiger Hotten

* **Heft-Nr. 119/1993** – „Gefrierschutz bei Fischen der Polarmeere", von Andreas P. A. Wöhrmann

* **Heft-Nr. 120/1993** – „East Siberian Arctic Region Expedition '92: The Laptev Sea – its Significance for Arctic Sea-Ice Formation and Transpolar Sediment Flux", by D. Dethleff, D. Nürnberg, E. Reimnitz, M. Saarso and Y.P. Savchenko. – „Expedition to Novaja Zemlja and Franz Josef Land with RV 'Dalnie Zelentsy'", by D. Nürnberg and E. Groth

* **Heft-Nr. 121/1993** – „Die Expedition ANTARKTIS X/3 mit FS 'Polarstern' 1992", herausgegeben von Michael Spindler, Gerhard Dieckmann und David Thomas

Heft-Nr. 122/1993 – „Die Beschreibung der Korngestalt mit Hilfe der Fourier-Analyse: Parametrisierung der morphologischen Eigenschaften von Sedimentpartikeln", von Michael Diepenbroek

* **Heft-Nr. 123/1993** – „Zerstörungsfreie hochauflösende Dichteuntersuchungen mariner Sedimente", von Sebastian Gerland

Heft-Nr. 124/1993 – „Umsatz und Verteilung von Lipiden in arktischen marinen Organismen unter besonderer Berücksichtigung unterer trophischer Stufen", von Martin Graeve

Heft-Nr. 125/1993 – „Ökologie und Respiration ausgewählter arktischer Bodenfischarten", von Christian F. von Dorrien

Heft-Nr. 126/1993 – „Quantitative Bestimmung von Paläoumweltparametern des Antarktischen Oberflächenwassers im Spätquartär anhand von Transferfunktionen mit Diatomeen", von Ulrich Zielinski

Heft-Nr. 127/1993 – „Sedimenttransport durch das arktische Meereis: Die rezente lithogene und biogene Materialfracht", von Ingo Wollenburg

Heft-Nr. 128/1993 – „Cruise ANTARKTIS X/3 of RV 'Polarstern': CTD-Report", von Marek Zwierz

Heft-Nr. 129/1993 – „Reproduktion und Lebenszyklen dominanter Copepodenarten aus dem Weddellmeer, Antarktis", von Frank Kurbjeweit

Heft-Nr. 130/1993 – „Untersuchungen zu Temperaturregime und Massenhaushalt des Filchner-Ronne-Schelfeises, Antarktis, unter besonderer Berücksichtigung von Anfrier- und Abschmelzprozessen", von Klaus Grosfeld

Heft-Nr. 131/1993 – „Die Expedition ANTARKTIS X/5 mit FS 'Polarstern' 1992", herausgegeben von Rainer Gersonde

Heft-Nr. 132/1993 – „Bildung und Abgabe kurzkettiger halogenierter Kohlenwasserstoffe durch Makroalgen der Polarregionen", von Frank Laturnus

Heft-Nr. 133/1994 – „Radiation and Eddy Flux Experiment 1993 *(REFLEX II)*", by Christoph Kottmeier, Jörg Hartmann, Christian Wamser, Axel Bochert, Christof Lüpkes, Dietmar Freese and Wolfgang Cohrs

* **Heft-Nr. 134/1994** – „The Expedition ARKTIS-IX/1", edited by Hajo Eicken and Jens Meincke

Heft-Nr. 135/1994 – „Die Expeditionen ANTARKTIS X/6-8", herausgegeben von Ulrich Bathmann, Victor Smetacek, Hein de Baar, Eberhard Fahrbach und Gunter Krause

Heft-Nr. 136/1994 – „Untersuchungen zur Ernährungsökologie von Kaiserpinguinen *(Aptenodytes forsteri)* und Königspinguinen *(Aptenodytes patagonicus)*", von Klemens Pütz

* **Heft-Nr. 137/1994** – „Die känozoische Vereisungsgeschichte der Antarktis", von Werner U. Ehrmann

Heft-Nr. 138/1994 – „Untersuchungen stratosphärischer Aerosole vulkanischen Ursprungs und polarer stratosphärischer Wolken mit einem Mehrwellenlängen-Lidar auf Spitzbergen (79°N, 12°E)", von Georg Beyerle

Heft-Nr. 139/1994 – „Charakterisierung der Isopodenfauna (Crustacea, Malacostraca) des Scotia-Bogens aus biogeographischer Sicht: Ein multivariater Ansatz", von Holger Winkler

Heft-Nr. 140/1994 – „Die Expedition ANTARKTIS X/4 mit FS 'Polarstern' 1992", herausgegeben von Peter Lemke

Heft-Nr. 141/1994 – „Satellitenaltimetrie über Eis – Anwendung des GEOSAT-Altimeters über dem Ekströmisen, Antarktis", von Klemens Heidland

Heft-Nr. 142/1994 – „The 1993 Northeast Water Expedition. Scientific cruise report of RV 'Polarstern' Arctic cruises ARK IX/2 and 3, USCG 'Polar Bear' cruise NEWP and the NEWLand expedition", edited by Hans-Jürgen Hirche and Gerhard Kattner

Heft-Nr. 143/1994 – „Detaillierte refraktionsseismische Untersuchungen im inneren Scoresby Sund/ Ost Grönland", von Notker Fechner

Heft-Nr. 144/1994 – „Russian-German Cooperation in the Siberian Shelf Seas: Geo-System Laptev Sea", edited by Heidemarie Kassens, Hans-Wolfgang Hubberten, Sergey M. Pryamikov and Rüdiger Stein

* **Heft-Nr. 145/1994** – „The 1993 Northeast Water Expedition. Data Report of RV ‚Polarstern' Arctic Cruises IX/2 and 3", edited by Gerhard Kattner and Hans-Jürgen Hirche

Heft-Nr. 146/1994 – „Radiation Measurements at the German Antarctic Station Neumeyer 1982 – 1992", by Torsten Schmidt and Gert König-Langlo

Heft-Nr. 147/1994 – „Krustenstrukturen und Verlauf des Kontinentalrandes im Weddell Meer/Antarktis", von Christian Hübscher
Heft-Nr. 148/1994 – „The expeditions NORILSK/TAYMYR 1993 and BUNGER OASIS 1993/94 of the AWI Research Unit Potsdam", edited by Martin Melles
Heft-Nr. 149/1994 – „Die Expedition ARCTIC '93. Der Fahrtabschnitt ARK-IX/4 mit FS ‚Polarstern' 1993", herausgegeben von Dieter K. Fütterer
Heft-Nr. 150/1994 – „Der Energiebedarf der Pygoscelis-Pinguine: eine Synopse", von Boris M. Culik
Heft-Nr. 151/1994 – „Russian-German Cooperation: The Transdrift I Expedition to the Laptev Sea", edited by Heidemarie Kassens and Valeriy Y. Karpiy
Heft-Nr. 152/1994 – „Die Expedition ANTARKTIS-X mit FS 'Polarstern' 1992. Bericht von den Fahrtabschnitten ANT X/1a und 2", herausgegeben von Heinz Miller
Heft-Nr. 153/1994 – „Aminosäuren und Huminstoffe im Stickstoffkreislauf polarer Meere", von Ulrike Hubberten
Heft-Nr. 154/1994 – „Regional and seasonal variability in the vertical distribution of mesozooplankton in the Greenland Sea", by Claudio Richter
Heft-Nr. 155/1995 – „Benthos in polaren Gewässern", herausgegeben von Christian Wiencke und Wolf Arntz
Heft-Nr. 156/1995 – „An adjoint model for the determination of the mean oceanic circulation, air-sea fluxes and mixing coefficients", by Reiner Schlitzer
Heft-Nr. 157/1995 – „Biochemische Untersuchungen zum Lipidstoffwechsel antarktischer Copepoden", von Kirsten Fahl
* **Heft-Nr. 158/1995** – „Die deutsche Polarforschung seit der Jahrhundertwende und der Einfluß Erich von Drygalskis", von Cornelia Lüdecke
Heft-Nr. 159/1995 – „The distribution of $\delta^{18}O$ in the Arctic Ocean: Implications for the freshwater balance of the halocline and the sources of deep and bottom waters", by Dorothea Bauch
* **Heft-Nr. 160/1995** – „Rekonstruktion der spätquartären Tiefenwasserzirkulation und Produktivität im östlichen Südatlantik anhand von benthischen Foraminiferenvergesellschaftungen", von Gerhard Schmiedl
Heft-Nr. 161/1995 – „Der Einfluß von Salinität und Lichtintensität auf die Osmolytkonzentrationen, die Zellvolumina und die Wachstumsraten der antarktischen Eisdiatomeen *Chaetoceros* sp. und *Navicula* sp. unter besonderer Berücksichtigung der Aminosäure Prolin", von Jürgen Nothnagel
Heft-Nr. 162/1995 – „Meereistransportiertes lithogenes Feinmaterial in spätquartären Tiefseesedimenten des zentralen östlichen Arktischen Ozeans und der Framstraße", von Thomas Letzig
Heft-Nr. 163/1995 – „Die Expedition ANTARKTIS-XI/2 mit FS 'Polarstern' 1993/94", herausgegeben von Rainer Gersonde
Heft-Nr. 164/1995 – „Regionale und altersabhängige Variation gesteinsmagnetischer Parameter in marinen Sedimenten der Arktis", von Thomas Frederichs
Heft-Nr. 165/1995 – „Vorkommen, Verteilung und Umsatz biogener organischer Spurenstoffe: Sterole in antarktischen Gewässern", von Georg Hanke
Heft-Nr. 166/1995 – „Vergleichende Untersuchungen eines optimierten dynamisch-thermodynamischen Meereismodells mit Beobachtungen im Weddellmeer", von Holger Fischer
Heft-Nr. 167/1995 – „Rekonstruktionen von Paläo-Umweltparametern anhand von stabilen Isotopen und Faunen-Vergesellschaftungen planktischer Foraminiferen im Südatlantik", von Hans-Stefan Niebler
Heft-Nr. 168/1995 – „Die Expedition ANTARKTIS XII mit FS 'Polarstern' 1994/95. Bericht von den Fahrtabschnitten ANT XII/1 und 2", herausgegeben von Gerhard Kattner und Dieter Karl Fütterer
Heft-Nr. 169/1995 – „Medizinische Untersuchung zur Circadianrhythmik und zum Verhalten bei Überwinterern auf einer antarktischen Forschungsstation", von Hans Wortmann
Heft-Nr. 170/1995 – DFG-Kolloquium: Terrestrische Geowissenschaften – Geologie und Geophysik der Antarktis
Heft-Nr. 171/1995 – „Strukturentwicklung und Petrogenese des metamorphen Grundgebirges der nördlichen Heimefrontfjella (westliches Dronning Maud Land/Antarktika)", von Wilfried Bauer
Heft-Nr. 172/1995 – „Die Struktur der Erdkruste im Bereich des Scoresby Sund, Ostgrönland: Ergebnisse refraktionsseismischer und gravimetrischer Untersuchungen", von Holger Mandler
Heft-Nr. 173/1995 – „Paläozoische Akkretion am paläopazifischen Kontinentalrand der Antarktis in Nordvictorialand – P-T-D-Geschichte und Deformationsmechanismen im Bowers Terrane", von Stefan Matzer
Heft-Nr. 174/1995 – „The Expediton ARKTIS-X/2 of RV 'Polarstern' in 1994", edited by Hans-W. Hubberten
Heft-Nr. 175/1995 – „Russian-German Cooperation: The Expedition TAYMYR 1994", edited by Christine Siegert and Dmitry Bolshiyanov
Heft-Nr. 176/1995 – „Russian-German Cooperation: Laptev Sea System", edited by Heidemarie Kassens, Dieter Piepenburg, Jörn Thiede, Leonid Timokhov, Hans-Wolfgang Hubberten and Sergey M. Priamikov
Heft-Nr. 177/1995 – „Organischer Kohlenstoff in spätquartären Sedimenten des Arktischen Ozeans: Terrigener Eintrag und marine Produktivität", von Carsten J. Schubert
Heft-Nr. 178/1995 – „Cruise ANTARKTIS XII/4 of RV 'Polarstern' in 1995: CTD-Report", by Jüri Sildam
Heft-Nr. 179/1995 – „Benthische Foraminiferenfaunen als Wassermassen-, Produktions- und Eisdriftanzeiger im Arktischen Ozean", von Jutta Wollenburg

Heft-Nr. 180/1995 – „Biogenopal und biogenes Barium als Indikatoren für spätquartäre Produktivitätsänderungen am antarktischen Kontinentalhang, atlantischer Sektor", von Wolfgang J. Bonn
Heft-Nr. 181/1995 – „Die Expedition ARKTIS X/1 des Forschungsschiffes 'Polarstern' 1994", herausgegeben von Eberhard Fahrbach
Heft-Nr. 182/1995 – „Laptev Sea System: Expeditions in 1994", edited by Heidemarie Kassens
Heft-Nr. 183/1996 – „Interpretation digitaler Parasound Echolotaufzeichnungen im östlichen Arktischen Ozean auf der Grundlage physikalischer Sedimenteigenschaften", von Uwe Bergmann
Heft-Nr. 184/1996 – „Distribution and dynamics of inorganic nitrogen compounds in the troposphere of continental, coastal, marine and Arctic areas", by María Dolores Andrés Hernández
Heft-Nr. 185/1996 – „Verbreitung und Lebensweise der Aphroditiden und Polynoiden (Polychaeta) im östlichen Weddellmeer und im Lazarevmeer (Antarktis)", von Michael Stiller
Heft-Nr. 186/1996 – „Reconstruction of Late Quaternary environmental conditions applying the natural radionuclides ^{230}Th, ^{10}Be, ^{231}Pa and ^{238}U: A study of deep-sea sediments from the eastern sector of the Antarctic Circumpolar Current System", by Martin Frank
Heft-Nr. 187/1996 – „The Meteorological Data of the Neumayer Station (Antarctica) for 1992, 1993 and 1994", by Gert König-Langlo and Andreas Herber
Heft-Nr. 188/1996 – „Die Expedition ANTARKTIS-XI/3 mit FS 'Polarstern' 1994", herausgegeben von Heinz Miller und Hannes Grobe
Heft-Nr. 189/1996 – „Die Expedition ARKTIS-VII/3 mit FS 'Polarstern' 1990", herausgegeben von Heinz Miller und Hannes Grobe
Heft-Nr. 190/1996 – „Cruise report of the Joint Chilean-German-Italian Magellan 'Victor Hensen' Campaign in 1994", edited by Wolf Arntz and Matthias Gorny
Heft-Nr. 191/1996 – „Leitfähigkeits- und Dichtemessung an Eisbohrkernen", von Frank Wilhelms
Heft-Nr. 192/1996 – „Photosynthese-Charakteristika und Lebensstrategien antarktischer Makroalgen", von Gabriele Weykam
Heft-Nr. 193/1996 – Heterogene Reaktionen von N_2O_5 und HBr und ihr Einfluß auf den Ozonabbau in der polaren Stratosphäre", von Sabine Seisel
Heft-Nr. 194/1996 – „Ökologie und Populationsdynamik antarktischer Ophiuroiden (Echinodermata)", von Corinna Dahm
Heft-Nr. 195/1996 – „Die planktische Foraminifere *Neogloboquadrina pachyderma* (Ehrenberg) im Weddellmeer, Antarktis", von Doris Berberich
Heft-Nr. 196/1996 – „Untersuchungen zum Beitrag chemischer und dynamischer Prozesse zur Variabilität des stratosphärischen Ozons über der Arktis", von Birgit Heese
Heft-Nr. 197/1996 – „The Expedition ARKTIS-XI/2 of RV 'Polarstern' in 1995", edited by Gunther Krause
Heft-Nr. 198/1996 – „Geodynamik des Westantarktischen Riftsystems basierend auf Apatit-Spaltspuranalysen", von Frank Lisker
Heft-Nr. 199/1996 – „The 1993 Northeast Water Expedition. Data Report on CTD Measurements of RV 'Polarstern' Cruises ARKTIS IX/2 and 3", by Gereon Budéus and Wolfgang Schneider
Heft-Nr. 200/1996 – „Stability of the Thermohaline Circulation in analytical and numerical models", by Gerrit Lohmann
Heft-Nr. 201/1996 – „Trophische Beziehungen zwischen Makroalgen und Herbivoren in der Potter Cove (King George-Insel, Antarktis)", von Katrin Iken
Heft-Nr. 202/1996 – „Zur Verbreitung und Respiration ökologisch wichtiger Bodentiere in den Gewässern um Svalbard (Arktis)", von Michael K. Schmid
Heft-Nr. 203/1996 – „Dynamik, Rauhigkeit und Alter des Meereises in der Arktis – Numerische Untersuchungen mit einem großskaligen Modell", von Markus Harder
Heft-Nr. 204/1996 – „Zur Parametrisierung der stabilen atmosphärischen Grenzschicht über einem antarktischen Schelfeis", von Dörthe Handorf
Heft-Nr. 205/1996 – „Textures and fabrics in the GRIP ice core, in relation to climate history and ice deformation", by Thorsteinn Thorsteinsson
Heft-Nr. 206/1996 – „Der Ozean als Teil des gekoppelten Klimasystems: Versuch der Rekonstruktion der glazialen Zirkulation mit verschieden komplexen Atmosphärenkomponenten", von Kerstin Fieg
Heft-Nr. 207/1996 – „Lebensstrategien dominanter antarktischer Oithonidae (Cyclopoida, Copepoda) und Oncaeidae (Poecilostomatoida, Copepoda) im Bellingshausenmeer", von Cornelia Metz
Heft-Nr. 208/1996 – „Atmosphäreneinfluß bei der Fernerkundung von Meereis mit passiven Mikrowellenradiometern", von Christoph Oelke
Heft-Nr. 209/1996 – „Klassifikation von Radarsatellitendaten zur Meereiserkennung mit Hilfe von Line-Scanner-Messungen", von Axel Bochert
Heft-Nr. 210/1996 – „Die mit ausgewählten Schwämmen (Hexactinellida und Demospongiae) aus dem Weddellmeer, Antarktis, vergesellschaftete Fauna", von Kathrin Kunzmann
Heft-Nr. 211/1996 – „Russian-German Cooperation: The Expedition TAYMYR 1995 and the Expedition KOLYMA 1995", by Dima Yu. Bolshiyanov and Hans-W. Hubberten

Heft-Nr. 212/1996 – „Surface-sediment composition and sedimentary processes in the central Arctic Ocean and along the Eurasian Continental Margin", by Ruediger Stein, Gennadij I. Ivanov, Michael A. Levitan, and Kirsten Fahl
Heft-Nr. 213/1996 – „Gonadenentwicklung und Eiproduktion dreier *Calanus*-Arten (Copepoda): Freilandbeobachtungen, Histologie und Experimente", von Barbara Niehoff
Heft-Nr. 214/1996 – „Numerische Modellierung der Übergangszone zwischen Eisschild und Eisschelf", von Christoph Mayer
Heft-Nr. 215/1996 – „Arbeiten der AWI-Forschungsstelle Potsdam in Antarktika, 1994/95", herausgegeben von Ulrich Wand
Heft-Nr. 216/1996 – „Rekonstruktion quartärer Klimaänderungen im atlantischen Sektor des Südpolarmeeres anhand von Radiolarien", von Uta Brathauer
Heft-Nr. 217/1996 – „Adaptive Semi-Lagrange-Finite-Elemente-Methode zur Lösung der Flachwassergleichungen: Implementierung und Parallelisierung", von Jörn Behrens
Heft-Nr. 218/1997 – „Radiation and Eddy Flux Experiment 1995 *(REFLEX III)*", by Jörg Hartmann, Axel Bochert, Dietmar Freese, Christoph Kottmeier, Dagmar Nagel, and Andreas Reuter
Heft-Nr. 219/1997 – „Die Expedition ANTARKTIS-XII mit FS 'Polarstern' 1995. Bericht vom Fahrtabschnitt ANT-XII/3", herausgegeben von Wilfried Jokat und Hans Oerter
Heft-Nr. 220/1997 – „Ein Beitrag zum Schwerefeld im Bereich des Weddellmeeres, Antarktis. Nutzung von Altimetermessungen des GEOSAT und ERS-1", von Tilo Schöne
Heft-Nr. 221/1997 – „Die Expedition ANTARKTIS-XIII/1-2 des Forschungsschiffes 'Polarstern' 1995/96", herausgegeben von Ulrich Bathmann, Mike Lucas und Victor Smetacek
Heft-Nr. 222/1997 – „Tectonic Structures and Glaciomarine Sedimentation in the South-Eastern Weddell Sea from Seismic Reflection Data", by László Oszkó
Heft-Nr. 223/1997 – „Bestimmung der Meereisdicke mit seismischen und elektromagnetisch-induktiven Verfahren", von Christian Haas
Heft-Nr. 224/1997 – „Troposphärische Ozonvariationen in Polarregionen", von Silke Wessel
Heft-Nr. 225/1997 – „Biologische und ökologische Untersuchungen zur kryopelagischen Amphipodenfauna des arktischen Meereises", von Michael Poltermann
Heft-Nr. 226/1997 – „Scientific Cruise Report of the Arctic Expedition ARK-XI/1 of RV 'Polarstern' in 1995", edited by Eike Rachor
Heft-Nr. 227/1997 – „Der Einfluß kompatibler Substanzen und Kryoprotektoren auf die Enzyme Malatdehydrogenase (MDH) und Glucose-6-phosphat-Dehydrogenase (G6P-DH) aus *Acrosiphonia arcta* (Chlorophyta) der Arktis und Antarktis", von Katharina Kück
Heft-Nr. 228/1997 – „Die Verbreitung epibenthischer Mollusken im chilenischen Beagle-Kanal", von Katrin Linse
Heft-Nr. 229/1997 – „Das Mesozooplankton im Laptevmeer und östlichen Nansen-Becken – Verteilung und Gemeinschaftsstrukturen im Spätsommer", von Hinrich Hanssen
Heft-Nr. 230/1997 – „Modell eines adaptierbaren, rechnergestützten, wissenschaftlichen Arbeitsplatzes am Alfred-Wegener-Institut für Polar- und Meeresforschung", von Lutz-Peter Kurdelski
Heft-Nr. 231/1997 – „Zur Ökologie arktischer und antarktischer Fische: Aktivität, Sinnesleistungen und Verhalten", von Christopher Zimmermann
Heft-Nr. 232/1997 – „Persistente chlororganische Verbindungen in hochantarktischen Fischen", von Stephan Zimmermann
Heft-Nr. 233/1997 – „Zur Ökologie des Dimethylsulfoniumpropionat (DMSP)-Gehaltes temperierter und polarer Phytoplanktongemeinschaften im Vergleich mit Laborkulturen der Coccolithophoride *Emiliania huxleyi* und der antarktischen Diatomee *Nitzschia lecointei*", von Doris Meyerdierks
Heft-Nr. 234/1997 – „Die Expedition ARCTIC '96 des FS 'Polarstern' (ARK XIII) mit der Arctic Climate System Study (ACSYS)", von Ernst Augstein und den Fahrtteilnehmern
Heft-Nr. 235/1997 – „Polonium-210 und Blei-210 im Südpolarmeer: Natürliche Tracer für biologische und hydrographische Prozesse im Oberflächenwasser des Antarktischen Zirkumpolarstroms und des Weddellmeeres", von Jana Friedrich
Heft-Nr. 236/1997 – „Determination of atmospheric trace gas amounts and corresponding natural isotopic ratios by means of ground-based FTIR spectroscopy in the high Arctic", by Arndt Meier
Heft-Nr. 237/1997 – „Russian-German Cooperation: The Expedition TAYMYR / SEVERNAYA ZEMLYA 1996", edited by Martin Melles, Birgit Hagedorn and Dmitri Yu. Bolshiyanov.
Heft-Nr. 238/1997 – „Life strategy and ecophysiology of Antarctic macroalgae", by Iván M. Gómez.
Heft-Nr. 239/1997 – „Die Expedition ANTARKTIS XIII/4-5 des Forschungsschiffes ‚Polarstern' 1996", herausgegeben von Eberhard Fahrbach und Dieter Gerdes.
Heft-Nr. 240/1997 – „Untersuchungen zur Chrom-Speziation in Meerwasser, Meereis und Schnee aus ausgewählten Gebieten der Arktis", von Heide Giese.
Heft-Nr. 241/1997 – „Late Quaternary glacial history and paleoceanographic reconstructions along the East Greenland continental margin: Evidence from high-resolution records of stable isotopes and ice-rafted debris", by Seung-Il Nam.

Heft-Nr. 242/1997 – „Thermal, hydrological and geochemical dynamics of the active layer at a continuous permafrost site, Taymyr Peninsula, Siberia", by Julia Boike.
Heft-Nr. 243/1997 – „Zur Paläoozeanographie hoher Breiten: Stellvertreterdaten aus Foraminiferen", von Andreas Mackensen.
Heft-Nr. 244/1997 – „The Geophysical Observatory at Neumayer Station, Antarctica. Geomagnetic and seismological observations in 1995 and 1996", by Alfons Eckstaller, Thomas Schmidt, Viola Gaw, Christian Müller and Johannes Rogenhagen.
Heft-Nr. 245/1997 – „Temperaturbedarf und Biogeographie mariner Makroalgen – Anpassung mariner Makroalgen an tiefe Temperaturen", von Bettina Bischoff-Bäsmann.
Heft-Nr. 246/1997 – „Ökologische Untersuchungen zur Fauna des arktischen Meereises", von Christine Friedrich.
Heft-Nr. 247/1997 – „Entstehung und modifizierung von marinen gelösten organischen Substanzen", von Berit Kirchhoff.
Heft-Nr. 248/1997 – „Laptev Sea System: Expeditions in 1995", edited by Heidemarie Kassens.
Heft-Nr. 249/1997 – „The Expedition ANTARKTIS XIII/3 (EASIZ I) of RV ‚Polarstern' to the eastern Weddell Sea in 1996", edited by Wolf Arntz and Julian Gutt.
Heft-Nr. 250/1997 – „Vergleichende Untersuchungen zur Ökologie und Biodiversität des Mega-Epibenthos der Arktis und Antarktis", von Andreas Starmans.
Heft-Nr. 251/1997 – „Zeitliche und räumliche Verteilung von Mineralvergesellschaftungen in spätquartären Sedimenten des Arktischen Ozeans und ihre Nützlichkeit als Klimaindikatoren während der Glazial/Interglazial-Wechsel", von Christoph Vogt.
Heft-Nr. 252/1997 – „Solitäre Ascidien in der Potter Cove (King George Island, Antarktis). Ihre ökologische Bedeutung und Populationsdynamik", von Stephan Kühne.
Heft-Nr. 253/1997 – „Distribution and role of microprotozoa in the Southern Ocean", by Christine Klaas.
Heft-Nr. 254/1997 – „Die spätquartäre Klima- und Umweltgeschichte der Bunger-Oase, Ostantarktis", von Thomas Kulbe.
Heft-Nr. 255/1997 – „Scientific Cruise Report of the Arctic Expedition ARK-XIII/2 of RV ‚Polarstern' in 1997", edited by Ruediger Stein and Kirsten Fahl.
Heft-Nr. 256/1998 – „Das Radionuklid Tritium im Ozean: Meßverfahren und Verteilung von Tritium im Südatlantik und im Weddellmeer", von Jürgen Sültenfuß.
Heft-Nr. 257/1998 – „Untersuchungen der Saisonalität von atmosphärischem Dimethylsulfid in der Arktis und Antarktis", von Christoph Kleefeld.
Heft-Nr. 258/1998 – „Bellingshausen- und Amundsenmeer: Entwicklung eines Sedimentationsmodells", von Frank-Oliver Nitsche.
Heft-Nr. 259/1998 – „The Expedition ANTARKTIS-XIV/4 of RV ‚Polarstern' in 1997", by Dieter K. Fütterer.
Heft-Nr. 260/1998 – „Die Diatomeen der Laptevsee (Arktischer Ozean): Taxonomie und biogeographische Verbreitung", von Holger Cremer
Heft-Nr. 261/98 – „Die Krustenstruktur und Sedimentdecke des Eurasischen Beckens, Arktischer Ozean: Resultate aus seismischen und gravimetrischen Untersuchungen", von Estella Weigelt.
Heft-Nr. 262/98 – „The Expedition ARKTIS-XIII/3 of RV 'Polarstern' in 1997", by Gunther Krause.
Heft-Nr. 263/98 – „Thermo-tektonische Entwicklung von Oates Land und der Shackleton Range (Antarktis) basierend auf Spaltspuranalysen", von Thorsten Schäfer.
Heft-Nr. 264/98 – „Messungen der stratosphärischen Spurengase ClO, HCl, O_3, N_2O, H_2O und OH mittels flugzeuggetragener Submillimeterwellen-Radiometrie", von Joachim Urban.
Heft-Nr. 265/98 – „Untersuchungen zu Massenhaushalt und Dynamik des Ronne Ice Shelfs, Antarktis", von Astrid Lambrecht.
Heft-Nr. 266/98 – „Scientific Cruise Report of the Kara Sea Expedition of RV 'Akademik Boris Petrov' in 1997", edited by Jens Matthiessen and Oleg Stepanets.
Heft-Nr. 267/98 – „Die Expedition ANTARKTIS-XIV mit FS 'Polarstern' 1997. Bericht vom Fahrtabschnitt ANT-XIV/3", herausgegeben von Wilfried Jokat und Hans Oerter.
Heft-Nr. 268/98 – „Numerische Modellierung der Wechselwirkung zwischen Atmosphäre und Meereis in der arktischen Eisrandzone", von Gerit Birnbaum.
Heft-Nr. 269/98 – „ Katabatic wind and Boundary Layer Front Experiment around Greenland (KABEG '97)", by Günther Heinemann.

* vergriffen/out of print
** nur noch beim Autor/only from the author